



**Queensland University of Technology**  
Brisbane Australia

This may be the author's version of a work that was submitted/accepted for publication in the following source:

Laycock, Bronwyn, [Nikolic, Melissa](#), [Colwell, John](#), Gauthier, Emilie, Halley, Peter, [Bottle, Steven](#), & [George, Graeme](#) (2017)

Lifetime prediction of biodegradable polymers.  
*Progress in Polymer Science*, 71, pp. 144-189.

This file was downloaded from: <https://eprints.qut.edu.au/105377/>

**© Consult author(s) regarding copyright matters**

This work is covered by copyright. Unless the document is being made available under a Creative Commons Licence, you must assume that re-use is limited to personal use and that permission from the copyright owner must be obtained for all other uses. If the document is available under a Creative Commons License (or other specified license) then refer to the Licence for details of permitted re-use. It is a condition of access that users recognise and abide by the legal requirements associated with these rights. If you believe that this work infringes copyright please provide details by email to [qut.copyright@qut.edu.au](mailto:qut.copyright@qut.edu.au)

**License:** Creative Commons: Attribution-Noncommercial-No Derivative Works 2.5

**Notice:** *Please note that this document may not be the Version of Record (i.e. published version) of the work. Author manuscript versions (as Submitted for peer review or as Accepted for publication after peer review) can be identified by an absence of publisher branding and/or typeset appearance. If there is any doubt, please refer to the published source.*

<https://doi.org/10.1016/j.progpolymsci.2017.02.004>

## Accepted Manuscript

Title: Lifetime prediction of biodegradable polymers

Authors: Bronwyn Laycock, Melissa Nikolić, John M. Colwell, Emilie Gauthier, Peter Halley, Steven Bottle, Graeme George



PII: S0079-6700(17)30054-0  
DOI: <http://dx.doi.org/doi:10.1016/j.progpolymsci.2017.02.004>  
Reference: JPPS 1017

To appear in: *Progress in Polymer Science*

Received date: 19-7-2016  
Revised date: 20-2-2017  
Accepted date: 20-2-2017

Please cite this article as: Laycock Bronwyn, Nikolić Melissa, Colwell John M, Gauthier Emilie, Halley Peter, Bottle Steven, George Graeme. Lifetime prediction of biodegradable polymers. *Progress in Polymer Science* <http://dx.doi.org/10.1016/j.progpolymsci.2017.02.004>

This is a PDF file of an unedited manuscript that has been accepted for publication. As a service to our customers we are providing this early version of the manuscript. The manuscript will undergo copyediting, typesetting, and review of the resulting proof before it is published in its final form. Please note that during the production process errors may be discovered which could affect the content, and all legal disclaimers that apply to the journal pertain.

## Lifetime prediction of biodegradable polymers

Bronwyn Laycock <sup>a\*</sup>, Melissa Nikolić <sup>b</sup>, John M. Colwell <sup>b</sup>, Emilie Gauthier <sup>a</sup>, Peter Halley <sup>a</sup>, Steven Bottle <sup>b</sup>, Graeme George <sup>b</sup>

<sup>a</sup> Cooperative Research Centre for Polymers, School of Chemical Engineering, The University of Queensland, St Lucia, QLD 4072, Australia.

<sup>b</sup> Cooperative Research Centre for Polymers, School of Chemistry, Physics and Mechanical Engineering, Queensland University of Technology (QUT), GPO Box 2434, Brisbane, QLD 4001, Australia

**Corresponding author:** b.laycock@uq.edu.au

### Abstract

The determination of the safe working life of polymer materials is important for their successful use in engineering, medicine and consumer-goods applications. An understanding of the physical and chemical changes to the structure of widely-used polymers such as the polyolefins, when exposed to aggressive environments, has provided a framework for controlling their ultimate service lifetime by either stabilizing the polymer or chemically accelerating the degradation reactions. The recent focus on biodegradable polymers as replacements for more bio-inert materials such as the polyolefins in areas as diverse as packaging and as scaffolds for tissue engineering has highlighted the need for a review of the approaches to being able to predict the lifetime of these materials. In many studies the focus has not been on the embrittlement and fracture of the material (as it would be for a polyolefin) but rather the products of degradation, their toxicity and ultimate fate when in the environment, which may be the human body. These differences are primarily due to time-scale. Different approaches to the problem have arisen in biomedicine, such as the kinetic control of drug delivery by the bio-erosion of polymers, but the similarities in mechanism provide real prospects for the prediction of the safe service lifetime of a biodegradable polymer as a structural material. Common mechanistic themes that emerge include the diffusion-controlled process of water sorption and conditions for surface *versus* bulk degradation, the role of hydrolysis *versus* oxidative degradation in controlling the rate of polymer chain scission and strength loss and the specificity of enzyme-mediated reactions.

**Keywords:** biodegradable polymers, lifetime, biodegradation, hydrolysis, erosion.

## Nomenclature

$\alpha$	Diffusion porosity constant	$c_1$	A constant of integration that accounts for the hydrolysis rate and crystallinity
$\beta$	A constant introduced to regulate the contribution of autocatalysis	$c_2$	Ratio of the initial concentrations of acids and ester bonds; $c_2 = [COOH]_0/[E]_0$
$\gamma$	Axial stretch ( $\gamma = 1 + \varepsilon$ ) (where $\varepsilon$ is the nominal strain)	$C_\infty$	The amount of starch degraded at the end point of the enzymatic hydrolysis reaction
$\delta^2$	Cohesive energy density of the polymer	$c_m$	Mole concentration of hydrolysed monomers
$\delta_1^2$	Disperse forces	$c_{ol}$	Molar concentration of ester bonds in the oligomers (mol/L)
$\delta_2^2$	Polar forces	$C_m^b$	Diffusion of monomers accounting for dissociation of acid end group
$\delta_3^2$	Hydrogen bonding forces	$C_t$	The starch degraded (expressed as mass per unit volume) at incubation time $t$
$\varepsilon$	Nominal strain	$D$	Diffusion coefficient
$\varepsilon_t$	Erosion number	$D_0$	Intrinsic diffusion coefficient
$\vartheta$	Fraction of the substrate surface occupied by the ES complex	$D^\infty$	Diffusivity of water into an intact, dry polymer
$\theta$	A rate constant that accounts for the differences in the reactivity of polymer functional groups	$D_{eff}$	Effective diffusion coefficient of water inside a polymer
$\Lambda$	Thiele modulus	$d_h$	Damage parameter (equivalent to $[1 - \sigma/\sigma_0]$ )
$\Lambda$	Hydrolysis rate constant specific to a polymer	$D_{ia0}$	Initial diameter of a cylinder
$\lambda'$	Pseudo first order rate constant	$D_{medium}$	Diffusion coefficient of the monomers produced following hydrolysis in the hydrolysis medium
$\lambda''$	Revised rate constant	$\bar{D}_{medium}$	Nondimensional form of $D_{medium}$
$\lambda_{Ei}$	Rate constant for hydrolysis of each corresponding type of ester bond ( $E_i$ )	$D_n$	Effective diffusion coefficient of an n-long polymer chain through the polymer matrix
$\mu g_p$	Polymer weight loss in $\mu g$	$\mathcal{D}_M$	Molar mass dispersity where $\mathcal{D}_M = M_w/M_n$
$\mu g_z$	Mass of enzyme present in $\mu g$	$DP$	Average degree of polymerization
$v_0$	Rate of a reaction	$DP_0$	Initial degree of polymerization
$\rho$	Polymer density	$E$	Young's modulus (in MPa)
$\rho_w^\infty$	Water density	$E_0$	Initial Young's modulus (in MPa)
$\sigma$	Polymer strength	$[E]$	Concentration of ester groups (in mol/L)
$\sigma_0$	Nominal stress	$[E]_0$	Initial concentration of ester groups (in mol/L)
$\sigma_x$	Tensile stress ( $N\ m^{-2}$ )	$E_a$	Activation energy
$\sigma_\infty$	Polymer strength at a theoretical infinite $M_n$	$E_D$	Activation energy for the diffusion reaction
$\varphi_A$	Concentration of ester bonds in the amorphous fraction (mol/L)	$E_h$	Polymer-dependent activation energy for the hydrolysis reaction
$\omega$	Inverse molar volume of the crystalline phase		
$\phi$	Coefficient ( $m^3\ mol^{-1}$ )		
$A$	A pre-exponential factor for the hydrolysis reaction rate coefficient		
$Area$	Substrate surface area		
$BSR$	Tensile breaking strength retention; $BSR = (\sigma_0 - \sigma)/\sigma_0$		

$E(t_n)$	Velocity of degradation (which is equivalent to $d[E]/dt$ )	$N_0$	Initial number of polymer chains
$f$	Fractional dissolution of a polymer at time $t$	$N_A$	Avogadro's number
$fP_n$	Fraction of polymer chains with degree of polymerization $n$	$N_{chains}$	Total number of polymer chains
$[H_2O]$	Concentration of water (in mol/L)	$N_{total}$	Sum of polymer units in a group of chains
$k$	Rate constant	$n$	Total number of chains in a group of chains
$k_1$	Non-catalytic reaction rate constant	$n_e$	Number of esters in a monomer unit
$k_2$	Autocatalytic reaction rate constant	$P_A$	Accelerated probability density function
$K$	Adsorption equilibrium constant (from the Freundlich equation)	$P_C$	The contributions to the accelerated probability density function due to autocatalysis
$K_0$	Arrhenius frequency factor	$P_F$	The contributions to the accelerated probability density function due to fundamental hydrolysis
$K_f$	Rate of bond rupture events	PBAT	Poly(butylene adipate- <i>co</i> -terephthalate)
$k_b$	Boltzmann's constant	PBS	Poly(butylene succinate)
$K_{EQ}$	Thermodynamic equilibrium constant for the polymer chain hydrolysis	PCL	Poly( $\epsilon$ -caprolactone)
$K_{COOH}$	Dissociation constant for the acid end groups	PDLA	Poly( <i>D</i> -lactic acid)
$k_p$	Depolymerization rate for the polymer chain hydrolysis	PGA	Poly(glycolic acid)
$L$	Thickness of the specimen	PHA	Polyhydroxyalkanoate
$L_{crit}$	Critical thickness of the specimen	PHB	Poly(3-hydroxybutyrate)
$L_{crit0}$	Initial critical thickness of the specimen	PHBV	poly(3-hydroxybutyrate- <i>co</i> -3-hydroxyvalerate)
$m$	Molar mass of a repeat unit (in g/mol)	PLA	Poly(lactic acid)
$M_{chain}$	Molar concentration of polymer chains (mol/L)	PLGA	poly( <i>D,L</i> -lactide- <i>co</i> -glycolide)
$M_{chain0}$	Initial molar concentration of polymer chains (mol/L)	PLLA	Poly( <i>L</i> -lactic acid)
$M_e$	Critical molecular weight for chain entanglement (in kg/mol)	$P_n$	An $n$ -long polymer chain
$M_n$	Number average molecular weight (in kg/mol)	$[P_n]$	Molar concentration of an $n$ -long polymer chain (in mol/L)
$M_{n0}$	Initial number average molecular weight (in kg/mol)	$R$	Radius of a cylinder or sphere or the half-thickness of a slab
$M_{nt}$	The value of $M_n$ after environmental exposure for time, $t$ (in kg/mol)	$R$	Gas constant
$M_t$	Water absorption at time $t$	$RH$	Relative humidity
$M_{th}$	Molecular weight threshold	$R_{ind}$	Molecular weight reaction index
$M_w$	Weight average molecular weight	$R_n$	Molar rate of formation by the collection of degradation chemical reactions
$M_\infty$	Water absorption at time $\infty$	$R_s$	Molar number of scissions per unit volume (mol/L)
$Mass_t$	Mass of polymer at time $t$	$R_{scissions}$	Ratio of random scissions to end scissions
$Mass_\infty$	Mass of polymer at infinite time	$S$	Number of scissions per number average chain
$MW$	Molecular weight (either $M_n$ or $M_w$ )	$s_c$	Critical number of chain scissions at the end of polymer lifetime
$N$	Number of polymer chains per unit volume	$[S]$	Substrate concentration
		$[S]_0$	Initial substrate concentration
		SEC	Size Exclusion Chromatography

$t$	Time
$T$	Temperature
$t_{AV}$	Average lifetime of the pixel rings in a Monte Carlo simulation
$t_{diff}$	Time for water to diffuse through a polymer matrix
$t_{fail}$	Time to fail
$u_s$	Strength decrease rate of a material
$V_{(t)}$	Volume fraction of polymer matrix at time $t$
$W_c$	Critical thickness (variation, analogous to but defined differently from $L_{crit}$ )
$W_m$	Total amount of water consumed in the hydrolysis region when mass loss starts
$W_s$	Solubility of water in the polymer
$W_\infty$	Mass of water absorption at infinite time
$W_t$	Mass of water absorption at time $t$
$x$	Average number of repeating units of the oligomers (set at 4).
$\langle x \rangle$	A mean distance
$X_c$	Degree of crystallinity
$X_{Ei}$	Molar fraction of each corresponding type of ester bond ( $E_i$ )
$x_i$	Monomer concentration at a given location
$z$	A random integer between 0 and 99
$[Z]$	Concentration of the unbound enzyme
$[Z]_0$	Initial enzyme concentration
$[ZS]$	Concentration of an enzyme-substrate complex

## 1. Introduction

Plastics are ubiquitous in our modern culture, having excellent and tailorable material properties, with controllable flexibility and strength and the ability to be moulded into shape. They are also cheap, durable, relatively impermeable, sterilizable, and with a high strength to weight ratio. The application of plastic film as packaging and other disposable items is particularly important, with approximately 40 million tonnes of plastic film and sheet produced from polyethylene alone [1-3].

There has been considerable interest in the use and optimization of biodegradable polymers as an alternative to polyolefins such as polyethylene for such applications. Much of this has been driven by increasing concerns about land, water and, in particular, marine pollution that arise from the inherent resistance of polyolefins to environmental degradation [4].

Biodegradable plastics can originate from renewable sources (e.g., starch and polyhydroxyalkanoates) or biodegradable synthetic polymers (e.g., petroleum derived polyesters). The most widely studied biodegradable polymers have been either polysaccharides (cellulose and its derivatives, particularly starch) or aliphatic and mixed aliphatic/aromatic polyesters. Fig. 1 summarises the stages in degradation for biodegradable polymers, where the primary mode of degradation is chain cleavage through hydrolysis (either through abiotic (non-enzymatic) hydrolysis or enzyme-promoted hydrolysis), unlike oxo-degradable systems which are very resistant to hydrolysis [5]. There are four key variables and the relationship between them, which are critical to the mechanism of polymer erosion (covered in detail in section 4.4):

- The rate of water diffusion into the polymer ( $D$ ) and the pseudo first order rate of hydrolysis ( $\lambda'$ )
- The thickness of the specimen ( $L$ ) and the critical thickness ( $L_{crit}$ )

Under a surface erosion mechanism ( $\lambda' > D$ ;  $L > L_{crit}$ ), polymer is eroded from the surface and the core polymeric material remains intact (average molecular weight  $M_w$  and mechanical properties), until the load bearing capability decreases steadily as the thickness of the polymer is less than the critical thickness. At this point the mechanism of erosion shifts to bulk erosion ( $\lambda' < D$ ;  $L < L_{crit}$ ), where the time to failure becomes dominated by the rate of auto-acceleration of hydrolysis where  $M_n$  reaches a critical value  $M_e$ . From this point, the polymer depolymerises into water-soluble products oligomer and monomers, which are then assimilated by micro-organisms into biomass or mineralised to  $\text{CO}_2$ ,  $\text{H}_2\text{O}$ ,  $\text{CH}_4$  and other metabolic products.

However, the use of biodegradable plastics has been limited by their higher cost, moisture sensitivity, narrow processing windows, low heat deflection temperatures, and/or poor barrier and conductivity properties [5]. In addition, thorough life cycle assessments (cradle to grave) need to be carried out to assess the relative environmental impact of each polymer type.

While technological solutions are being developed for many of the property limitations described above, the core challenge remains: to understand the factors that will ultimately control the time over which biodegradable polymers will maintain their integrity and material properties when exposed to different environments. The environmental stresses usually considered in association with the deterioration of performance outdoors are elevated temperatures and solar radiation as well as mechanical stresses and rainfall/moisture. However, other factors such as chemical conditions and, particularly for soil burial, biological activities including enzymatic and other microbial and biological processes (such as impacts of roots and fungal hyphae) are also factors.

*Figure 1*



In parallel with the use of polymers in the external environment, there is the increasing use of controlled-lifetime polymers in biomedical applications of drug delivery, tissue engineering, scaffolds and prosthetics. In this case the environment of concern is a particular part of a human or animal body. In these applications, “lifetime” has a different meaning depending on the function the polymer is performing in the body. The medical applications of a biodegradable polymer are the most challenging of all due to:

- The need for compatibility with body tissue of both the original polymer and its degradation products;
- The requirement for properties to continually change as the medical function is progressively met, e.g., a scaffold for tissue regeneration must progressively weaken so the new tissue can assume the biological function and replace the implant;
- In the case of polymer-controlled drug delivery, the kinetics of release will depend on whether the degradation of the carrier polymer is controlling release or whether this occurs through migration following water uptake and swelling. The rate of biodegradation may be less important if the polymer is orally administered compared to subcutaneous or pulmonary delivery.

If one is able to focus on the physical and chemical property changes in the polymer when exposed to different environments, then results in one application may be translatable to others. The key principle is the extent of degradation of the polymer that constitutes end-of-life when in that particular application. If the rate of change of the property is known for this environment then the lifetime can, in principle, be predicted.

Lifetime prediction therefore requires the measurement of the kinetics of the chemical, physical and/or biological reactions that result in bond scission and subsequent chemical transformations that constitute the degradation process under the combined environmental

stresses (shown in Fig. 1), together with knowledge of the extent of degradation that constitutes the end of the safe service life [7-9].

In this paper, the fundamental principles that underlie the biodegradation of biodegradable polymers are summarised and then recent literature on the environmental performance and prediction of the lifetime of these polymers is reviewed.

## 2. Definitions

The literature associated with biodegradable polymer degradation and biodegradation is inconsistent with respect to the terms used to describe different stages and aspects of degradation. In this review, we have adopted the definitions as listed in the Standards, PD CEN/TR 15351:2006 and ASTM D883 [10, 11]:

<b>Aerobic biodegradation</b>	Biodegradation under aerobic conditions (oxygen present)
<b>Anaerobic biodegradation</b>	Biodegradation under anaerobic conditions (oxygen absent)
<b>Bioassimilation</b>	Conversion of a polymeric item to biomass
<b>Bioavailability</b>	Property of being physically and chemically accessible to the action of cells and enzymes released by them
<b>Bioavailable</b>	Status of a plastic item that can be processed by cells
<b>Biodegradable</b>	Status of a polymeric item that can be biodegraded
<b>Biodegradable plastic</b>	A degradable plastic in which the degradation results from the action of naturally-occurring micro-organisms such as bacteria, fungi and algae
<b>Biodegradation</b>	Degradation of a polymeric item due to cell-mediated phenomena
<b>Biodisintegration</b>	Disintegration resulting from the action of cells
<b>Bioerosion</b>	Faster degradation at the surface than inside resulting from biodegradation
<b>Biofragmentation</b>	Fragmentation of a polymeric item due to the action of cells
<b>Biomass</b>	Material of biological origin excluding material embedded in geological formation or transformed to fossil
<b>Biom mineralization</b>	Mineralization caused by cell-mediated phenomena
<b>Bulk degradation</b>	Faster degradation inside than at the surface of a polymeric item

<b>Compostable plastic</b>	A plastic that undergoes biological degradation during composting to yield carbon dioxide, water, inorganic compounds, and biomass at a rate consistent with other known compostable materials and leaves no visually distinguishable or toxic residues
<b>Degradable</b>	Status of a polymeric item that can undergo degradation
<b>Degradable plastic</b>	A plastic designed to undergo a significant change in its chemical structure under specific environmental conditions resulting in a loss of some properties that may vary as measured by standard test methods appropriate to the plastic and the application in a period of time that determines its classification
<b>Degradation</b>	A deleterious change in the chemical structure, physical properties, or appearance of a polymer, which may result from chemical cleavage of the macromolecules forming a polymeric item, regardless of the mechanism of chain cleavage
<b>Disintegration</b>	Fragmentation to particles of an acceptable size (depending on the application)
<b>Dissolution</b>	Solution of macromolecules constituting a polymeric item in a liquid medium
<b>Enzymatic degradation</b>	Degradation caused by the catalytic action of enzymes under abiotic experimental conditions
<b>Erosion</b>	Faster alteration at the surface than inside
<b>Fragmentation</b>	Breakdown of a polymeric item to particles regardless of the mechanism
<b>Heterogeneous degradation or biodegradation</b>	Degradation or biodegradation occurring at different rates depending on the location within a matrix
<b>Homogeneous degradation or biodegradation</b>	Degradation or biodegradation that occurs at the same rate regardless of the location within a polymeric item
<b>Hydrolytic degradation</b>	Degradation identified as resulting from hydrolytic cleavage of macromolecules
<b>Hydrolytically degradable plastic</b>	A degradable plastic in which the degradation results from hydrolysis
<b>Maximum degree of biodegradation</b>	Maximum value of the degree of biodegradation that can be reached under selected experimental conditions
<b>Mineralization</b>	Conversion of an organic compound to methane or carbon dioxide and water and other minerals
<b>Oxobiodegradation</b>	Degradation identified as resulting from oxidative and cell-mediated phenomena, either simultaneously or successively
	NOTE: Similarly, prefixes like thermo (for the action of heat), photo (for the action of light) are to be used separately or in combination whenever one wants to indicate the involvement of various identified mechanisms of degradation

<b>Oxodegradation (or oxidative degradation)</b>	Degradation identified as resulting from oxidative cleavage of macromolecules  NOTE: Similarly, prefixes like thermo (for the action of heat), photo (for the action of light) are to be used whenever one wants to indicate an identified mechanism of degradation
<b>Theoretical degree of biodegradation</b>	Theoretical value of the degree of biodegradation corresponding to total conversion of the organic matter present in an original polymer-based item to minerals and biomass

### 3.0 Polymer degradation – an overview

The short overview of the principles of polymer degradation as a whole that is covered in this section is not a comprehensive review of the field but rather summarises the core concepts and formulae that need to be understood in order to undertake lifetime prediction in biodegradable polymers.

Polymer degradation can be defined as “a deleterious change in the chemical structure, physical properties, or appearance of a polymer, which may result from chemical cleavage of the macromolecules forming a polymeric item, regardless of the mechanism of chain cleavage” [12], see Section 3.0. Such degradation produces changes in: mechanical, optical or electrical characteristics, through crazing, cracking, erosion, discolouration and phase separation [13]. Polymer degradation can be classified as photo-oxidative, thermo-oxidative, ozone-induced, mechanochemical, hydrolytic, catalytic and/or biodegradation, depending on the mechanism [13]. However, for practical use, one critical parameter that needs to be determined is the useful lifetime of the polymer in the service environment.

#### 3.1 Mechanical criteria for failure

Polymers are deemed to have met the mechanical criteria for failure when their fracture energy, which is a measure of toughness, has fallen to a pre-determined fraction of the starting value. In the literature on service lifetimes of polymers, this predetermined set-point varies. For polyolefins such as polypropylene, for example, mechanical failure is frequently

taken as the point at which fracture energy has reached 50% of the initial value [14], although in practice this may be beyond the point at which the polymer is still serviceable. Another approach for assessing failure in thermoplastic polymers is to measure elongation to break. When this has fallen to 5% of the initial ultimate elongation when measured under tension, this indicates that the polymer can no longer yield and as such will fail in a brittle mode on the application of force. The direct measurement of the actual fracture toughness is also useful, if it is possible, since this enables the tracking of the dissipation of energy at the crack tip [15]. In practice, however, the total loss of toughness is most commonly indicated by the polymer fracturing when tapped or otherwise handled.

Overall, and at the simplest level, it is the underlying changes in the length of the polymer chain (and the associated dissolution of degradation products), the forces between the chains, and the extent and type of crystallinity that cause this mechanical failure [7].

### 3.1.1 The length of the polymer chain

The ideal length of a polymer chain (*i.e.* its degree of polymerization) for a given application is typically optimised to provide a balance between processability, strength and toughness. The latter properties require a high degree of chain entanglement (achieved by increasing the  $M_n$  while if the molecular weight is too high, then the material becomes difficult to process. The relationship between polymer strength,  $\sigma$ , and molecular weight is given by:

$$\sigma = A - B/\bar{M}_n \quad (1)$$

where  $A$  and  $B$  are constants for a particular polymer. When  $\sigma$  is zero, *i.e.*, when the polymer no longer has any strength and thus is at the end of its useful lifetime for a material application, then  $M_n$  becomes  $M_e$ , the critical molecular weight for chain entanglement, which for poly(lactic acid) (PLA) is ~8 to 10 kg/mol [16] and for polyhydroxyalkanoate (PHA) is

~13 kg/mol [17]. The constant,  $A$ , has been equated [18] to the strength at a theoretical, infinite  $M_n$  ( $\sigma_\infty$ ).

The hydrolytic degradation of a polymer results in polymer chain scission events (whether random or otherwise) that cause a reduction in molecular weight. The number of scissions per number average chain,  $s$ , is described by equation (2):

$$s = \left( \frac{\bar{M}_{n0}}{\bar{M}_{nt}} \right) - 1 \quad (2)$$

where  $M_{n0}$  is the initial number average molecular weight and  $M_{nt}$  the value after environmental exposure for time,  $t$ .

These chain scission events will rapidly reduce entanglements and thus strength and, as  $M_{nt}$  approaches  $M_e$ , the strength as given by equation (1) reduces to zero. A more detailed discussion of the type of chain scission events associated with different polymer types and their effect on polymer material properties is given in Sections 4.3 and 4.7.

### 3.1.2 Forces between polymer chains

Intermolecular forces between polymer chains play a critical role in determining polymer strength and toughness and depend on the functional groups in the repeat unit. These forces are measured through the Cohesive Energy Density  $\delta^2$  of the polymer, as described in equation (3). This is the sum of the components from disperse  $\delta_1^2$ , polar  $\delta_2^2$  and hydrogen bonding  $\delta_3^2$  forces, each of which may be determined from the solubility parameters for the polymer in appropriate solvents [19].

$$\delta^2 \text{ (MPa)} = \delta_1^2 + \delta_2^2 + \delta_3^2 \quad (3)$$

The Young's Modulus  $E$  of the polymer increases with  $\delta^2$ .

In hetero-atom systems such as polyamides and polyesters, the polar  $\delta_2^2$  and hydrogen bonding  $\delta_3^2$  forces make a major contribution, so that these polymers are typically stiffer than aliphatic polymers such as polyolefins, although the effect of crystallinity will also play a role.

### 3.1.3 Polymer crystallinity

Many of the biodegradable polymers in use are semi-crystalline, with the crystalline regions being effectively impermeable to water, hence slowing the hydrolysis reaction rates of such polymers (see Section 4.1). The crystalline blocks also reduce other transport processes such as gas and solvent diffusion and increase the stiffness and density of the polymer. It is also possible that inhomogeneity can increase following biodegradation, with localised regions of higher crystallinity and hence density. This can in turn result in a localised stress that exceeds the local tensile strength of the matrix, resulting in micro-crack formation [20, 21]. If the polymer film is thin enough, then this crack can cause embrittlement. In thicker films, crack propagation under load can result in loss of mechanical properties. Chain recrystallization following chain scission (through hydrolysis) may also play a role in changing the local crystalline environment, although this is not well-studied in biodegradable polymers.

## 3.2 Polymer lifetime estimation

An estimation of polymer lifetime is made, in most cases, through the use of accelerated ageing using increased temperature and/or higher radiation intensity. This approach measures the rate of degradation under controlled conditions, such that the time taken to reach an extent of degradation corresponding to failure under these conditions can be determined [22]. Extrapolation back to service conditions is then made through the use of a reciprocity relationship (whereby it is assumed, for example, that there is an equal radiation dose to failure regardless of the dose rate). This is coupled with estimation of the effect of

temperature on the reaction rate constant through the exponential dependency described by the Arrhenius relationship. However, the extent to which an Arrhenius relationship may be used is debatable, as curvature is frequently seen, invalidating the extrapolation [23]. Likewise, changes in activation energy for the hydrolytic degradation of biodegradable polymers, particularly above and below their glass transition temperature ( $T_g$ ), make it necessary to identify an upper limit for the testing temperature under which the Arrhenius relation is valid for different polymers [24]. There are also, in many cases, additional, polymer-specific factors that affect the extent to which the environmental parameters couple to accelerate the loss of properties over time. For this reason, it is important to characterise the degradability under a range of conditions for all new polymers, blends of existing polymers and even established formulations where the additives are changed.

This process has been studied in detail for oxidative degradation [7] and the methodology is well developed. In the case of polymers defined as “biodegradable”, it is the ultimate fate that frequently dominates considerations rather than the precise kinetics of the processes leading to the loss of mechanical properties [25, 26]. Thus, attention has very often been focussed on the total amount of carbon dioxide evolved or mass loss on soil burial [26] rather than the extent of degradation at which embrittlement occurs and the kinetics of the reactions leading to this embrittlement [27].

### **3.3 Interconnection of macroscopic, microscopic and chemical changes on degradation**

The first key measurable stage of polymer degradation is loss of physical properties, particularly toughness, such that the polymer material becomes mechanically embrittled (Fig. 1). As already described, it is the changes to the polymer molecular weight, intermolecular forces and crystallinity that underpin loss of physical properties for both oxodegradable and biodegradable polymers. These changes are frequently very non-uniform due in large part to the surface sensitivity of environmental degradation. These three factors are also



interdependent and hence a change in one produces changes to the others. As outlined in Nikolić et al. [15], one or more of the following measures can be used to track environmental degradation or polymer stabilization, depending on the type of polymer and the available techniques:

- Engineering measurements of **fracture toughness and fracture energy** under either slow strain rate or impact. Degradation often corresponds to a transition from a ductile to brittle mode of failure.
- Optical and electron microscope analysis of **surface cracking** responsible for the change in engineering properties.
- Measurement of **macromolecular properties** such as chain length (by Size Exclusion Chromatography (SEC)) and the degree of crystallinity (by X-Ray Diffraction and Differential Scanning Calorimetry) that produce the shrinkage forces leading to surface cracking. A common parameter determined by SEC is the number average chain scissions per polymer molecule,  $s$ , as defined by equation (2).
- Measurement of **chemical changes** (oxidation; hydrolysis; chemical reactions) that result in the physical changes due to scission or crosslinking of polymer chains as well as changes in intermolecular forces. Spectroscopic methods are often employed as well as oxygen uptake, wet-chemical analysis and gravimetry.
- Identification and quantification of volatile organic compounds and gases, particularly carbon dioxide, that indicates the ultimate end product of the degradation process in the environment.
- Measurement of weight changes of the sample during service. This may be a weight increase due to oxygen uptake at short times of exposure followed by weight loss due to dissolution of volatile organic compounds and gases (previous point) as well as ultimate mineralization to carbon dioxide and water. This is a very restricted measure

since leaching of additives etc. can be responsible for weight change rather than loss of degradation products due to hydrolysis or oxidation.

The monitoring of degradation can be undertaken at different levels, from averaged engineering measurements of the bulk polymer through to micromechanical and finally molecular level measures of degradation. Overall, however, the core underlying process controlling degradation and loss of mechanical properties in biodegradable polymers is hydrolysis, with a more detailed analysis of lifetime modelling of mechanical properties of biopolymers being given in Section 4.7.

#### **4.0 Hydrolytic biodegradation**

The processes involved in hydrolytic biodegradation are complex, in that the interactions of living organisms with susceptible (biodegradable) polymers such as polysaccharides, polyesters and their aliphatic and aromatic copolymers, and polyamides play a large role. Such polymers can be degraded through a variety of mechanisms (via photo, thermal, mechanical and chemical degradation), which can act alone or in combination, often synergistically [28]. It has, for example, been observed that the molecular weight of a custom made poly(*L*-lactic acid) (PLLA), with higher metal catalyst residue content than normal, decreased by more than half (from 431,000 to 202,000 g/mol) just upon storage in a desiccator at ambient temperature for an unspecified time [29]. However, as previously stated, the most important reaction that is associated with loss of mechanical properties in these polymers is hydrolysis of susceptible chemical bonds leading to chain scission and molecular weight decrease [8, 9, 30, 31].

The rate of this process is low when in air or water at neutral pH, and either acid, base or enzyme catalysis is required to achieve the rapid degradation in mechanical properties necessary for the first stage of degradation of biodegradable polymers (Fig. 1). Ester

hydrolysis, for example, can be either acid or base catalysed while poly(ortho esters) are resistant to basic pH but are hydrolysed more rapidly in the presence of acids [32]. The rate of hydrolytic degradation also depends on many other factors including the polymer chain length, crystallinity, molecular weight distribution, swellability, size, shape and geometry of polymer matrix, surface pretreatment, porosity, pore size and distribution, pore geometry, overall device dimensions, processing conditions, and water diffusivity in the polymer matrix [5, 26, 33, 34].

In making use of these biopolymers for tailored lifetime applications, and for understanding post-use degradation, it is important to understand the kinetics and mechanisms of polymer failure via hydrolytic degradation. In most studies of biodegradable polymers the primary focus has been on the time taken for mineralization, as indicated by evolution of carbon dioxide [25], rather than the time taken for the embrittlement of the polymers and the end of their useful lifetime as materials. Determination of this time to loss of mechanical integrity is of vital importance in biomedical polymers where the degradation must take place in the human body and the loss of mechanical strength may have to be synchronized with the growth of load-bearing tissue such as bone [9, 35]. The kinetic models developed for this process may also be applied to wider environmental degradation.

#### **4.1 Failure mechanisms in biodegradable materials**

The random scission of natural polymers and the determination of their scission rate constants were first described in 1930 by Kuhn [36]. Over recent years, there have been a number of more advanced models developed to predict the rate of hydrolytic degradation in biodegradable polymers, with a specific view to modelling the fate of materials intended for *in vivo* applications. The types of models range from empirical to phenomenological and deterministic to computational, with different computational models exploring different aspects of the chemistry utilizing molecular dynamics, cellular automata or Monte Carlo

modelling methods [37, 38]. Empirical models are those that build a relationship between degradation outcomes and experimental data (e.g., crosslink density, pH, temperature, etc.) through approaches such as regression or similar, such as in the discussion above. They provide little insight into the mechanisms of the process. By contrast, both the phenomenological and computational/probabilistic approaches are mechanistic. Phenomenological models are based on the transport models that govern reaction, diffusion, and dissolution and use deterministic equations. They are specific to a given system. Probabilistic models describe modifications to the polymer matrix (such as local polymer concentration or crystallinity) on a stochastic/probabilistic basis, typically using Monte Carlo simulations and cellular automata. There have been several reviews of the mathematical modelling of bio-erodible systems from the perspective of drug delivery [38-46]. Sackett and Narasimhan in particular [38] provided an excellent summary. The primary focus has been modelling changes in molecular weight on degradation, as opposed to modelling changes in mechanical properties and associated lifetime prediction (which will be dealt with in Section 4.7).

Central to an understanding of these hydrolytic degradation processes is an understanding of water fluxes in these systems. A common feature of both oxidative and hydrolytic degradation processes is that an increase in the degree of crystallinity lowers the rate of degradation. In hydrolytic degradation, this is because water is unable to penetrate readily into the highly ordered crystalline regions of polymers [47], and the sensitivity of mechanical properties to hydrolytic degradation thus depends on the structure and reactivity of the amorphous regions. The other factor that is important to retained mechanical properties is whether degradation occurs as a surface or a bulk process, which is controlled by the relative rates of the diffusion and hydrolysis in a given polymer (see Section 4.4). For both of these processes, an understanding of water flux in polymers is important.

## 4.2 Modelling water flux

According to Fick's law, the one-dimensional flux of water in a solid bounded by two parallel planes can be expressed as:

+

where  $[H_2O]_t$  is the concentration of the diffusing species (water) at time  $t$ ,  $D_1$ ,  $D_2$  and  $D_3$  are the diffusion coefficients of water in the polymer in the different directions, and  $x$ ,  $y$  and  $z$  are the distances of the diffusion in the  $x$ ,  $y$  and  $z$  directions. In the case of isotropic polymers, diffusion has no preferential direction and  $D_1 = D_2 = D_3 = D$ . Thus, for plane sheet geometry:

$$\frac{M_t}{M_\infty} = 1 - \frac{8}{\pi^2} \sum_{n=0}^{\infty} \frac{1}{(2n+1)^2} \exp \left[ -D \frac{(2n+1)^2 \pi^2}{L^2} t \right] \quad (5)$$

where  $M_\infty$  is the mass of water absorption at infinite time,  $M_t$  is the mass of water absorption at time  $t$ , and  $L$  is the thickness of the specimen [48]. When  $M_t/M_\infty$  is small enough ( $< 0.6$ ), i.e., in the early stages of the degradation process, equation (5) can be reduced to the Stefan's approximation:

$$\frac{M_t}{M_\infty} = \frac{4}{L} \left( \frac{Dt}{\pi} \right)^{1/2} \quad (6)$$

Restating equation (6) the time for water to diffuse ( $T_{diff}$ ) a mean distance  $\langle x \rangle$  can be estimated by applying random walk theory to the motion of water in a polymer [49]:

$$T_{diff} = \frac{\langle x \rangle^2 \pi}{4 D_{eff}} \quad (7)$$

where  $D_{eff}$  is the effective diffusion coefficient of water inside a polymer.

Other approaches to modelling water diffusion have also been taken, including the use of Finite Element Analysis [41]. However, all of these models ignore some of the factors that control uptake in typically complex matrix environments, such as the polymer's free volume, the physical state of the polymer, and the glass transition temperature (all of which can be influenced by the fabrication technique, as well as by polymer mobility and relaxation) [50]. The effect of molecular weight on water uptake is also unpredictable, based on the limited studies to date. Valenzuela et al. [50], for example, showed that annealing is necessary to obtain reproducible water uptake rates, which has implications for the prediction of polymer degradation rates more generally. Albertsson [51] showed that the first stage of degradation of poly(lactic acid) (PLA), as a typical hydrolytically degradable polymer, occurs in the amorphous regions. As discussed, this is because water penetrates through the disordered regions more readily, resulting in more rapid hydrolysis in the amorphous regions and thus more space between polymer chains, allowing the non-degraded chains to more readily reorient and to pack into more crystalline structures. And further, the increase in pore volume following degradation, as well as the increase in polymer mobility and the decrease in glass transition temperature ( $T_g$ ), all allow increased water uptake. Gautieri et al. [52] provided a detailed, atomistic molecular model of water diffusion for individual molecules during PLA degradation and showed that diffusivity is highly influenced by swelling, not degradation.

However, despite all this, hydrolytic degradation can be successfully modelled by assuming that the water concentration remains constant (see Section 4.5). It has been proposed that this is due to the existence of different water environments internally, with only a portion of the water, called the "bound water", being reactive [53]. It should be noted that the models at present do not take into account the water vapour to liquid transformation and associated calculations with respect to number of molecules required to coalesce before hydrolysis can begin.

### 4.3 Rate of hydrolysis – effect of chemical bond type

The kinetics of bond cleavage in the main polymer chain is dependent on the type of bond present. There have been many reviews on biodegradable polymers [25, 33, 34, 54-61], which describe the main classes of polymers and main chain bond types that fall into this category, whether bio-derived, synthetic or modified (Table 1). The relative rate of hydrolysis under non-catalysed conditions has been determined for a range of polymer types as well as for model compounds of low molecular weight. A summary of these main classes of hydrolysable bonds and the approximate half-lives in water at pH 7 and 25°C for the low molecular weight (methyl, ethyl) model compounds is given in Table 2 (adapted from [32, 62, 63]). However, the kinetics of these reactions can change vastly in the presence of catalysts or through the influence of neighbouring groups, such as through steric and electronic effects. For example, the hydrolysis rate of PLA is slower than that of other poly( $\alpha$ -hydroxy esters), at least in part due to the methyl group hindering the attack by water [32].

### 4.4 Bulk *versus* surface degradation

As noted previously, the relationship between the rate of water diffusion in a polymer and the kinetics of bond cleavage (hydrolysis) plays a critical role in the mechanism of degradation of biodegradable polymers (Table 2). Vieira [28] has summarised the three most common situations for erosion following hydrolysis as shown in Fig. 2 [9]. It should be noted that the term “degradation” in this case specifically refers to the polymer chain scission reaction, whereas “erosion” refers to the loss of polymer material as oligomers and monomers leave the polymer [40].

*Table 1*

*Table 2*

The complete erosion of a polymer takes substantially longer than the loss of tensile strength due to polymer chain scission, since, as outlined in Section 3.1, the loss of polymer strength occurs at  $M_e$ , at which point the polymer chain is still of significant molecular weight, well above that of oligomers and monomers.

**Surface eroding polymers** (Fig. 2) will decrease in thickness with a loss of material from the surface when the rate of hydrolysis exceeds the rate of diffusion of water into the bulk, or where the catalyst is unable to penetrate the bulk polymer (as with enzymes). In the former case, a higher rate of hydrolysis than diffusion can be due to hydrophobicity of the bulk polymer, a slow rate of water diffusion due to a high glass transition temperature or high crystallinity, and/or a very rapid hydrolysis rate [101]. The local water concentration can be determined from the diffusion coefficient and solubility of water in the polymer. In bulk eroding polymers, by contrast, the rate of diffusion of water exceeds the rate of the hydrolysis reaction. The simplest case of bulk erosion (Fig. 2) occurs when the rate of diffusion of the hydrolysis catalyst, particularly catalytic degradation products such as acidic oligomers, is also faster than the reaction rate. In this case, the degradation will occur uniformly through the thickness, with hydrolytic chain scissions (equation (2)) lowering  $M_n$  and thus the strength (equation (1), Section 3.1.1). The more complex situation, where bulk erosion occurs with autocatalysis leading to the formation of pores due to loss of the degraded material (Fig. 2), typically occurs only after extensive degradation, so will not control the loss of mechanical properties unless the pore reaches a critical size for the brittle cracking of material under a stress (which may be mechanically applied or result from swelling stresses). In this case, the accumulation of oligomers with acidic end groups that diffuse more slowly out of the polymer than water leads to higher local acidity internally, resulting in heterogeneous degradation [102, 103]. However, if the thickness of the polymer is sufficiently small and the degradation products diffuse rapidly, then autocatalysis is largely suppressed [104].



The polymers that tend to degrade through surface erosion include some polyanhydrides, some poly(ortho esters), and some polycarbonates [101], although fiber-forming polyanhydrides formed from aliphatic acids are susceptible to hydrolysis and thus bulk erosion. The erosion of poly(bis-(*p*-carboxyphenoxy)-methane) for instance is mostly via heterogeneous surface erosion. For such surface eroding polymers, the core of the polymeric article tends to retain its high molecular weight. Consequently, some material properties, such as modulus, remain relatively unchanged until late in the degradation process and other properties, such as load bearing capability, tend to decrease steadily as the thickness decreases.

### *Figure 2*

By contrast, bulk degradation is the dominant mechanism for polyesters such as PLA, poly(glycolic acid) (PGA), poly( $\epsilon$ -caprolactone) (PCL) and poly(butylene succinate) (PBS), as well as for polyamides, proteins, and cellulose and cellulose-derivatives such as starch and cellulose acetate [101]. The hydrolytic degradation of polyhydroxyalkanoates (PHAs) in water is also a bulk process, albeit a very slow one – although it tends to be regarded as a surface eroding polymer since that is its dominant mode of degradation under enzymatic hydrolysis [17].

Typically, during bulk erosion, a decrease in molecular weight of the polymer occurs before any mass-loss is observed. Most of the kinetic data and models, to date, relate to bulk eroding polymers. However, the situation even in relatively simple biodegradable polymers is often more complex than is typically modelled. In studies of poly( $\alpha$ -hydroxy acids) in aqueous media, for example, Li et al. [105-107] showed that the degradation of PLA was not only inhomogeneous, with a greater rate of degradation internally, but initially amorphous samples crystallised as degradation proceeded. It was also shown that amorphous samples retained

mechanical integrity for longer than semicrystalline samples, which was attributed to the sensitivity of the latter to stress and solvent micro-cracking.

Overall, it should also be noted that surface or bulk erosion modes are two extremes of the degradation process and the erosion of a polymer usually shows characteristics of both. The mathematical modelling of the transition between the two states is given in Section 4.6.

#### 4.5 Kinetics of hydrolysis in bulk eroding polymers

Hydrolysis is a very intricate process since a variety of different scission pathways can occur simultaneously [108]. Even though the reactivity of each bond might be equal, the effect of molecular weight and the inherent steric and crystalline environment, as well as chain branches and other factors such as local pH, may influence the rate of reaction at specific locations. Despite this complexity, some generalizations can still be made.

For instance, Lyu [16] has examined the kinetics of poly(lactic acid) (PLA) degradation and noted that there are four broad stages in the degradation of PLA copolymers implanted in the body. The first three of these stages are relevant for the total loss of mechanical properties (*i.e.*, decrease of  $M_n$  to  $M_e$ ), these being:

- (a) Water uptake controlled by the diffusion coefficient of water at the test temperature (which may be accompanied by polymer swelling);
- (b) Steady rate of hydrolysis controlled by the amount of water present;
- (c) Auto-acceleration of hydrolysis rate due to catalysis by increased number of acid chain ends, which could be identified with a critical value of  $M_n$ ; and
- (d) Evolution of water-soluble breakdown products with significant weight loss and eventual total dissolution.

These stages are characteristic of bulk eroding polymers, in general, both *in vivo* and in the broader environment. A schematic (Fig. 3) illustrates the general hydrolytic degradation processes in these polymers.

It has been shown that since the rate of water uptake is much faster than that of hydrolysis in bulk eroding polymers, such as PLA, then the kinetics of degradation are under chemical control [49, 107, 109] and the mechanisms of polyester hydrolysis in different media are relatively well understood [18].

### Figure 3

#### 4.5.1 Kinetics of Ester Hydrolysis

The simplest representation of the overall chemical reaction for ester hydrolysis in the presence of acid or base is:



The reverse esterification reaction is negligible. The detailed mechanisms for hydrolysis of aliphatic polyesters have been described [18] and aim to rationalise the empirical relationships for the rate of loss of ester groups, where the concentration of these ester groups is given by  $[E]$ . In the absence of diffusion control (*i.e.*, in thin samples), the rate of in-chain hydrolysis giving random chain scissions,  $s$ , is given by:

$$-\frac{d[E]}{dt} = \lambda[\text{H}^+][E][\text{H}_2\text{O}] = \frac{d[\text{COOH}]}{dt} = ds/dt \quad (9)$$

where each chain scission to lose an ester results in a carboxylic acid end group,  $-\text{RCOOH}$  [110], and  $\lambda$  is the rate constant for the hydrolysis reaction. In the early stage of hydrolysis where  $[E]$  and  $[\text{H}_2\text{O}]$  are constant and in the absence of added acid, the catalyst is provided

by the carboxylic acid chain ends so the system is self-catalysing and the rate of growth of chain end groups is:

$$\frac{d[COOH]}{dt} = \lambda' [COOH] \quad (10)$$

Solving this first order equation and noting the initial carboxyl end group concentration:

$$[COOH]_0 = 1/\bar{M}_{n0} \quad (11)$$

then the value  $M_{n0}$  after hydrolysis for time  $t$  is:

$$\bar{M}_n = \bar{M}_{n0} \cdot e^{-\lambda t} \quad (12)$$

It should be noted that:

$$s = \frac{\bar{M}_{n(0)}}{\bar{M}_{n(t)}} - 1 = e^{\lambda' t} - 1 \quad (13)$$

Lyu et al. [16] suggested a modification of these kinetic equations to account for the slower rates of early stage degradation. They suggested that there was a transition from a reaction without autocatalysis to one made much faster by the presence of acidic end groups following chain cleavage. In addition, rather than being dependent on the concentration of COOH end groups, the hydrolysis rate may be proportional to the dissociated hydrogen ion:

$$[H^+] = (K_{COOH}[COOH])^{1/2} \quad (14)$$

where  $K_{COOH}$  is the dissociation constant for the acid end groups. Combining equations (9) and (14) gives:

$$\frac{d[E]}{dt} = \lambda [H_2O][E]([COOH]K)^{1/2} \quad (15)$$

Siparsky et al. [111] found, from studies of PLA, PLA-co-PCL and PLA-poly(ethylene glycol) blends, that this equation matched the data well, although the analysis was carried out in solution rather than solid state, making it more likely that the acid groups could dissociate. PCL was not found to be self-catalysed under these conditions. Using the relationship in equation (12), an alternative kinetic equation was derived by Lyu et al. [16, 101]:

$$\left(\frac{1}{\bar{M}_n}\right)^{1/2} = \left(\frac{1}{\bar{M}_{n(0)}}\right)^{1/2} + \frac{1}{2}\lambda_{2.5}(K[E])^{1/2}[H_2O]t \quad (16)$$

where  $\lambda_{2.5}$  is the reaction rate constant, where the subscript 2.5 reflects the kinetic order for this mechanism. Expressing this in terms of  $s$ , the number of scissions per number average chain, given that  $s + 1 = M_{n0}/M_n$  (rewriting equation (13)):

$$s = \left(1 + \frac{1}{2}\lambda_{2.5}(\lambda[E]\bar{M}_{n0})^{1/2}[H_2O]t\right)^2 - 1 \quad (17)$$

Again assuming that  $[E]$  and  $[H_2O]$  are constant in the early stage of hydrolysis and in the absence of added acid, this equation collapses to:

$$s = 2\lambda''t + (\lambda''t)^2 \quad (18)$$

where  $\lambda'' = (1/2)\lambda_{2.5}(\lambda[E]M_{n0})^{1/2}[H_2O]$ ; this implies an exponential increase in number of chain scissions over time through the early stages of the hydrolysis reaction. However, neither equations (12) nor (15) alone were adequately able to replicate the observed experimental results.

Martens et al. [112] also took this approach recently in modelling the degradation of the glucosaminoglycan, hyaluronan, assuming a random chain scission process, as follows:

$$\frac{1}{\bar{M}_{nt}} - \frac{1}{\bar{M}_{n0}} = \frac{\lambda t}{m} = \lambda' t \quad (19)$$

where  $\lambda$  is the rate constant and  $m$  is the molecular mass of a repeat unit. Unlike equations 9 to 16 above, the underlying rate equation ignores water and acid concentration effects. Rate constants were determined from experimental data and there was good agreement between experimental and simulated results, indicating that acid hydrolysis of hyaluronan can be considered a random scission process.

Equation (19) can be rewritten, taking equation (2) into account, as:

$$s = \frac{M_{no}}{m} \lambda t = \overline{DP}_0 \lambda t \quad (20)$$

In a related approach, Charlier et al. [113] investigated drug release from thin poly(*D,L*-lactide-*co*-glycolide) (PLGA) films, adopting an empirical approach by assuming a first order degradation kinetic but modifying the equations to include a time dependent term for the diffusion coefficients (to take into account polymer degradation and erosion). While there was a good fit to the experimental data, this model was only applicable for thin films, not other geometries.

However, the broad applicability of these solutions for lifetime prediction is very limited due to the fact that many simplifying assumptions are necessary for the analytical treatment of the problem.

More recently, much more complex models have been developed, taking a range of approaches to try to develop a robust fit that can have predictive capability. Overall, the approaches to modelling of the degradation of biodegradable polymers can be broadly classed as empirical, probabilistic or phenomenological [38].

One of the earliest approaches to the modelling of polymer hydrolysis employed combinatorial statistics to derive analytical solutions to the evolution of molecular weight distribution. This approach assumed that bond scission could be described with a known probability density function (e.g., equiprobable random scission, central Gaussian, or parabolic) [36].

Another approach that has been adopted is to develop a system of differential equations that describe the depolymerization rates of individual bonds and then to integrate them to give the time evolution of the molecular weight distribution [114]. However, this requires a substantial set of equations to completely describe even a simple polymeric system, so approximations need to be made.

To this effect, Chen et al. [115] developed a hybrid mathematical model that combined stochastic (probabilistic) hydrolysis and diffusion-controlled autocatalysis to simulate polymer degradation and erosion. They considered three states – hydrolysable, hydrolysed and void. Equation (9) was used for ester hydrolysis, with the degradation process modelled as a stochastic event using a first order Erlang process in which the probability density function  $p$  that defines the probability of hydrolysis of a single hydrolysable element can be calculated as:

$$p(\lambda, t) = \lambda e^{-\lambda t} \quad (21)$$

where  $\lambda$  is the degradation rate constant, which can be determined from experimental data by linear regression. A hysteretic delay was imposed to account for the gradual transition from solid polymer to porous degraded material. This led to the following hybrid degradation model:

$$P_A = P_F + P_C = P_F + \beta (e^{C_m} - 1) P_F = \frac{\lambda_0 e^{-\lambda_0 t} (1 + \beta (e^{C_m} - 1))}{V_0 V_t} \quad (22)$$

where  $P_A$  is the accelerated probability density function;  $P_F$  and  $P_C$  are the contributions due to fundamental hydrolysis and autocatalysis, respectively;  $\beta$  is a constant introduced to regulate the contribution of autocatalysis;  $C_m$  is the time dependent concentration of hydrolysed monomers;  $\lambda_0$  is the degradation rate constant at time zero;  $V_t$  is the volume fraction of polymer matrix at time  $t$ ; and  $V_0$  is the initial volume fraction of the polymer matrix. An illustration of the effect of matrix thickness on the degradation process (both matrix morphology and acid catalyst concentrations) based on this model is given in Fig. 4. Overall, it was found that the architecture and thickness of the sample played a significant role in the degradation kinetics. The thicker the film, the higher the internal acid concentration and thus the higher the rate of pore formation and molecular weight loss. However, this modelling approach did not consider variability in the kinetics of the hydrolysis reactions and chain scission and did not allow for a prediction of molecular weight distribution. Also, the diffusive parameters were estimated and could not be readily measured experimentally for verification.

#### 4.5.2 Mechanistic (numerical) modelling

The use of molecular modelling, where polymer chains are modelled atom by atom, is also limited in its applicability. Such simulations can assess disrupted bonds and the influence of thermodynamic enthalpy on product formation, but give less insight into kinetic processes. Most simulations deal with bond breakage as a sub-nanosecond event occurring at the molecular level. The correlation to polymer degradation that occurs over weeks or months may therefore not be clear-cut. However, Karst and Yang [116] used this approach to rank relative degradation rates in PLLA/poly(*D*-lactic acid) (PDLA) polymer blends by comparing the states of polymer chains before and after an artificially introduced cleavage event and calculating the change in potential energy. The 50/50 blend was found to have the greatest



resistance to hydrolysis, due to its having stronger hydrogen-bonding and dipole–dipole interactions than pure PLLA or PDLA.

**Figure 4**

Peralé et al. [117] adopted a mechanistic approach to the modelling of polymer degradation through hydrolysis, using a population balance model that provided a detailed description of hydrolysis kinetics, as opposed to some of the more lumped models previously described. In this case, it was assumed that water molecules could break an ( $m$  unit)-long polymer chain at various sites, leading to an ( $n$  unit)-long and an ( $m-n$  unit)-long polymer chain, where the  $n$ -long oligomer could in principle diffuse out of the polymer matrix, according to the following equation:

$$\frac{\partial([P_n])}{\partial t} = R_n + D_n \nabla^2 [P_n] \quad (23)$$

where  $P_n$  is the  $n$ -long polymer chain,  $[P_n]$  is the molar concentration,  $R_n$  is the molar rate of formation by the collection of degradation chemical reactions, and  $D_n$  is its effective diffusion coefficient through the polymer matrix. The degradation kinetics can then be written as:

$$R_n = k_p \left\{ \sum_{j=1}^{n-1} [P_j] [P_{n-j}] - 2[P_n] \sum_{j=1}^{\infty} [P_j] \right\} + \frac{k_p}{K_{EQ}} \left\{ 2[H_2O] \sum_{j=n+1}^{\infty} [P_j] - [H_2O](n - 1) [P_n] \right\} \quad (24)$$

where  $k_p$  and  $K_{EQ}$  are the depolymerization rate constant and the thermodynamic equilibrium constant for the polymer chain hydrolysis respectively. For polyesters, the second term is the dominant one. To make the calculations tractable, a moments model describing the evolution in time and space of its first three statistical moments, representing the number of polymer

chains, their overall length and their dispersion, was adopted. A reasonable comparison between predicted and actual molecular weight over time for the degradation of PCL filaments was obtained. However, this model ignored many of the inhomogeneities in the material structure, in particular the effect of the crystalline phase in the matrix.

A mixed modelling approach was employed by Soares and Zunino [118] for a stent coating, i.e., effectively a one-sided film. In this multiscale study, the hydrolytic degradation of polymer chains was modelled at the molecular level and the diffusion of water and also reaction products was modelled at the bulk level according to Fick's laws. The numerical solution was, in this case, made tractable by the use of a finite element approach, where a limited number of polymer constituents were defined, each accounting for chains of an average size. The Thiele modulus,  $\Lambda$ , a non-dimensional number that relates time scales of reaction and diffusion, was defined as follows:

$$\Lambda = \frac{D^\infty}{L^2 \lambda \rho_W^\infty} \quad (25)$$

where  $\rho_W^\infty$  is water density,  $\lambda$  is the hydrolysis rate constant,  $L$  is the coating thickness and  $D^\infty$  is the diffusivity of water into an intact, dry polymer.  $\Lambda$  is the dominant parameter controlling the mode of erosion in this system, with a high  $\Lambda$  associated with bulk erosion and a low  $\Lambda$  with surface erosion. In effect this is a restatement of the condition summarised in Fig. 2: for  $D^\infty \gg k$ , the polymer degrades via bulk erosion, and for  $D^\infty$  is  $\ll k$ , the polymer degrades via surface erosion. A limitation is that the model does require as inputs the diffusion coefficients of water and each polymer subfraction. These authors noted that mass loss occurs earlier in samples with higher polydispersity.

Antheunis et al. used a diffusion-reaction model similar to that of Thombre et al. ([119], see Section 4.6) to characterise autocatalytic behavior in a range of aliphatic polyesters [120, 121], assuming constant mass and volume and a uniform molecular weight. The model was calculated using the number average, as opposed to the weight average molecular weight, with the following expression being derived for amorphous polymers:

$$\bar{M}_{nt} = \left( \frac{[COOH]_0}{\rho} \frac{e^{c_1 t} - 1}{1 + c_2 e^{c_1 t}} + \frac{1}{M_{n0}} \right)^{-1} \quad (26)$$

where  $[COOH]_0$  is the initial acid concentration,  $\rho$  is the polymer density,  $c_1$  is a constant of integration that accounts for the hydrolysis rate and crystallinity, and  $c_2$  is a constant of integration that is a ratio  $c_2$  between the initial concentrations of acids and ester bonds ( $c_2 = [COOH]_0/[E]_0$ ). This model was expanded for semi-crystalline polymers and copolymers by making a number of assumptions, including that the ratio between the different specific types of ester bonds remains constant through the reaction (since each has its own hydrolysis rate) and that only the ester bonds in the amorphous phase can be hydrolysed (due to the inability of water to penetrate the crystalline region), to give the following expression for  $c_1$  in Equation (26):

$$c_1 = ([E]_0 + [COOH]_0) \varphi_A \left( \sum_{i=1}^m x_{e_i} k_{e_i} \right) \quad (27)$$

where  $\varphi_A$  is the concentration of the ester bonds in the amorphous fraction,  $x_{e_i}$  is the molar fraction of each corresponding type of ester bond ( $E_i$ ) and  $k_{e_i}$  is the rate constant for hydrolysis of that ester bond. This model accurately predicted an initial sigmoidal decrease in  $M_n$  for PLA and PLGA in the initial period before mass loss. One limitation of this approach is that it does not take into account partial dissociation of the acid groups and that the

assumptions, particularly that of constant ratio of ester bond types, are unlikely to hold for extended periods.

Pan and coworkers, in a series of studies, have developed increasingly sophisticated derivations of models of polyester cleavage using classical theory, starting with an initial phenomenological model [122] in which biodegradation was modelled using a set of simplified reaction-diffusion equations in order to predict the effect of size and shape of a device on its degradation rate. This model took into account autocatalysed or non-catalysed hydrolysis or a combination of hydrolysis and monomer diffusion. It was extended to take into account the effect of polymer recrystallization following chain scission [123] by including modified equations based on Avrami's theory of crystallization. This was undertaken because the changing crystallinity that occurs during degradation affects both the degradation rate and mechanical properties of the material or device. The initial equations which were developed were then simplified [31, 124] and adjusted in order to relate the observed degradation trend in experimental data to different underlying mechanisms, including non-catalytic and auto-catalytic end-chain scission (in which only ester bonds at the end of polymer chains are cleaved) and non-catalytic and auto-catalytic random cleavage, where any ester bond can be cleaved. In summary, these authors developed an equation that allows the number average molecular weight  $M_n$  to be calculated as:

$$\bar{M}_n = \frac{(\varphi_A + \omega X_c)m}{N_{chain}} \quad (28)$$

where

$$N_{chain} = N_{chain0} + \left( R_s - \left( \frac{c_{ol}}{X} \right) \right) \quad (29)$$

and  $\varphi_A$  is the concentration of ester bonds in the amorphous chains (mol/L),  $\omega$  is the inverse molar volume of the crystalline phase, set at 17,300 mol/L,  $X_c$  is the degree of crystallinity,  $m$  (g mol<sup>-1</sup>) is the molar mass of each repeat unit,  $M_{chain}$  (mol/L) is the molar concentration of polymer chains, with  $M_{chain0}$  being the initial molar concentration of polymer chains,  $R_s$  (mol/L) the molar number of scissions per unit volume, and  $c_{ol}$  (mol/L) the molar concentration of ester bonds in the oligomers, respectively, and  $x$  is the average number of repeating units of the oligomers (set at 4). The term at the top of Equation (28) is the total weight of the crystalline and amorphous phases excluding oligomers (on the assumption that oligomers are too small to be measured experimentally). In this model, the rate of polymer chain scission due to hydrolysis is given by:

$$\frac{dR_s}{dt} = \lambda_1 c_e + \lambda_2 c_e \left( \frac{c_{ol}}{1 - X_c} \right)^{0.5} \quad (30)$$

where  $\lambda_1$  (day<sup>-1</sup>) and  $\lambda_2$  ([mol<sup>-1</sup>m<sup>3</sup>]<sup>0.5</sup>day<sup>-1</sup>) are the reaction constants for the non-catalytic and auto-catalytic hydrolysis reactions respectively.

In an extension/simplification of this work, Heljak et al. [125] developed a model to simulate the degradation of bulk-erosive polymers under different conditions of static medium as opposed to a medium that is flowing through the scaffold pores. This model assumed that the polymer bulk was instantly saturated with water, thus eliminating a water diffusion term from the equation, and assumed an autocatalytic mechanism, giving:

$$\bar{D}_{medium} = \frac{D_{medium}}{[E]_0^n k_2 L^2} \quad (31)$$

$$\begin{cases} \frac{\partial \bar{c}_m}{\partial \bar{t}} = \bar{k}_1 [\bar{E}] + \bar{k}_1 \bar{c}_m^n + \text{div}_{\bar{x}_i} \left\{ \bar{D} \text{grad}_{\bar{x}_i} (\bar{c}_m) \right\} & \text{for } \bar{x}_i \in \Omega_{polymer} \\ \frac{\partial \bar{c}_m}{\partial \bar{t}} = \text{div}_{\bar{x}_i} \left\{ \bar{D}_{medium} \text{grad}_{\bar{x}_i} (\bar{c}_m) \right\} & \text{for } \bar{x}_i \in \Omega_{medium} \end{cases} \quad (32)$$

where  $\bar{D}_{medium}$  is the nondimensional form of  $D_{medium}$ , which is the diffusion coefficient of the monomers produced following hydrolysis in the hydrolysis medium;  $[E]_0$  is the initial ester bond concentration; the power  $n$  accounts for the dissociation of the acidic end groups;  $k_1$  and  $k_2$  are phenomenological rate constants;  $L$  is the characteristic length of the object being subjected to degradation;  $c_m$  is the time dependent concentration of hydrolysed monomers, which could also be treated as the concentration of the degradation products and

$$\bar{c}_m = \frac{c_m}{[E]_0}; \quad \bar{k}_1 = \frac{k_1}{[E]_0^n}; \quad \bar{t} = k_2[E]_0^n; \quad \bar{x}_i = \frac{x_i}{L},$$

where  $x_i$  is the monomer concentration at a given location;  $\text{div}_{\bar{x}_i}$  and  $\text{grad}_{\bar{x}_i}$  are divergence and gradient respectively; and

$$\bar{D} = \frac{D_0}{[E]_0^n k_2 L^2} \left[ 1 + \alpha \left( 1 - \frac{c_m + [E]}{[E]_0} \right) \right] \quad (33)$$

Overall, then, the degradation process was modelled using the non-dimensional form of a series of reaction-diffusion equations, that were solved using a standard Euler scheme, with the equations being integrated using a finite element method at each time step. This gave a good fit to the degradation data presented by Agrawal et al. [126], who used both static and flow conditions. The model had a number of explicit limitations: it did not take into account the changing sample porosity with degradation, and changes of geometry could not be accommodated. It was also not possible to calculate the molecular weight distribution at successive stages.

Zhao et al. [127] adopted a mechanistic approach to modelling of degradation, accounting at the same time for changes in the effective diffusivity by modelling hindered diffusion and pore formation and growth over time. It was proposed that the rate at which soluble monomers and oligomers were formed was proportional to the rate of growth of average pore size. This model was an improved version of the earlier empirical relationships between

erosion rate and pore growth proposed by Batycky et al. [128] and Lemaire et al. [129]. Arosio and co-workers also developed mechanistic models based on a shrinking core (with polymer eroding from the centre out) and pseudo-first order degradation to describe a bulk eroding polymer in cylinder form. The production of oligomers and monomers was modelled and an equilibrium between hydrolysis and condensation (polymerization) reactions was included, although autocatalysis was not [130]. The model did not fit well to published data, presumably because of the oversimplicity of the assumptions.

Nishida et al. [131] used a statistical moments approach to solve for:

$$\frac{d[P]}{dt} = \lambda_h (\sum_{n=1}^{\infty} n [fP_n] - \sum_{n=1}^{\infty} [fP_n]) [H_2O] [COOH] \quad (34)$$

where  $fP_n$  is a fraction with degree of polymerization  $n$ ,  $[P] = \sum_{n=1}^{\infty} [fP_n]$ , assuming that  $[H_2O] \gg [COOH]$  throughout the hydrolysis reaction, and  $\lambda_h$  is the rate constant of hydrolysis of each step. Approximations for the polymer polydispersity, the average degree of polymerization, and the weight-average molecular weight were determined as a function of time, with reasonable fit.

Casalini et al. [132] also used a mass conservation and statistical moment-based approach to the derivation of equations for polymer degradation from first principles, in the modelling of the degradation of PLGA microparticles. The assumption was that only water and oligomers up to nonamers can diffuse inside the polymer. Autocatalysis was taken into account, as was the change in diffusivity over time as the hydrolysis proceeded. However, a limitation is that a single rate constant for polymer degradation (which was fitted from experimental data) was used for each system modelled.

### 4.5.3 Stochastic modelling

A number of studies have taken a Monte Carlo propagation approach to the modelling of random chain scission processes in bulk eroding polymers. In this approach, a virtual grid for the polymer matrix is established and a lifetime is assigned to each element (or pixel) within that grid. The probability of erosion of each element is then calculated using Monte Carlo methods. Guaita et al. [133] adopted this approach to investigate the key parameters that would help with elucidating differences in degradation mechanisms when volatilization was excluded. It was assumed that polymer fragments would interact with each other, but chain branching was not taken into consideration. These authors found that for completely random chain scission, the polydispersity index should trend to 2, regardless of any chain recombinations, which is in line with a typical Kuhn distribution [36]. The same was observed by Nishida et al. [131]. In non-random scissions, a different trend would be observed. In other early work, Emsley and Heywood [134] also took a Monte Carlo approach, in this case comparing the effect of bond cleavage at randomly determined points as opposed to specific systematic bond cleavage, such as by breaking the molecule in half or slicing off a fixed number or percentage of units. They found that non-random processes were needed in order to see a shift in molecular weight distribution.

Siepmann and coworkers in turn coupled a Monte Carlo approach for simulating polymer erosion to classic equations for mass transport for a sphere. As an example of how this approach was used to simulate monomer release from a poly(anhydride) matrix, their initial model assigned pixels within a 2-D matrix to be either crystalline or amorphous regions (Fig. 5) [39]. The crystalline polymer pixels were assigned a longer average lifetimes compared to amorphous pixels. As the solvent front moves from right to left within the grid, the resultant porosity,  $\epsilon$ , of the matrix can be calculated. As the number of eroded pixels increases across a



row, so does the overall porosity in that part of the device, which also then decreases the time to overall mechanical failure.

### *Figure 5*

In an expansion of this initial work, a 3-D model was developed [39, 135-137] in which each pixel had the same volume in the total sphere, although with varying widths in the two-dimensional cross-sections, and was assigned to be either polymer or drug. Each of these pixel rings that represents non-degraded polymer was assumed to have an equal probability of eroding on coming into contact with incoming water, with a lifetime expectancy ( $t_{LT}$ ) being given by:

$$t_{LT} = t_{AV} + \frac{(-1)^z}{\lambda} \ln \left( 1 - \frac{z}{100} \right) \quad (35)$$

where  $t_{AV}$  is the average lifetime of the pixel rings,  $\lambda$  is a constant specific to the polymer, and  $z$  is a random integer between 0 and 99.

Overall, the concept is that the erosion of any given pixel is a random event, which can be described by a Poisson first order process, with amorphous pixels having shorter lifetimes than crystalline ones. This model was successfully fitted to experimental data regarding drug release in buffer, but was still an oversimplification, failing to take into account variability in polymer crystallinity, for example, as well as autocatalysis.

Other authors have similarly used a Monte Carlo approach to simulate the effect of pH on porosity [103] and molecular weight distributions [138]. Of note is that of Mohammadi and Jabbari [103] who found that, in line with expectation, the higher the porosity of the scaffold (in this case, PLA), the higher was the modelled rate of mass loss in the bulk; all porosities showed a lag time of at least 7 weeks for both surface and bulk elements. Bose et al. [138]

also employed a semi-iterative algebraic exact statistical formulation method that gave a reasonable approximation of experimental data.

By contrast, Gleadall and Pan used a Monte Carlo approach to simulate molecular weight distributions for a PDLA at different times of degradation. They adjusted the kinetics by applying a scission rate, with the model results being successfully compared with experimental data from an earlier publication [139]. Random scissions were found to have over 1000 times greater impact on molecular weight reduction than end scissions, which were able to produce a significant fraction of water-soluble chains with little or no effect on  $M_n$ . For the degradation of poly(lactic acid) by random scission, it was found that  $M_n$  must reduce to  $< 5,000$  g/mol in order for a polymer to exhibit significant mass loss due to the diffusion of water-soluble short chains. Other authors have set this critical  $M_n$  value for PLA at around 10,000 g/mol [140], or 4,000 g/mol [141] – the latter value being at, or lower than, the molecular entanglement value  $M_e$  for PLA, hence the mechanical properties would be lost by this stage.

Lin et al. [142] simulated the effect of PLA molecular weight on chain scission, comparing random, central and chain-end scission. They compared amorphous and crystalline PLLA and introduced a parameter called the *molecular weight reaction index*,  $R_{ind}$ , which was used to define the reaction rate to be proportional to the molecular weight to the  $R$ -th power. They found that the molecular weight reaction index was equal to 0.4 in amorphous polymer, and remained constant, while for the crystalline material it changed through time, decreasing from 1.0 (at the highest molecular weight) to 0.7.

Another method that has been adopted for the modelling of bulk polymer degradation is a cellular automaton approach, which is a discrete dynamic modelling approach, similar to and extended from the Monte Carlo process, based on a virtual matrix defined in a cubic space, with a number of states being modelled (such as polymer, solvent, porosity, solid drug or

drug in its solubilised form) [143-145]. The life expectancy of a polymer cell (its probability of being eroded) changes as the number of direct neighbour cells containing solvent changes. This approach has been found to be a reasonable match to experimental data except when degradation is associated with surface erosion and bulk detachment.

#### 4.5.4 Experimental studies

Of note experimentally is the slow deacetylation of cellulose acetate film through hydrolysis of the ester chains to produce acetic acid. Film conservators have previously developed the concept of a critical or autocatalytic point for the concentration of this by-product acid that accumulates in archived materials over time. When the  $[H_3O^+]$  reaches  $5 \times 10^{-5}$  mol/L, the apparent rate of deterioration of film increases dramatically. While providing a practical limit for conservators, Knight [146] recently reviewed the evidence for such an autocatalytic point and found that the reaction is, in fact, autocatalytic at all values of hydrogen ion concentration, in line with the discussion above.

It should also be noted that more sophisticated approaches to the prediction of micro-environment pH in biodegradable films have also been published [147] that can be adapted for future models. Overall, therefore, there are a number of sophisticated stochastic and other models in the literature describing the hydrolysis of biodegradable polymers. However, erosion modelling is still not an ideal process given the need to choose the mode of degradation up front, the need to model different rates for different phases, the complexity of taking product fluxes into account in an environment of changing pore sizes and crystallinities, and the changes in microstructure and morphology with time and increased erosion. Some studies are seeking to address these issues by monitoring degradation progress in much more detail.

Schusser et al. [148], for example, presented a new method for characterizing the degradation of thin PLA films, based on a capacitance-voltage approach, measuring the polymer-covered electrolyte-insulator-semiconductor (EIS) sensors, enabling *in situ* monitoring of the process through monitoring increases in the accumulation capacitance as a result of both increases in the water content within the polymer matrix but more significantly due to thinning and/or decomposition of the polymer layer. Likewise Keller et al. [149] presented a microcantilever-based sensor for monitoring enzymatic degradation. Measurements of the resonance frequency allowed the calculation of the Young's modulus of both the uncoated cantilever and the coating material, with erosion of the biopolymer coating on the cantilever resulting in a shift of the resonance frequency towards the reference value measured for the uncoated device. Both of these techniques, while requiring specialised equipment, do give immediate feedback on the progress of degradation.

#### **4.6 Kinetics of hydrolysis in surface eroding polymers**

As for the bulk erodible polymers, the rate of degradation of surface eroding polymers depends on many factors, both environmental and material related. Regarding the polymeric matrix, factors such as polymer chain length, swellability, the reactivity of functional groups, polymer morphology and chain structure/composition, crystallinity and water diffusivity all play a role. In modelling the kinetics of degradation, there have again been a number of approaches, which were reviewed from the perspective of drug release by Göpferich and coworkers [39, 91]. The chemistry of ester hydrolysis will be the same as described in Section 4.5.1.

Empirical models of erosion take an approach of describing simply the observed kinetics of a system, without relating these to underlying mechanisms. In the case of surface eroding polymers, it is assumed that the degradation rates are related to the surface area and that there

is a shape factor to be taken into account [39]. Hopfenburg [150] derived a general equation for surface erosion of biodegradable polymers, assuming a linear moving erosion front:

$$\frac{Mass_t}{Mass_\infty} = 1 - \left(1 - \frac{\lambda t}{c_0 r}\right)^n \quad (36)$$

where  $Mass_t$  and  $Mass_\infty$  are the polymer mass at time  $t$  and at infinite time, respectively,  $c_0$  is a polymer concentration,  $\lambda$  is a rate constant,  $r$  is the radius of a cylinder or sphere or the half-thickness of a slab and  $n$  is in this case a “shape factor”, where  $n$  is 1, 2, or 3 for slabs, cylinders or spheres, respectively. This approach only considered heterogeneous erosion. Cooney extended this model [151] by assuming that there was an additional stage of release of the degradation products through an adjacent stationary solvent phase and applied the dissolution model to a number of different geometries. This led to the following equation for cylindrical polymer matrices, for example, with an initial length  $L_0$  and an initial diameter  $Dia_0$ :

$$f = \frac{(Dia_0 - 2\lambda t)^2 + 2(Dia_0 - 2\lambda t)(L_0 - 2\lambda t)}{Dia_0^2 + 2Dia_0 L_0} \quad (37)$$

where  $f$  is the fractional dissolution at time  $t$  and  $\lambda$  is a rate constant. Again, however, this is an over-simplistic model for a complex process [152].

Thombre and Himmelstein [119] proposed a diffusion-reaction model for poly(ortho ester) erosion based on a series of partial differential equations. This model was applied to surface erosion, using the concept of an erosion front that follows the water diffusion front through the polymer matrix. In this case, the polymer was treated as a slab, with simultaneous modelling of the reactions within the polymer as well as diffusive transport using an unsteady-state mass equilibrium. This approach was also applied by Larobina et al. [153] and Kipper and Narasimhan [154] to some surface eroding poly(anhydride) copolymers. This

latter work took into account the microstructure and phase behavior of such copolymer systems by modelling four fractions: the crystalline and amorphous regions of either a fast degrading or slow degrading phase of the polymer matrix. In doing this, the underlying assumption was that the amorphous regions would degrade more rapidly than the crystalline. Polymer degradation was assumed to be a first-order process dependent on the polymer type but not chain length. The changes in polymer pore size and porosity were also accounted for. However, while such models provide a description of the likely events and kinetics at a microscopic scale, model validation is difficult since molecular level measurements are not available, and overall such frameworks by necessity represent a much-simplified version of a complex matrix.

In another approach, mechanistic mathematical models have been used. Such models are based on the description of the real physical processes and include non-Monte Carlo-based and Monte Carlo-based models. Zygourakis developed a Monte Carlo approach to the modelling of degradation in surface eroding polymers [155, 156]. In this approach, a rectangular grid with  $n_x$  by  $n_y$  grid points was established, with each square or pixel in the grid being randomly assigned as drug, polymer or filler initially. The lifetime of a specific solid could be constant for all pixels of this type, or distributed according to some distribution (e.g., Poisson distribution). Degradation on any grid point was only initiated after contact with an eroded neighbour. The degree of degradation could then be estimated by the relative mass of non-eroded polymer pixels. These simulations helped explain the lack of significant mass loss in the early stages and the significance of percolation in the degradation and erosion of these polymers.

Göpferich et al. [157, 158] also took a similar Monte Carlo approach to modelling of polyanhydride degradation, assigning grid points as amorphous or crystalline (Fig. 6). The life expectation was a random variable, distributed according to a first order Erlang

distribution and being slower for crystalline regions. Other factors such as the diffusion of monomers, the crystallization of polymer degradation products, and microclimate pH effects were taken into account. These approaches matched moderately well with experimental data.

Yu et al. [144] proposed a three-dimensional extension of these probabilistic models to fit with more complex geometries. In this case, the cells (pixels) were considered to either be drug, solvent, or polymer, based on probability. Those pixels assigned as polymer cells were also assigned to be either in the crystalline or amorphous state, again based on probability, with the model thus taking account of the slower degradation of the crystalline phase.

### *Figure 6*

Rothstein et al. [141] developed a model that accounted for both surface and bulk erosion in a single model, taking into account the critical length, i.e., the polymer thickness at the point where the process makes the transition from surface to bulk degradation (Table 3). A diffusion-reaction relationship was established, based on the time-dependent water concentration profile, calculated using the diffusivity of water in the polymer matrix (taken as  $10^{-12}$  m<sup>2</sup>/s for a broad array of polymers). A degradation rate constant for the polymer bond hydrolysis was fixed, using a second order form of Equation (12), with water concentration explicitly included as opposed to being assumed constant (see Equation (50) in section 4.7). These time-dependent hydration kinetics were coupled with time- and space-dependent descriptions of matrix porosity, which explicitly took variation in matrix crystallinity into account. Overall, this lumped model fitted well to previously published experimental data for a range of bulk- and surface-eroding polymeric systems.

More recently, investigators have begun to model the hydrolysis of cross-linked biodegradable polymers, such as cross-linked polyanhydrides, which were also predicted to degrade via a surface eroding mechanism [159]. These molecules have a long induction

period of water uptake relative to their degradation rate. It was proposed that the most likely explanation for this effect was that since the network is eroded by hydrolysis, then only a fraction of the water in the voids can react with the surface of the surrounding matrix.

In a more general approach, von Burkersroda et al. [49] developed a theoretical (phenomenological) model to predict the erosion mechanism of surface eroding biodegradable polymer matrices and the critical thickness at which the transition from surface to bulk degradation occurs, deriving a measure for the velocity of degradation  $E(t_n)$  (which is equivalent to  $\frac{d[E]}{dt}$ ), as given by:

$$E(t_n) = \frac{1}{\lambda} \left( \ln \langle x \rangle - \ln \left[ \frac{\varepsilon \sqrt{\frac{M_n}{N_A(DP-1)\rho}}}{\sqrt{N_A(DP-1)\rho}} \right] \right) \quad (38)$$

where  $\lambda$  is a rate constant that accounts for the differences in the reactivity of polymer functional groups; it is equivalent to a first-order rate constant and is directly related to the half-life of a polymer bond.  $DP$  is the average degree of polymerization,  $N_A$  is Avogadro's number,  $\langle x \rangle$  is a mean distance, and  $\rho$  is the density of the polymer. An erosion number  $\varepsilon_t$  may be defined as follows, based on Equation (7):

$$\varepsilon_t = \frac{\langle x \rangle^2 \lambda \pi}{4D_{eff} \left( \ln \langle x \rangle - \ln \left[ \frac{\varepsilon \sqrt{\frac{M_n}{N_A(N-1)\rho}}}{\sqrt{N_A(N-1)\rho}} \right] \right)} \quad (39)$$

where  $\varepsilon_t$  is the ratio of both processes and indicates the mode of erosion, such that if  $\varepsilon_t < 1$  then the process of degradation is occurring in the bulk, and  $D_{eff}$  is the effective diffusion coefficient of water inside a polymer. However, if  $\varepsilon > 1$  then the mechanism of degradation is limited to the surface. When  $\varepsilon_t = 1$ , then the degradation mechanism is undefined and a critical device dimension  $L_{crit}$  can be calculated by substituting  $L$  for  $\langle X \rangle$  in Equation (39). If



the matrix dimension for a particular polymer is larger than  $L_{crit}$ , it will degrade through a surface erosion mechanism. Otherwise it will be occurring throughout the bulk. The estimated  $\varepsilon$  and  $L_{crit}$  values for a range of polymers are given in Table 3, assuming that for a 1 cm-thick device,  $D = 10^{-8} \text{ cm}^2 \text{ s}^{-1}$  and  $\ln\{M_w/[N_A(N-1)\rho]\}^{1/3} = -16.5$ , where  $D$  is the water diffusion coefficient in the polymer.

**Table 3**

These authors further developed this relationship to investigate the effect of temperature on the critical thickness, fitting an Arrhenius equation to both the diffusion coefficient and the rate constant to give:

$$L_{crit} = L_{crit0} e^{-\left(\frac{1}{2}(E_D - E_H)/RT\right)} \quad (40)$$

where  $L_{crit0}$  is the initial critical thickness and  $E_D$  and  $E_H$  are the activation energies for the diffusion and hydrolysis reactions, respectively,  $R$  is the gas constant and  $T$  is the temperature. For poly(carbonate) LEXAN 141 [161] for example, based on experimental data  $L_{crit} \approx 11 \text{ mm}$  at  $20^\circ\text{C}$  and  $L_{crit} \approx 2 \text{ mm}$  at  $70^\circ\text{C}$  [161].

This approach was extended by Lyu et al. [101], who correlated the erosion behavior with kinetic constants for hydrolysis along with thermodynamic and transport properties for the degrading polymer, to derive a different expression for critical thickness  $W_c$  (similar to  $L_{crit}$ ), below which the sample degrades via a bulk degradation process and above which surface degradation is the primary mode of degradation. This was given by:

$$W_c = \left(\frac{1}{1+c'}\right)^{1/2} (D/\lambda)^{1/2} \quad (41)$$

where  $\lambda$  is the degradation rate constant and  $C' = W_s/W_m$  where  $W_s$  and  $W_m$  are the solubility of water in the polymer and the total amount of water consumed in the hydrolysis region when mass loss starts, respectively.

#### 4.7 Modelling the effect of hydrolytic degradation on mechanical properties

As outlined in the previous sections, there are a large number of approaches to modelling the fundamental kinetics of polymer hydrolysis and understanding the transitions between surface and bulk hydrolysis. However, while it is important to have a fundamental understanding of these processes, these studies need to be related to the macroscopic scale of material performance. A great number of studies have measured the changes in molecular weight and/or dispersity as a function of time in the hydrolysis of biodegradable polymers. However, there have been very few attempts to link these changes to impacts on the mechanical properties, and particularly to modelling these changes to enable lifetime prediction.

It is accepted that hydrolysis (catalysed either enzymatically or chemically) may occur either at random along the polymer backbone or specifically from the end of the chain [31, 162]. The loss of the mechanical properties will be greatest if the molecular weight is decreased by random scission (Sections 3.1.1, 4.5 and 4.6) even though the end-group attack will produce low molecular weight reaction products that may be a proxy for the degradation process. In order to determine the fundamental hydrolysis kinetics of polyesters and their relationship to mechanical properties, studies were made of the water-soluble oligomers of PLA [163] with between 2 and 9 repeat units, hydrolysed at pH 2. This enabled the rate coefficients for hydrolysis of ester groups adjacent to carboxylic or hydroxyl end-groups ( $\alpha$ -esters) to be determined. When compared to the in-chain  $\beta$ -esters these were found to be greater by a factor of  $\sim 2.5$ . From the measured activation energy and pre-exponential factors, this difference was attributed to steric effects of in-chain *versus* end groups, as well as the more

hydrophobic environment of  $\beta$ -esters. Since a typical commercial PLA has a degree of polymerization  $> 1000$ , there will be  $> 500$   $\beta$ -esters for every  $\alpha$ -ester so this difference becomes significant only at large extents of hydrolysis. Thus, random chain scission should control the early stage of hydrolysis and, as discussed previously, lead to rapid loss of strength.

Characterization of the  $M_e$  values for biodegradable polymers, and more generally of the relationship between molecular weight and material properties following degradation, is an area of study that is not as well developed as for oxidative degradation. However, as noted above, there have been recent advances due to the need to model the degradation of mechanical properties of biomedical polymers in tissue engineering.

Taking Equation (1) for the general strength dependence on molecular weight from Section 3.1.1, and substituting for  $M_e$  in Equation (12) (Section 4.3), then the strength,  $\sigma$ , is given by:

$$\sigma = \sigma_{\infty} - \frac{B}{M_{n0} e^{-k't}} \quad (42)$$

where  $\sigma_{\infty}$  is the fracture strength at infinite molecular weight, and  $B$  is a material constant (see Equation (1)). This relationship is plotted in Fig. 7 for different initial molecular weights and has been tested for hydrolysis of PLA, poly(glyconate) (a copolymer of glycolic acid and trimethylene carbonate) and PLGA [18, 164-166]. This relationship was determined to be of limited value in describing the loss of strength, which was attributed [18] to the unsuitability of Equation (1) (Section 3.1.1) when applied to amorphous polymers below their  $T_g$ . It may also be that it is inappropriate to apply the Flory equation to tensile strength data other than in the brittle failure regime where it has been shown to successfully model failure [30].

Instead, an empirical equation was developed by Deng et al. [165] to relate strength and  $\overline{M}_n$ :

$$BSR = a + b \ln MW \quad (43)$$

where  $BSR$  is the tensile breaking strength retention (given by  $BSR = (\sigma_0 - \sigma)/\sigma_0$ ),  $MW$  is the molecular weight (either  $M_n$  or  $M_w$ ), and  $a$  and  $b$  are polymer specific constants to be defined for each new system. Unique relations between  $M_n$  and both the modulus and strain retention were also observed. By contrast, Weir et al. [164, 167] found that there was a linear relationship, while Farrar and Gillson [18] and Tsuji [166] used empirical curve fitting to characterise the relationship, as did Lewitus et al. [168] for the degradation of tyrosine-derived terpolymers.

### Figure 7

In the case of the bulk eroding PLA-co-PCL, Vieira et al. also found that a simple first order strength loss relationship was satisfactory for describing the retained strength,  $\sigma$ , during the first eight weeks of immersion [9], with the tensile strength and  $\bar{M}_n$  decreasing at the same relative rate:

$$\sigma = \sigma_0 e^{-\lambda[E][H_2O]t} \quad (44)$$

where  $[E]$  is the concentration of ester groups,  $[H_2O]$  is the water concentration in the bulk and  $\lambda$  is the rate coefficient for hydrolysis.

The damage due to hydrolysis ( $d_h$ ) was then defined as:

$$d_h = 1 - \frac{\sigma}{\sigma_0} = 1 - e^{-\lambda[E][H_2O]t} \quad (45)$$

In the specific case studied, the bulk eroding polymer PLA-PCL copolymer fiber lost only 10% of its mass but 80% of its initial strength after 16 weeks of immersion in phosphate buffered saline solution at pH 8.

In cases where the degradation is homogeneous with instant diffusion, the hydrolysis rate is constant and material property loss depends only on time. However, there are many cases where these underlying assumptions do not apply. These results indicate that the strength-property relationship for the hydrolytic degradation of polyesters is not yet sufficiently well developed to have any predictive capability. It may also mean that the initial kinetic equation, which again is based on assumptions of hydrolysis more appropriate to solution kinetics, may not be applicable.

With regard to defining material lifetimes, there have been a number of approaches. Bellenger et al. [161] developed a relationship for predicting lifetime (or time to fail)  $t_{fail}$  in linear polymers based on a given molecular weight as a criterion for end-of-life, selected as  $M_e$  (the critical molecular weight for chain entanglement), assuming that the scission number per mass unit relative to initial ester concentration is much less than 0.1 (since these materials typically become brittle at very low conversions) and that the hydrolysis rate is much slower than the water diffusion rate. This is given as:

$$t_{fail} = \frac{\Phi}{K[H_2O]} \text{ where } \Phi = \frac{1}{n_e DP_0} \left( \frac{M_{n0}}{M_e} - 1 \right) \quad (46)$$

where  $n_e$  is the number of esters in a monomer unit,  $DP_0$  is the initial number average degree of polymerization,  $M_{n0}$  is the initial number average molecular weight and  $K$  (the apparent rate constant) =  $\lambda[E_0][H_2O]$ , with  $\lambda$  the rate constant for the hydrolysis reaction,  $[E_0]$  the initial ester concentration,  $[H_2O]$  the water concentration,.

If we define  $s_c$  as the critical number of chain scissions at the end of polymer lifetime, as given by:

$$s_c = \left( \frac{\overline{M}_{n0}}{M_e} - 1 \right) \quad (47)$$

then

$$t_{fail} = \frac{s_c}{n_g K [H_2O] DP_0} \quad (48)$$

which is similar to Equation (20) (Section 4.5.1).

Pickett [8], in a study of the time to fail of mechanically stressed hydrolysable engineering thermoplastics (poly(carbonate), poly(ethylene terephthalate) and resorcinol poly(arylate)) at different moisture contents (controlled by the relative humidity), noted the following:

(a) the polymers lost ductility when the  $M_n$  decreased by 20 to 50% (*i.e.*  $s_c$  is  $\sim 0.25$  to 1, based on Equation (47))

(b) the time to fail ( $t_{fail}$ ) for these polymer films under a strain of 4% to 9.6% (depending on thickness) followed a relation:

$$t_{fail} = \frac{e^{E_h/RT}}{A(RH)^2} \quad (49)$$

where  $E_h$  is the polymer-dependent activation energy for hydrolysis,  $RH$  is the relative humidity, and for bulk eroding polymers such as polysaccharides, polyesters and their aliphatic and aromatic copolymers, and polyamides,  $A$  is a pre-exponential factor for the hydrolysis reaction rate coefficient. In the case of strength loss of hydrolysable engineering thermoplastics on exposure to moist air [8], the term for  $[H_2O]$  is now the variable so the simplification of Equation (9) (Section 4.3) becomes, by incorporating  $[E]$  into the pseudo-first order rate coefficient,  $\lambda'$ :

$$-d[E]/dt = \lambda'[H_2O] = \lambda' RH \quad (50)$$

where  $RH$  is the relative humidity, since the solubility of water in a polymer is constant. However, comparison of Equation (50) with the experimental data, Equation (49) shows that there should be a second-order dependence of polyester hydrolysis on  $RH$ . Pickett has noted that for most reports in the literature, ester hydrolysis in the absence of acid or base has been determined as being second order in  $[H_2O]$ . This indicates that the reaction mechanism involves two molecules of water in the transition state [8]. This both rationalises and provides a mechanistic basis for the empirical Equation (49) for predicting the lifetime of the polyester in the neutral pH, moist atmosphere environment.

Chemical reaction kinetics in solid polymers may be affected by reagent or product diffusion effects [169]. Different monomers in copolymers can also hydrolyse at different rates [153] and micro phase separation is also common, which affects the rate of water diffusion in the different domains [170]. Solubility, diffusivity and reaction rates can also be dependent on pH and temperature. In a drawn fiber, *er*-oriented chain will have a different effect on mechanical properties than scission of the non-oriented fiber.

It has been widely observed that there is typically a sharp reduction in molecular weight during the first few weeks of hydrolysis of bulk degradable polymers, such as PLA and PGA. However, the material properties typically do not follow this pattern. In a number of studies, it was observed that at physiological temperatures the Young's modulus initially decreased very slowly on hydrolysis before then sharply dropping [171-175]. In some cases, there was even an increase in Young's modulus in the early stages, which was attributed to "stabilised chain packing in the amorphous regions in the presence of water molecules" [166]. Karjalainen et al. [176] found that for copolymers of  $\epsilon$ -caprolactone and lactic acid the tensile modulus increased during hydrolysis, whereas that of PLLA decreased from the start. The yield stress response to hydrolysis was likewise either increased or decreased slightly for the

copolymers while for PLLA it again dropped consistently over time. By contrast, there was no change in molecular weight or mechanical properties in PCL after 70 days.

Wang et al. [177] suggested that for amorphous polymers, an entropy-driven model could explain this, in that the entropic elasticity of an amorphous polymer is not significantly affected by isolated chain scissions – it is the removal of entire chains from the system that has a strong effect. From entropy theory, the Young's modulus,  $E$ , of a polymer can be related to the number of polymer chains per unit volume,  $N$ , according to:

$$E = 3Nk_bT \quad (51)$$

with  $k_b$  Boltzmann's constant and  $T$  the absolute temperature. One understanding of this equation is that, as chain scissions occur, the number of chains per unit volume,  $N$ , should increase, resulting in an increase in  $E$ . However, Wang et al. argued that when individual polymer chains are highly constrained, an isolated scission may have little effect on the overall chain configuration. Once a molecular weight threshold  $M_{th}$  is reached (at which point the polymer is divided into many small chains) then it no longer contributes to the entropy increase during deformation, and hence  $N$  is reduced by 1, reducing  $E$  in turn. Through the use of Monte Carlo simulations, a relationship was developed, based on the empirical curve fitting of Tsuji [166], which fitted the experimental data well. The assumption was that the effective Young's modulus could be determined using a composite theory, such as that of de Oca and Ward [178], based on the contributions from the crystalline and amorphous regions.

Expanding on this and earlier work by Wang et al. [122], Shirazi et al. coupled a phenomenological (reaction-diffusion) model that captures changes in molecular weight during bulk eroding polymer, PLGA, degradation (as per Wang's approach, including Equation (51)) with a polymer chain model that captures the relationship between the molecular weight distribution and the mechanical properties [179] (Fig. 8). In this case, the



model was calibrated using experimental data. Again, it was concluded that the autocatalytic effect was very significant, with a prediction that Young's modulus would decrease faster for thicker films because of the increased concentration of acidic groups.

### *Figure 8*

Ding et al. used a molecular dynamics approach to study the atomic effects of polymer chain scission, with a focus on the effect on Young's modulus [174]. This study also took into account the tie chains that pass through several crystalline and amorphous regions and transmit the tensile loads in semicrystalline polymers. In this case, the generic model was based on a united atom model of polyethylene, where the methylene groups are treated as a single entity since the structures of polyethylene and PGA are very similar. It was found that below the  $T_g$ , the elasticity of the interlamellar amorphous phase is controlled by the van der Waals interactions between the polymer chains. Hence, chain cleavages lead to an immediate reduction in the Young's modulus. However, above the  $T_g$ , the elasticity is instead controlled by the entropy change during deformation. Therefore, isolated cleavages do not lead to an immediate reduction in Young's modulus. It should be noted that in one study it was found that PLA films with higher initial crystallinity underwent faster hydrolysis, in contrast to expectation [172]. This result was explained as being due to the decreased density of effective tie chains in the more crystalline material as well as to a larger number of defects in the amorphous region, which could promote hydrolysis by enhancing water diffusion. Gleadall [180, 181] has recently developed a model to explore the effect of chain scission and increasing crystallinity due to recrystallization of polymer fragments during the initial phases of PLA degradation on mechanical properties. Atomic scale simulations were used to determine a value of Young's modulus by calculating the force required for a vertically applied strain. The effect of polymer chain scission was analysed by studying the forces that individual atoms transfer vertically through the structure. It was found that there are regions

above and below the polymer that do not transfer as much vertical force after chain scission. It was proposed that chain cleavage be represented by effective cavities around the scission. The volume fraction and crystallinity were determined experimentally from Duek's results [182].

Chen et al. [183] used the empirical modified Flory-Fox Equation (1) to model PGA strength with degradation time, coupling this to a molecular dynamics simulation approach for estimation of the parameters, to systematically model the PGA degradation mechanism at different temperatures, external loads and molecular weights (Fig. 9). A density functional theory calculation was used to derive the degradation rate constants under the different conditions. The ultimate strength of PGA of an infinite chain length was estimated by extrapolating the ultimate strength of three different PGAs of different molecular weights. Although this approach can only give a qualitative estimate of degradation and, being empirical, is specific for individual polymeric systems, it does provide another option for estimating comparative degradation rates.

Vieira and coworkers have also published a series of papers on studying and modelling the effect of degradation on mechanical properties of biodegradable materials [28, 184-186]. They proposed a novel 4D approach to prediction of the mechanical behavior over time, based on the relationship between fracture strength and molecular weight for thermoplastic polymers. A relationship similar to Equation (44) was defined:

$$\sigma = \sigma_0 e^{-u_s t} \quad (52)$$

where  $u_s$  is the strength decrease rate of a material, and seems to be directly related to the molecular weight, although this equation is not dimensionally stable. Several constitutive equations for incompressible hyperelastic materials were used to model mechanical behavior,

with the axial nominal stress for the three models, Neo-Hookean ( $\sigma^{NH}$ ), Mooney-Rivlin ( $\sigma^{MR}$ ) and a reduced second-order equation ( $\sigma^{2nd\ red}$ ), being given by:

$$\sigma^{NH} = \mu_1 \left( \gamma - \frac{1}{\gamma^2} \right) \quad (53)$$

$$\sigma^{MR} = \mu_1 \left( \gamma - \frac{1}{\gamma^2} \right) + \mu_2 \left( 1 - \frac{1}{\gamma^3} \right) \quad (54)$$

$$\sigma^{2nd\ red} = (\mu_1 - \mu_3) \left( \gamma - \frac{1}{\gamma^2} \right) + (\mu_2 - \mu_3) \left( 1 - \frac{1}{\gamma^3} \right) + \mu_3 \left( \gamma^2 - \frac{1}{\gamma^4} \right) \quad (55)$$

where  $\gamma$  is the axial stretch ( $\gamma = 1 + \varepsilon$ ) (where  $\varepsilon$  is the nominal strain), that satisfies  $\gamma \geq 1$ , and  $\mu_1$ ,  $\mu_2$  and  $\mu_3$  are material properties (usually called the shear modulus for  $\mu_1$ ), where the values for  $\mu_i$  are  $> 0$ .

### Figure 9

Only  $\mu_1$  was modelled to vary linearly with hydrolytic damage, as proposed by Soares et al. [187]. These equations were implemented in a Finite Element Method approach, changing the material parameter as a function of hydrolytic damage or degradation time. The Neo-Hookean equation gave the least best fit to the degradation of PLA-PCL fibers, but still gave a reasonable approximation of the experimental tensile test results (Fig. 10). However, the limitation with Equations (54) and (55) is that they can violate the second law of thermodynamics by allowing negative values for the material parameters  $\mu_2$  and  $\mu_3$ . For this reason, the neo-Hookean material model was further developed and implemented in ABAQUS standard, which is a finite element software package [188]. However, this model is based on an empirical equation, so that the model parameters need to be determined experimentally for each material and during degradation. In addition, it is assumed that the hydrolytic degradation rate is constant. In such heterogeneous systems, this is a significant oversimplification.

Tang et al. [189] also used ABAQUS to model damage to biodegradable polymers under bulk erosion. In this case, the heat transfer function was used to simulate Fickian diffusion, given its ready availability and the analogous mathematical relationships. The rate of decrease in molecular weight was assumed to be related to the local water concentration  $[H_2O]$ , with  $0 < [H_2O] < 1$ , as given by:

$$\frac{dM_w}{dt} = -\beta[H_2O] = -\lambda\bar{M}_w \quad (56)$$

where  $\beta$  was assumed to be  $4000 \text{ day}^{-1}$  [140]. A first-order kinetic for the rate of molecular weight loss for hydrolytic scission of ester bonds in polyesters such as PLA was assumed, with the degradation rate constant fixed at  $0.0117 \text{ day}^{-1}$ , a value taken from [190].

#### *Figure 10*

It was determined that the critical concentration of water at which autoacceleration begins (at a critical  $M_w$  of 10,000 g/mol) is  $0.0293 \text{ g cm}^{-3}$ . On that basis, the predicted change in mechanical properties for three different polymer morphologies is given in Fig. 11, including the damage variable,  $d = 1 - E/E_0$ , where  $E$  is the Young's modulus and  $E_0$  is the initial Young's modulus. While this approach was developed, in this case, for porous scaffold materials of around 86% starting porosity and is again limited by fixed rate constants, it does offer another approach to mechanical property modelling.

#### *Figure 11*

According to a study by Deroiné et al. [191], hydrolytic degradation for poly(3-hydroxybutyrate-co-3-hydroxyvalerate) (PHBV) is not uniform because hydrolysis is faster than diffusion, i.e., it is a surface erosion phenomenon. The rate of water absorption in PHAs is temperature dependent and the activation energy for the diffusion coefficient was found to be  $70 \text{ kJ.mol}^{-1}$ , which is high because PHAs are hydrophobic and highly crystalline. Similar

reports in the literature place the value at  $43.7 \text{ kJ}\cdot\text{mol}^{-1}$  in deionised water and  $56.5 \text{ kJ}\cdot\text{mol}^{-1}$  in distilled water [191]. Differences can be explained by a number of factors (PHA type, thermal processing, aqueous environment, etc.).

While Deroiné et al. found that molecular weight decreased from the beginning of each hydrolysis experiment at all temperatures, the relationship between mechanical properties and molecular weight showed what was described as a two-phase relationship (Fig. 12), but what could be interpreted as the variation of strength with  $M_n$  as given by Equation (1). On plotting the curves of the stress-at-break and the strain-at-break, it can be seen that both changed slope below  $110,000 \text{ g/mol}$ . Above this threshold, most mechanical properties were not altered with molecular weight loss. Below the threshold, however, PHBV degradation occurs faster and the material loses its mechanical integrity, corresponding to an “end of use” criterion. The strain-at-break was therefore used as an indicator of aging since it is governed by surface properties, whereas some of the other mechanical property parameters relate to the bulk. It was possible to fit an Arrhenius curve to the strain at break result to give an activation energy of  $93 \text{ kJ/mol}$  for the hydrolytic degradation, as well as to undertake a lifetime estimation at different temperatures; in this case, the authors assumed that a 20% or 30% loss in strain at break was equivalent to end of use, less than otherwise quoted herein.

### *Figure 12*

## **5 Enzyme promoted degradation – effect on kinetics and mechanism**

So far, this review has focussed on abiotic processes and their modelling. However, biodegradation is in large part driven by enzymatic processes. Enzymes work through lowering of the activation energy of a reaction such that the reaction rate can be increased under conditions that are otherwise unfavourable, e.g., at room temperature in water at neutral pH. In the presence of enzymes, an increase in reaction rates by  $10^8$  to  $10^{20}$  can

commonly be observed [192]. Enzymes are proteins that have a complex three-dimensional structure, with enzyme activity being closely related to the specific conformational structure adopted. Specific regions on the protein structure related to enzyme activity are associated with characteristic primary sequences (active sites), and these are where the interaction with the substrate takes place [193]. Different enzymes can operate through different mechanisms, depending on the specific reagents available and the environment in which the reaction is occurring. Endozymes, for example, induce random chain scission of the main chain polymer bonds, leading to a rapid decrease in molecular weight, while exoenzymes cleave terminal monomer units sequentially. Some enzymes need specific cofactors such as metal ions (sodium, potassium, magnesium, calcium or zinc) or organic cofactors (or coenzymes). Chemical modification (crosslinking, removal or introduction of chemical groups in the polymer chain) can potentially affect the rate of reaction, as it may affect the ability of the enzyme to recognise the substrate. The adsorption and rate of reaction can also be influenced by the inherent characteristics of the specific enzymes involved (activity, stability, composition and conformation) as well as by external factors such as pH and temperature. Enzymes such as lipases are only activated after binding to the substrate and changing conformation. As previously described, enzymes are too bulky to penetrate into the polymer matrix, hence **enzymatic hydrolysis is a surface erosion process**. It is possible to reach a point with enzyme attack on solid polymers where additional enzyme does not increase the rate of degradation further, which is attributed to saturation of the surface.

The enzymes that are typically involved in biodegradation include amylolytic enzymes such as  $\alpha$ -amylase (which attacks starches) and lysozyme (which attacks chitin). Lipase is another important enzyme as it can catalyse the hydrolysis of  $\gamma \sim \omega$  ester bonds in aqueous media as well as hydrolyse aliphatic and aromatic polyesters such as PHAs, PCL, PLA and a PET-based degradable polyester [194]. As well as these key enzymes, there are also extracellular

PHA depolymerases that hydrolyse PHAs, and the enzymes pronase, proteinase K, and bromelain, all of which can attack  $\alpha$ -ester bonds such as in PLA [195]. The enzymatic degradation of cellulose-based materials is carried out by endo-1,4- $\beta$ -glucanases, which cleave the chains randomly. These include exo-1,4- $\beta$ -glucanases, which act on the polymer chain ends, and  $\beta$ -glucosidases, which catalyse the cellobiose to glucose conversion.

Synthetic polymers are able to be degraded by enzymes, but must be able to fit into the enzyme's active site [34], which is at least in part why rigid aromatic polyesters are non-degradable while flexible aliphatic polyesters do degrade.

The kinetics of abiotic hydrolysis do not apply for the full life cycle when considering the case of enzyme-promoted hydrolytic degradation, and lifetime prediction in the presence of bacteria or fungi that can secrete the appropriate enzymes becomes even more challenging. Most of the enzyme-promoted degradation studies reported in the literature are conducted in phosphate buffered saline solution, which is a simple model system.

The active promotion of hydrolysis by enzymes is a very significant process for naturally occurring biopolymers such as polysaccharides, proteins (gelatin and collagen), and poly(hydroxyalkanoic acids) (PHAs), where organisms capable of secreting the appropriate enzymes are commonly present in the environment [32]. Shah et al. have listed different microorganisms known to be capable of degrading different groups of polymers [60]. Only a few PLA-degrading microorganisms have been found and are not thought to be widely distributed in the environment, which is in part why PLA is slow to degrade in the soil at ambient temperatures [196], although the high  $T_g$  of these polymers also plays a large role.

The use of microorganisms in establishing ultimate biodegradation (to carbon dioxide and water) is well known and used commonly in standardized tests with known organisms (e.g., ISO 14852, ASTM D6691 – 09). However, these tests focus on carbon dioxide evolution and

mass loss, which, particularly in the presence of enzymatic degradation (which proceeds via a surface eroding mechanism), can have little relationship to the material properties and practical lifetime of the polymer in question. So, while there are a great many studies on the enzymatic degradation of biodegradable polymers, particularly PHAs, there are a limited number that relate enzymatic degradation to the change in molecular weight and in particular to changes in mechanical properties of the matrix.

Typically, biodegradation occurs via a multistep process with different mechanisms [197]. For example, for PLA, the initial degradation occurs after exposure to moisture via an abiotic hydrolytic process (non-living chemical and physical factors) as previously described, leading to random chain scission and molecular weight reduction with consequent embrittlement of the polymer. Subsequent to this, PLA oligomers can diffuse out of the bulk polymer and be degraded by microorganisms. In parallel with this, an enzymatic process of biodegradation can be promoted at the surface of the polymer, but cannot proceed in the bulk due to the size of the enzymes, which limits their diffusion into the matrix. Thus, the enzymatic degradation of the polymer interior can only occur once there are sufficient voids and pathways for the large biomolecule to enter.

Azevedo and Reis reviewed the enzymatic degradation of biodegradable polymers [198] and summarised the typical stages in solution as:

- Diffusion of the enzyme from the bulk solution to the solid surface
- Adsorption of the enzyme onto the substrate, resulting in the formation of the enzyme-substrate complex
- Catalysis of the hydrolysis reaction at the surface
- Diffusion of the soluble products into the solution



From a morphological perspective, it has been shown across a number of different polymers, particularly PHA, that there is preferential erosion of an amorphous interlamellar phase in these spherulitic semicrystalline polymers, which are subjected to substantial hydrolysis degradation processes by enzymes such as poly(3-hydroxybutyrate) (PHB) depolymerase [199].

The use of static or agitated conditions for testing can also influence the kinetics. Agrawal et al., for example, found that fluid flow actually decreased the degradation rate of poly(*D,L*-lactide-*co*-glycolide), which was attributed to the lack of an autocatalytic effect with reaction products being dispersed [200].

Other factors that affect the rate of enzymatic degradation include pH, oxygen levels, microbial population, and available nutrients for supporting the microbial population. In general:

- A higher hydrophilic/hydrophobic ratio promotes enzymatic degradation
- Carbon-chain polymers are not susceptible to enzymatic degradation
- Chain branching inhibits biodegradation
- Lower molecular weight polymers are more susceptible to enzymatic degradation
- Crystallinity reduces biodegradability
- Crosslinking reduces biodegradability

It is also necessary to take into account the processing additives used in polymer production, such as plasticizers, lubricants, antioxidants, salts and stabilizers, which may leach out after immersion to enhance or inhibit the degradation process.

## 5.1 General models for enzymatic degradation of biodegradable polymers

There have been a number of models developed for the interaction of solid substrates with enzymes, which could potentially serve as the basis for more complex modelling of biodegradable polymer degradation through enzyme-promoted hydrolysis.

In an early study, McLaren used a heterogeneous approach to the kinetics, recognising that only the surface of the insoluble substrate was accessible in the digestion of such substrates by hydrolytic enzymes [201]. It was also assumed that the adsorption of the enzyme onto the substrate obeyed a Freundlich adsorption isotherm of the form given in Equation (57):

$$[ZS] = K[Z]^n \quad (57)$$

where  $[ZS]$  is the concentration of the enzyme-substrate complex,  $K$  and  $n$  are constants for a given adsorbate and adsorbent at a particular temperature, and  $[Z]$  is the concentration of the unbound enzyme.  $n$  was predicted to be between 2 and 3 for adsorption of enzyme from a solution phase onto a two-dimensional insoluble surface.

Duguay et al. [202] developed a much more detailed mathematical model of the degradation of biomedical poly(urethanes), in which they incorporated elements of polyurethane surface chemistry, surface dynamics, non-enzymatic hydrolysis, enzyme adsorption and inactivation, and enzyme-mediated hydrolysis. They modelled enzyme adsorption using a Langmuir model to describe the concentration of free and adsorbed enzyme as well a loss of activity in the adsorbed enzyme, using a set of thirty-one kinetic equations to describe transformation rates. The reaction of an enzyme with a solid surface was assumed to operate via the well-known Michaelis-Menten equation. However, for the purposes of this review, the model was limited in that it was not validated with experimental observations and also only considered the production of surface and free products and did not consider the relationship of these processes to mechanical properties.

Mukai et al. [203] also recognised that with an insoluble substrate, the Michaelis-Menten approach does not describe the data adequately and modelled the kinetics of PHA degradation by PHB depolymerase to reflect this. Likewise, Timmins et al. [204] developed the model by Mukai et al. further by including both enzyme and substrate concentrations in the rate equations, as well as taking into account the fractional concentration of free substrate sites as opposed to the absolute concentration of such sites. The adsorption reaction was assumed to obey a Langmuir isotherm:

$$v_0 = \lambda[Z][S] / [S_0] = \frac{\lambda[Z]_0[S]_0(K+[S]_0)}{(K+[S]_0+[Z]_0)^2} \quad (58)$$

where  $v_0$  is the rate of the reaction,  $\lambda$  is the hydrolysis rate constant,  $[S]$  and  $[Z]$  are the substrate and enzyme concentrations, respectively, while  $[S]_0$  and  $[Z]_0$  are the initial substrate and enzyme concentrations, respectively, and  $K$  is the adsorption equilibrium constant. Based on this model, a value for  $\lambda$  was calculated at  $10 \mu\text{g}_p \text{ min}^{-1} \mu\text{g}_z^{-1}$  (where  $\mu\text{g}_p$  is polymer weight loss in  $\mu\text{g}$  and  $\mu\text{g}_z$  is mass of enzyme present in  $\mu\text{g}$ ) for a 55 kDa PHB polymer in  $20 \mu\text{g mL}^{-1}$  enzyme, where the enzyme was the PHB depolymerase from *Pseudomonas lemoignei*. A fungal enzyme had a smaller rate constant, but the overall relationship still applied.

Scandola et al. [205] in turn developed a simpler two-step kinetic model analogous to the Michaelis-Menten approach while still taking into account the solid nature of the substrate, whereby:

$$v_0 = \lambda A \vartheta \quad \text{where} \quad \vartheta = \frac{K[Z]}{(1 + K[Z])} \quad (59)$$

which in a linear form can be represented as:

$$\text{Area}/v_0 = \left(\frac{1}{K\lambda}\right) \left(\frac{1}{[Z]}\right) + 1/\lambda \quad (60)$$

where  $Area$  is the substrate surface area,  $\vartheta$  is the fraction of the substrate surface occupied by the Enzyme-Substrate complex,  $ZS$ ,  $v_0$  is the rate of reaction,  $K$  and  $\lambda$  are the adsorption equilibrium and hydrolysis rate constants, respectively, and  $[Z]$  is the initial enzyme concentration. The model as developed predicts that a plateau will be attained at high enzyme concentration, at which point the surface will be saturated. It was noted that this simple model ignores the development of increased surface roughness as degradation proceeds and the amorphous regions are eroded. It was further noted that in reconciling all the experimental and modelling data to date for enzymatic degradation, it is important to correctly quantify the area changes associated with selective enzymatic degradation of the substrate surface. In addition, the relative rates of degradation of the amorphous *versus* crystalline states of the substrate need to be characterized.

Tayal et al. [206] modelled the enzymatic hydrolysis of the water-soluble polysaccharide, guar galactomannan, as a model for the solid polymer. In this case, where the polymer was in solution rather than in a solid state and hence the water diffusion kinetics did not come into play, it was found that there was an inverse relationship between molecular weight and time  $1/M_w \propto \lambda t$ , with  $\lambda$  varying inversely with polymer concentration. The true order of the reaction could be determined from the dependence of reaction rate on polymer concentration and the solution viscosity was found to be very sensitive to the extent of guar hydrolysis.

Overall, there is no general model developed to date that adequately describes in full the progress of enzymatic degradation of biodegradable polymers, taking into account the heterogeneity of the systems and so on. This is an area that requires further development. However, many studies have been conducted on enzyme reactions with specific biodegradable polymer substrates and these are described in the following sections. Since enzymatic degradation occurs via a surface erosion process, the general principles for lifetime prediction as outlined in Sections 4.4 and 4.7 can be applied, including: rate of thickness

decrease, which can be used to predict a reduction in load-bearing capacity over time, and the formation of surface defects leading to a decrease in surface morphology dependent properties such as elongation-at-break.

## 5.2 Enzymatic hydrolysis reactions with specific biodegradable polymer substrates

### 5.2.1 Enzymatic hydrolysis of PLA

Zeng et al. [207, 208] found that the enzymatic degradation of PLA by proteinase K followed nearly zero-order kinetics. The effect of number, and molecular weight, of chain branches in PLA has also been explored through the synthesis and degradation of branched and star-shaped PLA molecules [209-211]. In particular, Numata et al. [212] used Atomic Force Microscopy (AFM) to monitor the effect of number of chain ends of branched PLAs on the enzymatic hydrolysis of PLA monolayers produced using Langmuir-Blodgett techniques. It was found that degradation was accelerated by an increase in the number and a decrease in the molecular weight of the branches.

Vasanthan and Gezer [213] also showed in a study of PLA films annealed at different temperatures, with different initial crystallinities, that the higher the crystallinity, the slower the enzymatic degradation rate. It has also been observed that for aliphatic polyesters more generally, the enzymatic hydrolysis rate is accelerated as the temperature increases, with quite rapid hydrolysis rates when the temperatures were 10 to 20°C lower than the melting temperature [214], although no activation energy for PLA was given – only for PCL (see Section 5.2.2).

In trying to understand and model the mechanism of this degradation process in more detail, novel techniques are being developed to monitor polymer degradation *in situ*. As an example, Yamashita et al. [215] used a combination of quartz crystal microbalance and AFM measurements to study the effect of proteinase K on an amorphous PLLA film. It was found

that the degradation rate reached a steady state when the concentration of proteinase K was greater than 100  $\mu\text{g/mL}$ , with the erosion rate being determined by the amount of adsorbed enzyme. Nanometre-scale surface patterning was seen, with the observed “footprint” of the hollow associated with an enzyme being larger than the estimated size of a given enzyme, indicating that the adsorbed enzyme may migrate at the surface.

### 5.2.2 Enzymatic hydrolysis of poly( $\epsilon$ -caprolactone) (PCL)

PCL-degrading bacteria are widely distributed in the environment, although little is known about these PCL depolymerases [216]. PCL is degraded by lipases and esterases [217] and it has also been shown [218] that cutinases in fungal pathogens can degrade this polymer.

Three kinds of lipase isolated from microorganisms have been found to accelerate the degradation of PCL: *Rhizopus delemere*, *Rhizopus arrhizus* and *Pseudomonas cepacia* [219]. Ozsagioglu et al. [220] tested different enzymes (an esterase, a lipolase and savinase) on PCL films and found that while the lipolase was able to erode the PCL, the esterase was only able to undertake chain scission, and the savinase had a much slower rate of reaction overall. Hydrolase type enzymes such as protease can also in theory degrade PCL.

In one study, which analysed the hydrolysis of model ester compounds as well as PCL at different temperatures, the activation energy for PCL under enzyme catalysis was estimated at 200 kJ/mol compared to 31 kJ/mol for the model dibutyladipate [221], although this was a poor model for PCL since there are significant structural dissimilarities. The high value in PCL was attributed to chain mobility being limited in the crystallites of the polyester.

In a study analysing the effect of enzymatic and hydrolytic cleavage of a PCL network (as opposed to linear PCL), hydrolysis was associated with swelling and degradation of the bulk matrix whereas the enzyme driven degradation was a surface related phenomenon, affecting the amorphous phase [222]. For all samples, the Young's modulus initially increased to week

5 of the experiment then decreased slightly. This is believed to be due to two competing effects where degradation occurs more rapidly in the amorphous phase and, therefore, the crystallinity initially increases, however, mass loss and increasing porosity results in a decrease in modulus. The former effect was found to dominate initially. Under enzyme treatment, the total crystallinity increased less and the change in material properties was also smaller.

Sekosan and Vasanthan [223] also showed that the enzymatic degradation rate of PCL depends strongly on the crystallinity of the matrix, decreasing as crystallinity increases. In films of lower crystallinity, the degradation occurs preferentially in the amorphous phase. However, there was evidence that at a higher crystallinity, both phases are attacked. Hayashi et al. [224] confirmed that for PCL fibers, enzymatic degradation using lipase proceeds via a surface degradation mechanism, with the rate of degradation being dependent on the draw ratio and crystallinity of the PCL fibers. The rate of loss of strength in these fibers was faster than the rate of weight loss, with the rate of loss being higher than could be explained by a decrease in fiber diameter due to erosion. This failure was tentatively attributed to the presence of cracks or stress concentration points in the samples.

In single crystal studies, Jiang et al. [225] has shown that for block copolymers of PCL with PEO and methoxy and amino terminal functional groups, the PEO phase is located in an amorphous surface layer. This alters the mode of degradation in that, for PCL single crystals, the enzymatic degradation predominantly occurs on the edges where the chain packing is loose. However, for the block copolymers, the crystal surfaces are also significantly affected. Increases in roughness and layer-by-layer loss of material were observed.

### 5.2.3 Enzymatic hydrolysis of poly(butylene succinate)

Lee et al. [226] reported that the enzymatic (lipase) degradation of poly(butylene succinate) (PBS) was slower than that of its copolymers poly(butylene succinate-*co*-*L*-lactate) and poly(butylene succinate-*co*-6-hydroxycaproate), which was attributed to fewer surface adsorption points on PBS. The preferred mode of attack was found to be *exo*-type scission from the chain ends, with a surface-etching mechanism proposed.

### 5.2.4 Enzymatic hydrolysis of PHAs

The ability to degrade short-chain-length PHAs is widely distributed among bacteria and filamentous fungi and a large number of depolymerases have been purified and characterized [227]. These PHA depolymerases are carboxylesterases and belong to the  $\alpha/\beta$ -hydrolase fold family [228-231]. Their protein sequences contain four regions: a catalytic domain containing the lipase box (a catalytic triad of serine, aspartate and histidine residues); a substrate-binding domain that acts as an adsorption site for polymer substrates; a signal sequence; and a domain that links the catalytic and substrate-binding domains. The substrate binding domain is responsible for the initial adsorption of the enzyme to the substrate surface. Once attached, the catalytic domain can interact with the polymer chains to hydrolyse the ester linkages. It has been shown that the adsorption depends not only on hydrogen bonding between hydroxyl groups of serine in the enzyme and carbonyl groups in the poly(3-hydroxybutyrate) (PHB) polymer but also on the hydrophobic interaction between non-polar residues in the enzyme and alkyl groups in the PHA polymer [232].

Various models [233-237] for the degradation of single crystals of PHB by PHB depolymerase have been proposed, in which the enzyme binds to the planar crystal surface, possibly generating disordered chain-packing regions on binding, and then erodes the end (and also the edges, for some enzymes) of the crystals along the crystallographic *a*- and *b*-



axes, with limited erosion along the *c*-axis. However, Numata et al. [238] characterised the real-time degradation of PHB and PHBV thin films using a combination of quartz crystal microbalance and AFM measurements (as above for PLA) and showed that the degradation occurred in the *a*-, *b*- and *c*-axes of the crystals (see model in Fig. 13). The same group recently reviewed the enzymatic processes for biodegradation of PHA crystals [239]. The enzymatic erosion rate of PHA copolymer films has been found to decrease with an increase in lamellar thickness in PHA films [240].

### ***Figure 13***

It has been shown that the apparent (calculated) cross-sectional area for one enzyme molecule binding to the PHA surface is around  $17 \pm 8 \text{ nm}^2$  [241], with the adsorption isotherms being found to follow the Langmuir adsorption equation. The activation energy of enzymatic hydrolysis of the PHB chain was found to be 82 kJ/mol. This compares with activation energies of 88.4 kJ/mol for crotonic acid formation and 78.9 kJ/mol for 3-hydroxybutyric acid formation in the base-catalyzed hydrolysis of PHB [242]. PHB depolymerases are able to degrade all (*R*) chains of PHAs as well as cyclic (*R*) oligomers and polymers composed of *rac*-hydroxybutyrates. They are unable to degrade all-(*S*) or syndiotactic (*R,S*) chains.

Ishida et al. [243] reviewed the effect of copolymer composition on biodegradability for finely fractionated PHBV copolymers of well-defined monomer unit content. It was found that PHA depolymerases degraded copolymers adopting the PHB crystal type far more rapidly than those adopting the comonomer crystal type (e.g., poly-3-hydroxypropionate). The amorphous films were almost not degraded by some enzymes, indicating that degradation rate is not only affected by the crystallinity but also by the chemical structure and the substrate specificity. It is believed that the binding site of the enzymes needs a crystalline structure in order to adhere.

Doi et al. [17, 244] found that the molecular weight of PHA samples did not change significantly during enzymatic hydrolysis but the sample mass did decrease. Enzymatic erosion rates were given, with SEM analysis showing surface roughening due to the erosion process. Luo and Netravali [245] also found that the molecular weight of PHBV samples degraded in compost remained almost unchanged, that it was enzymatic as opposed to hydrolytic degradation and was a surface degradation process. Modulus and crystallinity remained almost unchanged while ultimate tensile strength and elongation-at-break decreased as degradation increased. However, the tensile strength as reported was not corrected for the change in cross sectional area. Hermida et al [246] showed that when this correction was applied, the tensile strength remained constant, i.e., surface erosion was taking place and there was no critical crack formation to alter the properties of the bulk.

Doi et al. undertook comparative studies of hydrolytic and enzymatic degradation of PHBV and poly(3-hydroxybutyrate-co-4-hydroxybutyrate) (P(3HB-co-4HB)) [244]. Over the first 58 days of hydrolytic degradation without enzyme at 55°C in phosphate buffer solution, no weight loss was observed, but all samples showed a decrease in molecular weight associated with random chain scission. By contrast, during the course of enzymatic degradation (which took place over 20 hours as opposed to 58 days), the molecular weight remained relatively unchanged while weight loss was of the order of 1 to 5%. This indicated that, in this case, only the polyester chains on the surface were being hydrolysed via a surface erosion mechanism. The rate of degradation was found to be dependent on copolymer composition, with the presence of 4HB accelerating the rate of both hydrolytic and enzymatic degradation.

There have been a number of mechanistic enzyme degradation studies on solution-grown lamellar single crystals of PHA, which give further insight into the mechanism. Murase et al. [235] used a hydrolytic-activity-disrupted mutant of PHB depolymerase, to examine the enzymatic process without the influence of hydrolysis, and concluded that there is an

intermediate stage after the initial enzyme adsorption, which involves disturbance of the molecular packing in the crystal.

The effect of crystal structure was also explored in a number of studies. Zhang et al. [247] undertook cold drawing of both PHB and the novel PHA copolymer, P(3HB-*co*-4HB), achieving shish kebab structures with draw ratios of up to 1200%. A crystalline structure of a planar zigzag conformation ( $\beta$  form) was produced in this process. The overall susceptibility of the drawn materials to enzyme-catalysed hydrolysis did not change for PHB since the crystallite size was unchanged. However, for P(3HB-*co*-4HB) the rate of erosion increased with increased draw ratio. This result was attributed to an overall decrease in crystallinity and crystallite size for this stretched copolymer. Enzymatic degradation proceeded via attack on the amorphous regions first, then the pseudo-crystalline ( $\beta$ -form) crystal regions between the lamellar crystals. Once these were exposed, there was enzyme attack at the lamellar crystals of the  $\alpha$ -form. Tanaka and Iwata [248] also explored the enzymatic degradation of PHBV films, including cold-drawn films and found that the more drawn the film, the slower it was to degrade; this was felt to be reflective of higher crystallinity as well as the long period of the crystal structure. The drawn films had a shish-kebab morphology, with both the  $2_1$  helix ( $\alpha$ -form crystal) and the planar zigzag ( $\beta$ -form crystal) present. It should also be noted that the solvent-cast form of PHBV (8 mol% HV) was much faster to degrade than the melt-produced form, presumably because of a looser packing arrangement due to solvent evaporation. It was also found that the rate of enzymatic degradation increased with a decrease in crystallinity of melt crystallised PHB films, whereas the size of the spherulites made little difference [249].

In studies of different PHA copolymers, with co-monomer units of different chain length, it was found that the longer the side chain, the more the co-monomers acted as defects in the PHB crystal structure, limiting lamellar size and reducing crystallinity. The growth rate of

spherulites also decreased with chain length at the same crystallization temperature [250]. Overall, the rate of enzymatic degradation was found to be dependent on both crystallinity and lamellar thickness, hence increasing with increasing co-monomer chain length (Fig. 14).

By contrast, Li et al. found that the longer the side chain in the copolymer, the lower the rate of degradation (using the PHA depolymerase produced by *Ralstonia pickettii* T1) [251]. This was attributed to the higher proportion of long-chain comonomer units in the copolymers used in this study (at 15 – 20 mol%), which at this higher concentration could have a surface effect, inhibiting enzyme attachment and hence slowing the reaction.

#### **Figure 14**

Low molecular weight additives such as dodecanol, lauric acid, tributyrin and trilaurin have been found to act as plasticizers for PHB [252], and it was found that small amounts (1 wt% addition) act as accelerants for enzymatic degradation while larger amounts (9 wt%) slow the degradation rate. This was ascribed to migration of the additives to the surface, where they are believed to inhibit enzyme binding. At the low addition rate, it is thought that thinner lamellae and more mobile polymer chains in the amorphous phase may be responsible for the increased susceptibility.

#### 5.2.5 Enzymatic hydrolysis of starch

The enzymatic digestion kinetics of starch, and blends of starch with other polymers such as poly(vinyl alcohol), PLA or cellulose acetate, have been extensively reviewed and analysed [253-255]. In starch, the linear polymer, amylose, makes up about 20 wt% of the granule, and the branched polymer, amylopectin, the remainder. Both fractions are readily hydrolyzed at the acetal link by enzymes (Fig. 15). The  $\alpha$ -1,4-link in both components of starch is attacked by amylases and the  $\alpha$ -1,6-link in amylopectin is attacked by glucosidases. To date, there have to our knowledge been no reports on the modelling or prediction of in-use lifetimes in

starch-based plastics. However, a number of authors [256-259] have analysed the kinetics of glucose polymer degradation. A first-order equation is typically fitted, as given by:

$$C_t = C_\infty(1 - e^{-kt}) \quad (61)$$

where  $C_t$  is the starch degraded (expressed as mass per unit volume) at incubation time  $t$ ,  $C_\infty$  is the corresponding amount of starch degraded at the end point of the reaction and  $k$  is the first-order degradation rate coefficient. Values for  $k$  can be determined by plotting  $\ln(dC/dt)$  against  $t$ .

### *Figure 15*

Li et al. [256], however, studied the enzymatic degradation of a range of starch films of different initial molecular, crystalline and granule structure, and found that there were two distinct stages of degradation: an initial, much more rapid stage, typically over the first 100 minutes or so, and a second, slower stage. This initial, rapid degradation was attributed to two mechanisms: 1) the presence of small molecules that enter the solution and are readily degraded and 2) the likely presence of highly disordered and accessible chains at the film surface that are more susceptible to degradation. However, in parallel with this there was a tendency observed for the smaller molecules once formed to retrograde more rapidly to form more ordered, less readily degradable structures.

Consistent with this outcome, it has been demonstrated [257] that the enzymatic degradation of structurally complex starch substrates can be adequately described by the use of two sequential rate processes with different rate coefficients,  $k_1$  and  $k_2$ , with  $k_1$  typically being larger than  $k_2$ .

Increased crystallinity in starch has been shown to slow enzyme degradation [260] while a decrease in molecular size was associated with an increase in  $k_1$ . The increase in the amount

of amorphous material at the surface of a film was strongly correlated with the binding efficiency of the  $\alpha$ -amylase, and, therefore, the degradation rate [258].

Recent analysis of the enzymatic digestion of a high amylose starch by Gidley et al. [261] revealed that for extruded starches, undigested residues had increasing levels of crystallinity during the digestion, which was consistent with either selective hydrolysis of non-crystalline regions or recrystallization during digestion. However, the enzymatic digestion rates were all very similar, regardless of differences in initial crystallinity, moisture content or storage conditions. Given that the crystallinity levels in the residues were still relatively low overall, this indicates that enzyme resistance in these starches is actually associated with a dense solid phase structure that is only weakly crystalline and that measures of crystallinity are not sufficient to predict enzyme resistance. Zheng et al. [262] also showed that Gingko starch, with a higher amylose content, lower swelling factor and different crystalline structures compared to other starches also had higher resistance to enzyme degradation.

#### 5.2.6 Enzymatic hydrolysis of other polysaccharides

Chitin is a linear copolymer of *N*-acetyl-glucosamine and *N*-glucosamine, with a  $\beta$ -1,4 linkage, and is found in the shells of crabs, lobsters, shrimps and insects. Chitin can be considered to be an amino cellulose, and it can be degraded by chitinase through hydrolysis of the *N*-acetyl- $\beta$ -1,4-glucosaminide linkage. It can be processed to chitosan by partial alkaline *N*-deacetylation, with the degree of deacetylation affecting the crystallinity, surface energy and degradation rate of chitosan. Increasing degrees of deacetylation lead to decreases in the degradation rate. Kean and Thanou [87] have recently reviewed studies on the biodegradation of chitosan, with enzymes such as chitosanase or lysozymes being known to degrade it [263].

Cellulose esters represent an important class of biodegradable polymers, with cellulose acetate being used in high volume applications such as fibers, films and injection moulding thermoplastics. The biodegradation of cellulose acetate has been demonstrated in a number of studies, including under anaerobic conditions, and has recently been reviewed [264]. The degree of substitution is an important factor with respect to controlling biodegradation rates, with rates increasing as degrees of substitution fall. For example, Reese et al. [265] showed that cellulose acetates with a low degree of substitution (0.76 sites esterified per anhydroglucose monomer) were fully degraded by esterase while the fully substituted cellulose triacetate showed no sign of degradation. Likewise, Cantor and Mechals [266] found evidence of esterase activity on cellulose acetate membranes while there was none evident in cellulose triacetate materials. Gardner et al. [267] also showed that at a degree of substitution of 2.2, the cellulose acetate had a comparable biodegradability in compost to that of PHBV.

#### 5.2.7 Enzymatic hydrolysis of polymers containing main chain nitrogen bonds

Natural proteins tend to form disordered structures since they usually do not contain repeating units. As a result, they are generally susceptible to enzyme attack [34]. By contrast, synthetic polyamides have short and regular repeating units as well as strong inter-chain hydrogen bonding and thus have highly ordered crystalline morphologies, which makes them much more resistant to enzymes [34]. A decrease in molecular weight or modification of the structure through the introduction of substituents such as benzyl, hydroxy and methyl groups increases the rate of biodegradation [34]. Poly(amide-esters) and poly(amide-urethanes) have long repeating chains and are not as crystalline as polyamides, hence have a degradation rate that is between that of proteins and synthetic polyamides [34]. Poly(amide-enamines) are also susceptible to hydrolysis and biodegradation, both by fungi and enzymes. Polyureas prepared from lysine esters with 1,6-hexane diisocyanate and poly( $\epsilon$ -caprolactone) diol are readily

biodegradable [268]. Polyphosphazene, which contains alternating phosphorous and nitrogen atoms on the polymer backbone, which may be hydrolysed by enzymes to give phosphoric acid and ammonia derivatives [269, 270].

### **5.3 Non-hydrolytic enzymatic polymer degradation**

Some enzymatic processes are non-hydrolytic. For example, some fungi can secrete enzymes (peroxidases) that catalyse the oxidation of cellulose itself or of lower molecular weight oligomers produced from the enzymatic hydrolysis of cellulose. These enzymes produce hydrogen peroxide, which then undergoes free radical attack at the C2 – C3 positions of cellulose to form “aldehyde” cellulose, which is in turn very reactive and can hydrolyse to form oligomers (Fig. 16) [34].

In addition to degrading cellulose, peroxidases can be used to degrade polymers with carbon backbones, such as poly(vinyl alcohol) (PVA). PVA is widely used because of its solubility in water, and it can be easily degraded by microorganisms as well as enzymes such as secondary alcohol peroxidase [271].

### *Figure 16*

## **6 Environmental biodegradation**

Enzymatic degradation of polymers in a controlled aqueous environment, although complex, is still relatively predictable. In contrast, real world (environmental) biodegradation becomes much more complex to understand and predict. To our knowledge, to date, there is no model for predicting lifetimes in these circumstances for any class of biodegradable polymer. The prediction of polymer lifetime requires all elements of degradation to be accounted for [272] and this can be difficult to achieve in complex environments such as soil and seawater, where different processes such as swelling, cracking, creep, hydrolysis, leaching, and biodegradation can occur simultaneously [272].



Although there is no consensus in the literature as to what constitutes “biodegradation”, for the purposes of this review it is described as, “degradation of a polymeric item due to cell-mediated phenomena” (see Section 2.0). In essence, biodegradation refers to the process whereby polymers degrade due to biological activity (especially through enzymatic action) leading to a significant change in the chemical structure of that material. For a polymer to be classed as biodegradable according to CEN/TR 15351:2006, the material is also required to be mineralised into carbon dioxide, water and biomass during biodegradation [10], and that this biodegradation can be measured by standardised tests which specify extent of conversion in a given period of time under specific environmental conditions that must be met for the material to comply with a given standard [273-275]. This section of this review focuses on environmental/ambient conditions and so does not include degradation under composting conditions.

Since biological energy is obtained through the oxidation of reduced materials, biodegradation is essentially an electron transfer process [276], with electrons moving through metabolic pathways via electron transfer reactions to terminal electron acceptors. Typically in aerobic environments this terminal acceptor is oxygen. However, facultative or obligate anaerobic organisms can use other chemical species such as nitrate or sulphate as the terminal acceptor in the absence of oxygen.

There are a plethora of organisms and their associated enzymes that are capable of degrading polymer materials, with the three main types of microorganisms that are of particular importance in the degradation of biodegradable polymers being bacteria, fungi and algae.

For fungi, bacteria and algae, the primary influence they have on polymer degradation is through the enzymes they produce. The process of biodegradation is commonly presented as a sequence of steps [26]. Typically these are given as: biofragmentation, wherein the polymeric material is fragmented into smaller particles, followed by depolymerization

wherein the polymeric molecules are broken down into lower molecular weight oligomers, dimers and monomers (confusingly often called biofragmentation), then bioassimilation, whereby those products of depolymerization that can be taken up as a carbon source by microorganisms are used to produce energy, biomass, and various primary and secondary metabolites etc. The final stage, where these metabolites are completely oxidised and converted to carbon dioxide, nitrogen gas, methane, water and different salts is called mineralization.

However, in practice, in the natural environment, biotic and abiotic factors frequently act synergistically on biodegradable polymers in a complex interplay of processes and chemistries. Processes such as disintegration, dispersion, dissolution, erosion (which can be through enzymatic processes), abiotic hydrolysis and enzymatic degradation all come into play. Biodegradation processes can affect polymers through mechanical (grinding) processes, chemically-promoted degradation (acid/base catalysed hydrolysis), and particularly through excretion of substances other than enzymes that can change the environmental conditions such as pH or redox environment. Microscopic fungi and bacteria or other biological agents (such as earthworms, insects, roots, and rodents) can also fragment the product.

Soils in themselves are complex ecosystems with very divergent chemistries that encompass an enormous diversity of organisms. Numerous factors can affect the rate of biodegradation at any given location, including: soil moisture content, porosity, soil temperature, soil pH, oxygen availability, the presence of suitable microbes, the presence of contaminants and their concentration, the availability of nutrients, the presence of other electron acceptors, redox potential etc. [276].

The microbial degradation of polymers via enzymatic hydrolysis has further stages compared to that of isolated enzymes in aqueous solutions, including:

- 1) Attachment of microorganisms to the polymer surface
- 2) Release of enzymes
- 3) Enzymatic attack at the surface
- 4) Ester cleavage of macromolecular chains
- 5) Formation of oligomer fragments
- 6) Dissolution of fragments and subsequent surface erosion
- 7) Uptake of soluble fragments by microorganisms and growth of biomass

This process is also sensitive to all the parameters associated with polymer composition and material properties as described in Section 4.0 above.

The range of environments experienced by polymer materials during degradation can include: dry air, humid air, soil, a landfill, a composting environment, sewage, fresh-water or a marine environment. The kinetics of polymer degradation in the environment depends on the particular combination of key factors in that environment: oxygen concentration, water, other chemicals, daylight, degrading microorganisms, soil chemistry etc. [277]. More specifically, the environmental factors affecting the rate of degradation that is due to microorganisms include temperature, moisture level, atmospheric pressure, oxygen pressure, concentrations of acids and metals, and degree of exposure to light. Microorganism-specific factors include the community present, the concentration of organisms, whether or not they have enzymes for which the polymer is a substrate, the presence of trace nutrients for the microorganisms and the presence of inhibitors or predators.

Woolnough et al. [278] have identified that the colonization of biodegradable polymer surfaces by biofilms in a soil environment is dependent on factors such as surface roughness, hydrophobicity, charge, microbial population and whether or not the colonising population is capable of degrading the polymer in soil. In addition, there was found to be a correlation between biofilm coverage, surface roughness and rate of degradation. Both weight loss and

biofouling were found to follow the order: PHBV  $\approx$  PHB > polyhydroxyoctanoate > poly(*D,L*-lactide-*co*-glycolide) > poly(*D,L*-lactide) > ethyl cellulose.

Eubeler et al. [194] summarised the results of investigations into the biodegradation of different groups of synthetic polymers under different environmental conditions. Most of these studies focused on soil and compost, and polyesters were the main group of polymers investigated.

In another early study, Doi et al. [279] compared the biodegradation rates for biosynthetic and chemosynthetic polyesters in river water at 25°C under aerobic conditions in a temperature-controlled reactor. Based on weight loss and biological oxygen demand of the test solution, the rate of degradation of the synthetic polyesters were strongly dependent on the chemical structure and decreased in the following order: poly(ethylene succinate) > PCL > poly(ethylene adipate) > poly(butylene adipate) > poly(butylene sebacate) > poly(ethylene sebacate) = poly(butylene succinate) = poly(hexylene succinate) = poly( $\beta$ -propiolactone).

The following sections describe results from environmental degradation studies conducted on specific biodegradable polymer substrates.

## **6.1 Environmental degradation of biodegradable polymers**

### **6.1.1 Environmental degradation of PLA**

The processes and rates of PLA degradation in soil and compost have been studied for many years. Li and Vert [67] provided a comprehensive review of the biodegradation of aliphatic polyesters in 2002, with Hayes et al. providing an overview of the degradation of agricultural mulching films including those from PLA [280], and Shah et al. providing an update on biodegradable polymers in general in 2008 [60]. Overall, the accepted mechanism for PLA degradation is that it degrades through a two-stage process, involving abiotic hydrolysis at elevated temperatures as a first stage followed by biotic activity (microbial breakdown of the

hydrolysis degradation products) [281-285] (Fig. 17). It should be noted that in this Figure all strength and elongation of the polymer article will be lost in the hydrolysis stage. The chain scissions per number average polymer molecule(s) at embrittlement are 2.5 and at total fragmentation 4.4. In this period only 20% of the total carbon dioxide evolution has occurred.

*Figure 17*

Given this, the role of microorganisms in environmental degradation is still unclear. It is well known that PLA is less susceptible to environmental degradation than other aliphatic biodegradable polymers. The complete degradation in soil, for example, has been reported to take around a year [286], and around 60 to 100 days in compost at elevated temperature. Studies by Briassoulis and coworkers have also shown that PLA film in soil under field conditions is very slow, much slower than PHBV [287, 288]. In long term studies of PLA films and fibers in Mediterranean soils [288], it was found that the thinner the films, the more pronounced the degradation in general; all films became brittle after just one month, which was associated with cracks in thin films, with worms and roots clearly contributing to the degradation. Changes in elongation-at-break were much more evident than changes in other mechanical properties such as tensile strength. However, full disintegration took a much longer time, with limited degradation after 11 months. Overall, it was found that the type of soil (including pH, microorganisms present, temperature, humidity, etc.), *D* enantiomer content of initial PLA tested, and the shape and thickness and form of the material (*i.e.* the surface area of material exposed to soil; film *versus* fibers; single specimens *versus* mass of material) had a significant effect on the rate of biodegradation of PLA following soil burial.

Agarwal et al. [289] presented evidence that microorganisms were not involved in the environmental biodegradation process for PLA and that the degradation was purely due to abiotic hydrolysis. However, there is other evidence that microbial enzymes do play a role and that some exist that can degrade high molecular weight PLA [290-292]. This difference

can be attributed to the lower populations of PLA-degrading microorganisms in the environment, as well as variability of distribution. Sangwan and Wu [286] used molecular ecological techniques to directly identify the microbes associated with PLA degradation in compost and identified them as belonging to the genera *Paecilomyces*, *Thermomonospora*, and *Thermopolyspora*. Other microorganisms that have been identified as degrading PLA include *Actinomyces Amucolatopsis* type and a bacterium, *Bacillus brevis* [293]. By comparing PLLA degradation in natural compost (containing both fungi and bacteria) with sterilised soil inoculated with fungi, it has also been shown that degradation is faster in the former, potentially because there are synergistic effects between the microorganisms present in the soil [293, 294]. Karamanlioglu and Robson [295] compared the degradation of PLA coupons in sterile water, soil and compost at different temperatures with degradation in microorganism-rich soil and compost, and found that there was an acceleration of degradation in the microorganism-rich environments. All tensile strength was lost after 36 days in the microorganism-rich environments at 50°C, compared to 54-57 days for the sterile environments. However, no change in tensile strength or molecular weight was observed in any environment at either 25°C or 37°C after 1 year.

The molecular weight changes over time from a number of field studies have been collated and show a reasonable fit to a first-order kinetic model, while having very different rate constants, particularly for low temperature compost (at temperatures ranging from 9 to 42°C) *versus* soil (at ambient temperatures ranging from 5 to 21°C) [288]. This was attributed to a difference in number of microorganisms and the fact that they were able to consume the degradation by-products more rapidly, although the actual reason is likely to be much more complex.

Ho et al. in a series of studies [296-299] investigated the degradation of PLA under a range of environmental conditions, including in Costa Rican soils, compost rows, a banana field and in

soil-based respirometers. They also tested degradation in humidity and temperature-controlled chambers. In the laboratory studies, they found that the films started to lose their tensile properties when the  $M_w$  was in the range of 69,000 – 90,000 g/mol. Degradation was increased by an increase in temperature and humidity. A triple-layer film degraded faster under all conditions than a monolayer film, most likely due to the monolayer film having a higher initial molecular weight than the triple-layer film. Likewise, in the soil respirometer, an increase in temperature led to a very large increase in rate of biodegradation. In field-based soil studies, the degradation performance was comparable to the laboratory soil studies; it was estimated that the PLA films would be visibly degraded after 6 months in banana field soil as compared to 3 weeks in compost rows. However, in the Costa Rican banana field study, where the average temperature and humidity were higher and the material was exposed to additional stressors, the average degradation rate of PLA shrouds and ropes discarded into soil after use was higher than before and the materials lost their mechanical integrity after just 9 to 15 weeks. The  $M_w$  at embrittlement, where the materials had lost all of their tensile properties to the point of fragmentation, was higher than for the previous studies as well (at 90,000 to 140,000 g/mol), although the same starting materials were used. The  $M_w$  values at embrittlement reported in these studies are quite high, considering that the  $M_e$  of PLA is much lower than this (see Section 4.5.3) and other studies have shown that a much lower molecular weight is required before embrittlement/fragmentation is observed [197].

#### 6.1.2 Environmental degradation of Poly( $\epsilon$ -caprolactone) (PCL)

Fungal species are well known to promote the catalytic degradation of biodegradable polymers. Cook et al. [300] clearly showed the effect of degradation by *Penicillium funiculosum* mycelium on PCL solvent-cast films, with the degradation occurring in the amorphous regions between spherulites initially, before starting to degrade the crystalline regions at a later stage (Fig. 18).

### *Figure 18*

The biodegradation of PCL in both soil burial and activated sludge tests was found to be relatively fast, with rapid weight loss, indicating a bulk degradation mechanism. However, abiotic hydrolysis occurred more slowly [76], indicating that microorganisms play a significant role in the environmental biodegradation of PCL.

Tsuji and Suzuyoshi [301] found that the relative degradation rate, as judged by weight loss, tensile strength and Young's modulus results, decreased in the order PCL > PHB >> PLLA. In contrast to the study above, both the PCL and PHB films degraded by surface erosion rather than bulk degradation mechanism and this occurred inhomogeneously on the film surface due to the attachment of microbes, which caused the formation of pores and cracks, resulting in the loss of material properties.

#### 6.1.3 Environmental degradation of Poly(butylene adipate-*co*-terephthalate) (PBAT)

The use of PBAT as an agricultural mulch film for raised pineapple beds has been explored by Kijchavengkul et al. in a series of studies [302-304]. Above ground, photodegradation played a major role in film breakdown, causing the film to lose mechanical integrity after just 8 weeks, at a total solar irradiation dose of 800 MJ/m<sup>2</sup>. At this point, the gel content was 25% due to crosslinking and the  $M_w$  of the sol fraction plateaued at 10,000 g/mol. This cross-link formation limited the extent of subsequent mineralization and it was suggested that carbon black additives could limit the formation of gels by UV screening [305]. From FT-IR analysis, the degradation was found to be initiated on the upper (exposed) side of the film and then propagate through the matrix. The part of the film that was buried under the soil was much slower to degrade, with only a 50% decrease of  $M_w$  after 40 weeks.

In another application, Bilck et al. [306] outlined a field trial that employed biodegradable mulch films prepared by extrusion from cassava starch and poly(butylene adipate-*co*-



terephthalate) (PBAT) blends for use in strawberry production. It was found that the PBAT blend film had small cracks five weeks after being laid on the soil, and after another eight weeks there was a noticeable reduction in tensile strength, elongation-at-break and water sorption.

#### 6.1.4 Environmental degradation of Poly(butylene succinate) (PBS)

Some linear aliphatic polyesters such as PBS have been shown to be totally biodegraded in soil, through depolymerases or lipases produced by microorganisms. However, the degradation rate is strongly affected by the microbial community present as well as by a dynamic equilibrium between the microbial components [307].

Koitabashi et al. [308], for example, have trialled the use of a phylloplane fungi isolated from gramineous plants to accelerate the biodegradation of poly(butylene succinate-*co*-adipate) (PBSA) (Bionolle<sup>®</sup> 3001 G) and PBS (Bionolle<sup>®</sup> 1001G) films as well as a commercial PBS, PBSA and PBAT blend. Treatment of these films with the fungal strain on unsterilized soil resulted in 91, 24 and 15 wt% weight loss respectively after just 6 days, indicating that it was a very effective biodegradation agent for PBS-based polymers.

In another study, PBS plaques, prepared by compression moulding, showed a substantial decrease in molecular weight and the formation of vinyl groups and a range of oxygenated species when exposed to natural weathering in Malaysia for up to 6 months [309]. The neat PBS surfaces were severely deteriorated, with some large surface cracks, possibly due to thermal contraction and/or natural weathering. Chain scission during ageing due to degradation via a Norrish type II mechanism was proposed but is unlikely under terrestrial conditions due to the very limited absorption of the carbonyl groups of aliphatic polyesters in the region above 300 nm [310, 311].

### 6.1.5 Environmental degradation of PHA

Overall, PHA is very readily degraded in the environment, including the marine environment. Copolymers such as PHBV and poly(3-hydroxybutyrate-*co*-3-hydroxyhexanoate) have consistently been shown to degrade faster than PHB, regardless of environment [312], and, as expected, amorphous regions are also preferentially degraded. The following studies illustrate the typical fate of PHA under environmental conditions.

Hermida et al. [246] studied the effect of microbial degradation of PHBV (12 wt% HV) in a water-based culture on mechanical and other properties. They found that the rate of weight loss was sigmoidal and related to the cellular growth and activity of the bacteria. Colony-forming units increased through time as surface roughness and hence surface area increased. Crystallinity and molecular weight remained unchanged. The elastic modulus decreased only 10% after 45 days while the decrease in tensile strength was found to be proportional to the decrease in cross-sectional area. The rate of degradation decreased with an increase in crystallite size. The surface degradation behavior, therefore, was found to affect neither the elastic nor plastic behavior of the bulk. As the degradation proceeds, the size of the pores and microcracks at the surface increase until they achieve a critical size. At this size, the stress concentration factor around the crack is so high that a low stress promotes a catastrophic failure with practically no plastic deformation.

Sang et al. [313] showed that the degradation of PHBV films in soils was the result of a concerted effect of a microbial consortium comprising fungi, bacteria and actinomycetes. Over time, there was a distinctive increase in the fungal population, resulting in its eventual dominance. Fungi were shown to have a combination of high degradation ability as well as the ability to expand hyphae in three dimensions. This process was modelled mathematically [314] by taking into account the surface growth rate of hyphae as well as the degradation

ability of the fungal depolymerase. PHA degradation rates were shown to correlate with fungal biomass.

Hong and Yu [315] explored the effect of bacterial cells isolated from soil on PHBV degradation. They found that mixed bacterial cultures had a higher degradation rate and shorter adaptation time than a pure strain. The aerobic degradation rate was faster because of the higher cell growth and the greater number of attached proteins. Barren soil was shown to have fewer microbes rather than different species and was slower to degrade PHBV as a result. Because the amount of cell attachment remains constant, there is a zero-order rate model for PHBV degradation by soil microbes in an aqueous environment. The enzyme activity and the polymer degradation rate increase with an increase in temperature with an activation energy of around 67.8 kJ/mol. The enzymatic hydrolysis is the critical step in the degradation.

Arcos-Hernandez et al. [316] in soil-based degradation studies of a range of PHBV copolymers showed that a surface erosion mechanism dominated, and that the biodegradation rate was controlled by a combination of copolymer composition, crystallinity, micro-structure and surface morphology.

Tsuji et al. [317] evaluated the effect of pretreatment of PCL and PHB with alkali prior to soil degradation and found that this treatment enhanced the surface hydrophilicity of the films as well as the rate of biodegradation (as judged by weight loss and visual inspection). The relative rate of biodegradation was of the order  $PCL > PHB > PLLA$ , in agreement with other studies.

Blends of PHB with poly(butylene adipate-*co*-terephthalate) (PBAT) copolyesters, some containing 30 wt% wood flour, have been aged in simulated compound soil [318]. Mechanical properties were tracked over that time, and again there was significant mass loss

after 90 days and surface changes were evident, but there was little change in the bulk material properties. Similarly, samples of PHB with PHBV were aged in simulated soil at 24°C [319] as well as in compost. The decrease in tensile strength was the most significant change observed in mechanical properties over time, and the change was much more significant at higher temperatures, as expected. Surface roughness was used as an indicator of degree of biodegradation.

Mergaert et al. [320] showed evidence that confirmed the typical trend whereby mass loss of PHB and PHBV films was accelerated in soil at 40°C in comparison with 15 or 28°C. More importantly, while molecular weight declined slowly at the lower temperatures, the  $M_w$  decreased by more than a third in 200 days at 40°C. The PHBV copolymer degraded more rapidly than PHB.

Molitoris et al. [321] examined the effect of bacterial degradation on the surface properties of partially degraded sheets of poly(3-hydroxyvalerate) (PHV), PHB, PHBV and poly(3-hydroxyoctanoate) and derivatives following inoculation with selected species and found that the rate was dependent on surface area from all samples, with PHV being very slow to degrade relative to the other polymers. Film surfaces were pitted, with bacteria commonly found in the pits, and erosion patterns consistent with spherulitic banding were observed, indicating that amorphous areas were more rapidly degraded. Fracture surfaces showed that PHV and PHBV erosion was a surface phenomenon only while PHB samples showed the presence of deep fissures (attributed to the mechanical forces during manipulation and handling, i.e., artefacts of the experimental process).

Lim et al. [322] extended this work to study the degradation of the same medium chain length PHA films as used by Molitoris et al. [321] in tropical forest and mangrove soils for 112 days. At that stage, there was around 17% weight reduction for the samples buried in acidic forest soil, and only 3.0% reduction for those buried in alkaline forest soil by the side of a

stream and 4.5% reduction for those buried in mangrove soil. Only the films buried in the acidic forest soil showed any change in molecular weight, although this was slight. Mechanical properties were not tested.

Under anaerobic conditions, Abou-Zeid et al. [323] found that while PHA degraded more slowly than under aerobic conditions in sludge, PHB homopolymer degraded faster than PHBV in a range of environments, in contrast to the situation under aerobic conditions. PCL degraded slower than both. Other synthetic polyesters had only very limited biodegradability, particularly when aromatic groups were present. Overall, this was attributed to the types of organisms present in these environments, which seem to be specialised for PHB degradation and which are promoted by anaerobic degradation products such as acetate, crotonate or citrate. Morse et al. [312] found that annealing resulted in the acceleration of anaerobic degradation of poly(3-hydroxybutyrate-*co*-3-hydroxyhexanoate) copolymers in an anaerobic digester, which was attributed to an increase in void content after thermal annealing, allowing easier access for water and enzymes.

In the seawater accelerated aging of PHBV, Deroiné et al. [272] found that the water uptake was less than for distilled water, possibly due to the presence of mineral salts, and that a plateau was reached at different temperatures after 100 days. Again there was a good fit to the Arrhenius equation. Surface roughness increased for all samples, more so for natural seawater, which was assumed to be either due to surface hydrolysis or erosion due to microbial attack. In this case, the microbial population was as important as other factors such as temperature, with enzymatic degradation occurring from the surface via an erosion mechanism. The coexistence of two simultaneous degradation mechanisms was demonstrated – enzyme promoted chain scission at the surface and non-catalysed hydrolysis through the matrix, which was accelerated by increasing the temperature.

Kasuya, Doi and others also compared the biodegradabilities of a range of aliphatic esters in different natural waters, including fresh and marine. The samples tested included a range of PHAs along with some benchmark synthetic aliphatic polyesters such as PCL, PBS etc. [324-326]. PHBV (14 mol% 3HV) was very rapid to degrade under these conditions, with 100% weight loss and ~78% of theoretical maximum BOD produced after only 28 days under all conditions. By contrast, PHB was more resistant, particularly in seawater, with only 23% weight loss after 28 days, while P(3HB-*co*-4HB) was intermediate in performance. Poly(3-hydroxypropionate) (P(3HP)) and P[(*R*)-3HB-*co*-92%(*S*)-3HB] both lost only 1% of weight in that time. The synthetic polyesters were much more sensitive to composition, with weight losses ranging from 95% to 1% (see Section 6.0). The molecular weights of PHBV and P(3HB-*co*-4HB) decreased slightly as erosion proceeded while molecular weight dispersities remained constant, consistent with a surface degradation mechanism. By contrast, the strain-at-break decreased during exposure and the material gradually turned brittle, again reflecting the very significant effect of surface defects on mechanical properties.

In another river water study, Ho et al. [327] found that in natural tropical river water, a medium-chain-length PHA (mcl-PHA) lost 71.3% of its mass after 86 days. When the water was sterilised, the degradation rate slowed but did not stop, with 11% of mass lost in 28 days. The degradation rate of medium-chain-length-PHA in river water was faster than for other copolymers of PHA and may be due to the low crystallinity nature of the copolymer [327]. The PHA copolymer used in this study was composed in the main of 3-hydroxyoctanoate (C8) monomers, followed in decreasing order by 3-hydroxydecanoate (C10) monomers, 3-hydroxydodecanoate (C12) monomers, and 3-hydroxytetradecanoate (C14) monomers. It was noted that the C8 monomers were more readily removed from the polymer matrix, unlike the C10, 12 and 14 monomers, indicating that the rate of PHA hydrolysis depended on the side chain length of the monomers in these medium-chain-length materials.

Boskhomdzhev et al. [328] likewise showed that PHB and PHBV degradation *in vivo* in animal tissue and *in vitro* with enzymes occurred via two parallel pathways: abiotic polymer hydrolysis and enzymatic degradation.

Eldsäter et al. [329] clearly showed that water and air alone had little effect on the degradation of PHBV in a garden compost over 50 days, with the degradation being due to microbial action alone.

In a marine biodegradation study, Thellen et al. [330] explored the biodegradation of melt-processed films of PHB and three different PHBV copolymers (of differing 3HV content) in a simulated marine environment, which was inoculated with 13 marine microorganisms. All materials were highly degradable under static conditions, showing 89-99% biodegradation (based on mass loss) after 49 days. Under open, aquarium conditions with fluctuating temperatures and natural nutrient supply variation, however, the extent of degradation after 90 days was only between 30 and 73%.

Kaplan et al. [331] explored the effect of different environments on cellophane and two different PHBV films, and found that (as is commonly reported) the mechanical properties were lost more rapidly in soil contact than in marine water in the order soil > marine sediment > marine water. Composition also played a role, with the higher HV content copolymer degrading faster. Likewise, in another study by Mergaert, there was a significant difference in degradation rate depending on the environment (increasing in rate from freshwater ponds to seawater to soils to composts), particularly for PHBV copolymers [320]. Loss in elongation-at-break was significant from the start in soils, much more than in sterile buffers. It was thought that an increase in surface roughness may contribute to loss of toughness. In further studies [332, 333], they also found that PHB and PHBV degradation in low-temperature compost, freshwater, and seawater did not result in loss of molecular weight (presumably again because of surface erosion and solubilization/microbial consumption of

oxidised degradation products). Mass loss was less than 7% after half a year submerged in water and only 20% after 150 days in compost, with faster mass loss in seawater, and the PHBV samples degraded faster than PHB. However, again elongation-at-break for the PHBV samples was dramatically affected after just 30 days, although PHB (which had a low elongation-at-break to start with) was relatively unaffected.

Voinova, Volova and others [334-338] have also studied the degradation of PHAs in a wide range of natural environments. They presented evidence that the degradation of PHBV in natural water reservoirs may be slowed by lower inorganic phosphorus levels, and was also slower under anaerobic as opposed to aerobic conditions. It depends to a great extent on a complex set of weather-climatic conditions. In the tropical marine environment, the degradation rate is significantly influenced by the shape of the polymeric article and the preparation technique (compacted pellets versus films) rather than by the chemical composition. After 160 days there was significant molecular weight loss and increased dispersity; however, the crystallinity remained unchanged.

In blends of atactic and semicrystalline PHBV exposed to either a marine environment or compost with activated sludge, the degradation rate was dependent on the atactic content, with the amorphous phase degrading first, resulting in increased crystallinity. This in turn resulted in an initial increase in tensile strength and tensile modulus. The elongation-at-break, however, declined consistently and significantly from the start. Again, molecular weight was not significantly affected [339].

#### 6.1.6 Environmental degradation of starch

The hydrophilic and readily degradable nature of starch means that starches are generally modified to form a thermoplastic that is then blended with synthetic degradable polymers, such as PCL or poly(vinyl alcohols) or other polyesters [340]. A number of starch-containing



film products such as Mater-Bi<sup>®</sup> from Novamont have been commercialised and trialled extensively in the field [341].

Briassoulis et al. [342] tested Mater-Bi<sup>®</sup> films in low tunnel, direct cover and mulching film applications over a period of three years in four different European locations and found that the mechanical degradation of the films was directly related to their thickness. In only 1 week, the 12 micron films had lost both tensile strength and elongation-at-break, with crack/tear propagation resulting in loss of material integrity. The starch component was shown to degrade first.

Martin-Closas et al. [343] reviewed the in-field performance of the commercial mulch films Mater-Bi<sup>®</sup>, Biofilm<sup>®</sup> and Bioflex<sup>®</sup> (Bi-OPL) (the first two of which are thermoplastic starch – polymer blends, and the last is a PLA-based blend). The site was in Spain (under a Mediterranean-Continental climate), and the use was for tomato plants. The films were found to have a high near-IR transparency but very low photosynthetically active radiation (PAR) transmittance, both being comparable to polyethylene. The long-wave infrared transmittance was lower than polyethylene in all biomaterials, increasing the greenhouse warming effect. However, the films were twelve times more permeable to water vapour than polyethylene. In line with the research outlined above, the elongation-at-break was the most sensitive parameter to aging, declining rapidly in the first 30-60 days in the above-ground portion, with Mater-Bi<sup>®</sup> being particularly fast. Strength also declined for all biodegradable polymer films, though less significantly. On a qualitative scale, the rate of degradation for the films overall (both above and below ground) was assessed as Biofilm<sup>®</sup> > Mater-Bi<sup>®</sup> > Bioflex<sup>®</sup> (Bi-OPL) >> polyethylene.

The degradation of an acylated starch-plastic mulch film was evaluated by Fernando et al. [344] in a grey lowland and a volcanic andosol soil. In both laboratory and field experiments, the weight loss of the plastic films was on the average 50% greater in the volcanic andosol

soil than in the grey lowland soil. Elongation-at-break decreased to < 30% (from 250%) after ~4-8 weeks in both the lab and field in both soils. By contrast, while there were significant losses in tensile strength over time, this was a much slower process, particularly in the field.

Another study of Mater-Bi® for soil mulching and low tunnel applications was undertaken in Italy [345]. In this case, the lifetime of the mulches was assessed to be 9 months while that of the tunnels was 6 months, although this was based on the films remaining “almost intact” for that period. The difference was in part attributed to the increased temperature under the tunnels. After one year under soil, 96% of the initial mass was lost.

Calmon [346] compared the degradation on soil-burial of twenty different sample types (including PHBV/HV, PLA, PCL, PCL-starch, paper, PE and PE-starch) at four different locations for up to 24 months. Biodegradation was monitored through weight and area loss (using image analysis). The general behavior of polymers was the same at different sites, and there was no correlation between weight loss and location. The aim of this work was to ultimately be able to predict biodegradability based on laboratory results and site characteristics (climate and soil). However, to date, such correlations have not been developed.

#### 6.1.7 Environmental degradation of cellulose-based polymers

Andrady et al. [347] reviewed, in 1992, a Navy research program that assessed chitosan and regenerated cellulose for use as marine-degradable polymers in a range of environments. After 6 weeks of marine exposure, regenerated cellulose samples disappeared; after 10 weeks, chitosan samples became brittle and separated. It was found that while chitosan was faster to degrade in anaerobic soil environments, the opposite occurred in the marine sediment environment. Aerobic degradation was much higher than anaerobic degradation for

both biopolymers. The addition of urea and potassium phosphate increased the soil degradability of the cellulose.

## **6.2 Biodegradable polymer degradation and extrapolated lifetime prediction under elevated temperatures**

In general, the thermal degradation of thermoplastic biodegradable polymers occurs at polymer melt temperatures, well in excess of those experienced under ambient environmental conditions and thus beyond the scope of this review. However, as previously discussed, the kinetics of the hydrolytic processes of biodegradation have a temperature dependence which fits the Arrhenius equation in nature, and are also strongly influenced by the crystalline nature of the sample and the glass transition temperature, both of which can be affected by temperature and/or changed during the reaction process. For example, some biodegradable materials have melting temperatures close to ambient, such as PCL ( $T_m \sim 60^\circ\text{C}$ ) and polyester-starch composites such as Mater-Bi<sup>®</sup> ( $T_m \sim 64^\circ\text{C}$ ) [26]. As discussed in Section 3.2, polymer properties change very significantly above and below the  $T_g$ . It is important to understand the kinetics above and below the  $T_g$  to understand whether or not it is appropriate to extrapolate higher temperature data back to ambient conditions.

Regarding glass transition, the  $T_g$  often decreases during hydrolytic degradation as a result of chain scission allowing the polymer chains to move relative to one another. If the  $T_g$  shifts from above to below the testing temperature for mechanical properties, this could cause an interpretation of a sudden increase in material property loss due to increased molecular weight decrease whereas the actual mechanism is different. For example, the kinetics of diffusion of water and reaction products, increasing the mobility within the polymer matrix and changing the degradation rate. In addition, there can be a shift in the crystalline structure with temperature. An example is the polymer poly(butylene adipate), which is found in the  $\beta$ -

crystalline form below 27°C, in the  $\alpha$ -crystalline form above 32°C, and in a mixed form in between. The  $\alpha$ -crystals are more readily hydrolysed by lipase [348].

Accelerating the degradation rate of biodegradable polymers is a very attractive proposition as a way of estimating lifetime in use. For example, PLLA interference screws (used for fixation of bone-tendon-bone and soft tissue grafts) took 4 years to fully degrade as an implant in body at ~ 37°C, whereas similar polymers took only 25 days to fully degrade at 70°C ([24] and refs therein). However, the concern again is whether or not the change in temperature affects the mechanism.

Of significance in this work and the work by Lyu et al. [16] was the observation that a master curve could be constructed using the time-temperature equivalence principle so the lifetime could be predicted for a range of exposure conditions [16]. Both Deng et al. [165] and Weir et al. [164] also studied the effect of temperature on changes in mechanical properties and found that, regardless of temperature, a plot of tensile strength as a function of  $M_n$  fell on the same curve. This principle should be translatable to conditions found in environmental exposure.

In terms of using accelerated (higher temperature) aging for lifetime prediction, Lyu et al. [16] explored the simple system of hydrolysis of amorphous PLA in distilled water. They found that there was a slow to fast degradation rate transition at around 100 to 110 kDa. At this point, the dispersity also went from constant with molecular weight loss to broadening.

Deroiné et al. [191] investigated the accelerated aging and lifetime prediction of 4 mm-thick plaques of PHBV in distilled water. They found that under these simple conditions, strain at break did show a temperature dependence governed by surface properties. However, water diffusion did show an Arrhenius dependence.

Similarly, this team [272] investigated the degradation of PLA in seawater and found that there was a shift in mechanism of degradation above 40°C, presumably due to plasticization, making lifetime prediction through accelerated aging difficult for this material. The increased rate of degradation was thought to be due to a number of possibilities: osmotic cracking, or creation of diffusion paths induced by cracks, or hydrolysis process products such as carboxylic acids having a strong water affinity, but most likely due to pore formation through the autocatalytic effect. A linear relationship between water uptake and stress-at-break was observed.

### **6.3 Accelerated biodegradable polymer degradation under ultraviolet exposure**

In lifetime prediction of polymers, the effect of exposure to the outdoor environment is frequently simulated in the laboratory using accelerated weathering devices. These combine ultraviolet (UV) light irradiation with controlled temperature, humidity and “rainfall” exposure to assess the combined effects of photodegradation, photooxidation and abiotic hydrolysis. The ASTM standard G155 - 13 outlines one such protocol using a Xenon-arc lamp to simulate the natural sunlight spectrum. The assumption behind such tests is that through application of the Arrhenius equation and calculation of the total irradiation exposure (assuming a reciprocity relation, *i.e.*, the total dose to fail is independent of dose rate) a relationship can be derived to estimate polymer lifetime under natural weathering exposure.

Such accelerated weathering is less commonly applied to biodegradable polymers since their lifetime in the environment is dependent on many complex factors, particularly biotic, as outlined above, and therefore weathering studies conducted in isolation of the other environmental factors are unlikely to permit robust predictive models to be developed.

Of the studies that have been conducted, some have been performed under short-wave irradiation rather than wavelengths found in terrestrial sunlight. The C=O bond in the main chain of polyesters such as PLA has absorption bands at 280 nm (due to  $n-\pi^*$  excitation) and

~190 nm (due to  $n-\sigma^*$  excitation) [310]. The molar extinction coefficient for PLA at 280 nm is very low (less than 100 L/(mol cm)), but nevertheless photodegradation can occur [310]. However, because radiation intensities in shorter wavelengths below 280 nm are very weak in sunlight and rapidly drop in intensity below 300 nm the mechanisms of photodegradation under short-wave irradiation do not correlate well with those under natural weathering.

Under short-wave radiation, photodegradation can affect biodegradable polymers through Norrish Type I/II reactions and/or crosslinking reactions and oxidative processes [349]. Ikada for example showed that for PHBV (in the form of the commercial product Biopol) and PCL, C=C double bonds and carboxylic OH groups increased significantly under UV irradiation from a medium pressure mercury lamp, which was attributed to a Norrish Type II mechanism and associated with rapid chain scission [350]. These effects were not observed under terrestrial exposure. Similarly, when a Pyrex<sup>®</sup> plate was used to cut off radiation from a lamp below 300 nm, Janorkar et al. showed that PLA photodegradation was minimised [351] compared to the effects of irradiation using wavelengths from 232–500 nm. However, these authors proposed a different mechanism for the accelerated photodegradation of PLA involving photolysis of the backbone at C=O leading to dehydrogenation plus photooxidation of the main chain tertiary carbons leading to formation of hydroperoxide derivatives that subsequently degrade to carboxylic acids and unstable diketones.

Other studies have used natural sunlight simulators as opposed to short-wave radiation, to more appropriately model environmental exposure. Kijchavengkul et al., for example, found that for a range of PBAT aromatic-aliphatic copolyester films, long-range UV exposure (320 – 400 nm) resulted in crosslinking of polymer chains with the formation of a gel fraction, with aromatic groups playing a significant role in the crosslinking [302]. These authors found that crosslinking was associated with a reduction in the rate of biodegradation as given by reduced mineralization. By contrast, Stloukal et al. also found that polyesters with in-chain

aromatic groups experienced a significant degree of crosslinking under long-wave irradiation (320 – 400 nm), but found that this was not associated with any decrease in biodegradation rate with the key factor being the change in specific surface area. For PLA, however, irradiation resulted in both chain scission and chain recombination rather than cross-linking [305]. This is consistent with the natural weathering study of a PLA-cloisite nanocomposite [352], where natural weathering exposure led to the formation of vinyl unsaturation, carbonyls, anhydrides and hydroperoxide groups as a result of the occurrence of several chemical mechanisms simultaneously, with chain scission presumed to be the dominant phenomenon.

Overall, the use of accelerated weathering chambers for the lifetime estimation of biodegradable polymers appears to be a problematic strategy, with further research required to determine the mechanism of degradation and whether the UV exposure alters the rate of biodegradation of the polymer.

#### **6.4 Mechanical and other effects on biodegradable polymer degradation**

The effects of mechanical forces on biodegradable polymer degradation need to be taken into account in lifetime prediction. Mechanical degradation can occur due to compression, tension and/or shear forces [26]. Such stresses can activate or have an impact on the kinetics of biodegradation processes, either as a result of loading under service or due to residual stress arising during manufacturing [353]. For instance, fungal or algal growth on and in polymeric substrates can be associated with physical deformation, such as small-scale swelling and bursting [354].

Degradation due to loading in-service is more significant in materials subjected to mechanical stress such as sutures, scaffolds for tissue engineering, and fixation devices [32]. Physical forces such as heating/cooling, freezing/thawing, or wetting/drying, as well as air and/or water turbulence, can cause mechanical damage such as the cracking of polymeric materials

[355]. Such Environmental Stress Cracking (ESC) has recently been reviewed by Robeson [19], with the mechanisms being discussed in detail. Such environmental failures of semi-crystalline and amorphous engineering thermoplastics can occur in the absence of apparent chain scission events or obvious chemical changes to the polymer [19]. This failure mechanism may be seen when a polymer is under mechanical stress well below the yield point and in contact with a swelling, but non-reactive, solvent or chemical. In identifying environmental factors responsible for shortening the service life of a polymer, it is important to account for physical effects such as ESC which could otherwise mask the underlying oxidative or hydrolytic processes ([356] p. 546 et seq.). This important mechanism of degradation is not often taken into account in the case of biodegradable polymers. One study by Farias et al. [357] showed that sodium hydroxide may act as a strong stress cracking agent for PHBV copolymers, significantly affecting the mechanical properties. SEM imaging confirmed that catastrophic failure was associated with extensive surface damage. The magnitude of the effects increased with decreasing crosshead speed and increasing load level during mechanical testing. Even though effects from hydrolysis could not be ruled out, the study demonstrated that mechanical stress during ageing of biodegradable polymers can have a significant impact on material property changes over time.

A recent review by Li et al. [358] summarises the effects of external stress on biodegradable orthopaedic materials, effects that may be generalized to the broader domain of biodegradable polymers under a range of environmental stresses. In that review, the response of biodegradable polymers to both static and dynamic stress is described, with studies on the effects of dynamic stress on the degradation of biodegradable polymers being summarised in

#### *Table 4*



The influence of static tensile loading on polymers can be described using the Zhurkov equation (62), as follows:

$$K_f = K_0 e^{[-(E_a - \phi \sigma_x)/RT]} \quad (62)$$

with  $K_0$  the Arrhenius frequency factor,  $K_f$  the rate of bond rupture events,  $E_a$  the activation energy,  $\sigma_x$  the tensile stress, and  $\phi$  the coefficient linked to the activation volume. This equation can be coupled to the broader biodegradation models outlined above to include static stress effects into models of lifetime prediction by lowering the activation energy for chain scission due to applied stress.

Another approach is to assume that degradation is driven by strain alone, ignoring the effects of hydrolysis, UV radiation, oxygen diffusion and temperature [364]. This approach was adopted by Soares et al. [365, 366] who developed a sophisticated model to account for the accelerated breakdown of PLA articles (in this case, stents) under uniaxial extension. This model explicitly took into account both surface and bulk erosion. With more complex geometry, inhomogeneous deformation and hence inhomogeneous degradation takes place, with failure most likely occurring at stress points such as stent rings and junction points. Equations were developed to model this response based on a constitutive modelling approach, taking into account characteristics such as stress relaxation and creep. Hayman et al. [175] in turn explored the effect of static and dynamic load on the degradation of PLLA stent fibers *in vitro* over 15 months. Both types of loading increased the rate of loss of mechanical properties, more significantly under dynamic load. The conditions used during processing of the polymers may also have an impact on the kinetics of polymer degradation. Melt-based processing techniques (injection moulding, extrusion, compression moulding) are performed at higher than melt temperatures, and in the case of the first two processes, under high shear. Thus, some molecular weight loss through thermal degradation or

mechanoscission is common. In addition, there can be partial material orientation, particularly in the case of injection moulding, which is typically higher in the skin than the bulk. This leads to differences in degradation rates, with the skin being slower to degrade than the bulk [198].

## **7 Summary and conclusions**

The ultimate goal of lifetime modelling for all classes of polymers is to predict the degradation rate, taking all controlling variables as input. However, at this point, both existing models and the fundamental understanding of degradation mechanisms and interactions, particularly in a natural environment, are not sufficiently advanced as to be able to achieve this with a single unified theory. From this review, common approaches have emerged that are able to be translated from the disparate fields of degradation chemistry, drug delivery, and enzyme chemistry by using the broader framework of structure-property relations to relate macromolecular and chemical changes to engineering properties. Important concepts that are translatable across the broad class of biodegradable polymers are:

1. The controlling factors for hydrolytic degradation are the kinetics of hydrolysis reactions and whether under the conditions of exposure the sample thickness is such that the degradation will occur in the bulk or progressive surface erosion will occur. This is controlled by the kinetics of water diffusion versus the chemical kinetics of hydrolysis. Many of the models reviewed here collapse back to this single concept.
2. The changes to the polymer strength over time may be related to the progressive increase in the number of polymer chain scissions that can in turn be linked to polymer hydrolysis kinetics in 1, above, and so modelled.
3. Stochastic modelling offers the opportunity to visualize the processes that control the change in properties and recognizes the heterogeneity of the degradation process. In principle

the growth of the degradation zones to the critical size for fracture under the applied stress provides a link to the engineering properties of the polymer.

4. Environmental biodegradation introduces enzyme-mediated processes that unlike hydrolysis are more readily steric and surface restricted. Comprehensive studies of only a few polymers (e.g., the polyhydroxyalkanoates: PHBV etc.) have been made and demonstrate the complexity of degradation reactions and the sensitivity of the kinetics of degradation to the microbial environment.

Further development in the field will draw on the sensitive analytical techniques available to detect the earliest changes in polymer chemistry signalling the onset of rapid loss in properties and thus safe service lifetime. This may provide an adjunct to the accelerated ageing methodologies that are currently employed in lifetime prediction.

### **Acknowledgements**

The authors would like to thank and acknowledge the Cooperative Research Centre for Polymers and Integrated Packaging for financial support of this work. Dr Paul Luckman is acknowledged with thanks for his assistance with graphic design and artistry.

## References

- [1] Lemos W. Polymers demand in Africa to grow nearly 50% by 2020. <http://www.icis.com/resources/news/2014/10/14/9829036/polymers-demand-in-africa-to-grow-nearly-50-by-2020/>. 2016. 1 pp. accessed February 2017
- [2] Anonymous, Plastemart.com. Strong growth in global polyethylene industry expected to continue at a CAGR of 3.5% over next 5 years. <http://www.plastemart.com/Plastic-Technical-Article.asp?LiteratureID=1971&Paper=strong-growth-global-polyethylene-industry-3.5-percent-over-5-years/>. 2014. 1 pp. accessed February 2017
- [3] Rappaport H. Ethylene and polyethylene global overview. SPI Film & Bag Confer; 2011. 46 pp.
- [4] Rochman CM, Browne MA, Halpern BS, Hentschel BT, Hoh E, Karapanagioti HK, Rios-Mendoza LM, Takada H, Teh S, Thompson RC. Classify plastic waste as hazardous. *Nature* 2013;494:169-71.
- [5] Reddy MM, Vivekanandhan S, Misra M, Bhatia SK, Mohanty AK. Biobased plastics and bionanocomposites: Current status and future opportunities. *Prog Polym Sci* 2013;38:1653-89.
- [6] Bat E, Zhang Z, Feijen J, Grijpma DW, Poot AA. Biodegradable elastomers for biomedical applications and regenerative medicine. *Regener Med* 2014;9:385-398.
- [7] Verdu J. Oxidative ageing of polymers. New York: John Wiley and Sons; 2012. 355 pp.
- [8] Pickett JE, Coyle DJ. Hydrolysis kinetics of condensation polymers under humidity aging conditions. *Polym Degrad Stab* 2013;98:1311-20.
- [9] Vieira AC, Vieira JC, Ferra JM, Magalhaes FD, Guedes RM, Marques AT. Mechanical study of PLA-PCL fibers during in vitro degradation. *J Mech Behav Biomed Mater* 2011;4:451-60.
- [10] Anonymous. PD CEN/TR15351:2006 Plastics - Guide for vocabulary in the field of degradable and biodegradable polymers and plastic items. London: British Standards; 2006. 23 pp.
- [11] Anonymous. ASTM Standard D883-12 "Standard terminology relating to plastics". West Conshohocken, PA: ASTM International; 2012. 16 pp.
- [12] Pospisil J, Horak Z, Krulis Z, Nespurek S. The origin and role of structural inhomogeneities and impurities in material recycling of plastics. *Macromol Symp* 1998;135:247-63.

- [13] Singh B, Sharma N. Mechanistic implications of plastic degradation. *Polym Degrad Stab* 2008;93:561-84.
- [14] Fayolle B, Colin X, Audouin L, Verdu J. Mechanism of degradation induced embrittlement in polyethylene. *Polym Degrad Stab* 2007;92:231-8.
- [15] Nikolic M, Gauthier E, Colwell J, Laycock B, Yeh CL, Cash G, Halley P, Bottle S, George GA. Real-world factors that impact polyolefin lifetimes. In: Lewicki JPP, Overturf G, editors. *Lifetimes and Compatibility of Synthetic Polymers*. Beverly, MA: Scrivener Publishing LLC; 2017. Chapter 7, *in press*.
- [16] Lyu SP, Schley J, Loy B, Lind D, Hobot C, Sparer R, Untereker D. Kinetics and time-temperature equivalence of polymer degradation. *Biomacromolecules* 2007;8:2301-10.
- [17] Doi Y, Kanesawa Y, Kawaguchi Y, Kunioka M. Hydrolytic degradation of microbial poly(hydroxyalkanoates). *Makromol Chem, Rapid Commun* 1989;10:227-30.
- [18] Farrar DF, Gillson RK. Hydrolytic degradation of polyglyconate B: The relationship between degradation time, strength and molecular weight. *Biomaterials* 2002;23:3905-12.
- [19] Robeson LM. Environmental stress cracking: A review. *Polym Eng Sci* 2013;53:453-67.
- [20] Choi BH, Chudnovsky A, Paradkar R, Michie W, Zhou ZW, Cham PM. Experimental and theoretical investigation of stress corrosion crack (SCC) growth of polyethylene pipes. *Polym Degrad Stab* 2009;94:859-67.
- [21] Naebe M, Abolhasani MM, Khayyam H, Amini A, Fox B. Crack Damage in Polymers and Composites: A Review. *Polym Rev* 2016;56:31-69.
- [22] Celina MC. Review of polymer oxidation and its relationship with materials performance and lifetime prediction. *Polym Degrad Stab* 2013;98:2419-29.
- [23] Celina M, Gillen KT, Assink RA. Accelerated aging and lifetime prediction: Review of non-Arrhenius behaviour due to two competing processes. *Polym Degrad Stab* 2005;90:395-404.
- [24] Han XX, Pan JZ, Buchanan F, Weir N, Farrar D. Analysis of degradation data of poly(*L*-lactide-*co-L,D*-lactide) and poly(*L*-lactide) obtained at elevated and physiological temperatures using mathematical models. *Acta Biomater* 2010;6:3882-9.

- [25] Ammala A, Bateman S, Dean K, Petinakis E, Sangwan P, Wong S, Yuan Q, Yu L, Patrick C, Leong KH. An overview of degradable and biodegradable polyolefins. *Prog Polym Sci* 2011;36:1015-49.
- [26] Lucas N, Bienaime C, Belloy C, Queneudec M, Silvestre F, Nava-Saucedo JE. Polymer biodegradation: Mechanisms and estimation techniques. *Chemosphere* 2008;73:429-42.
- [27] Gutierrez-Wing MT, Stevens BE, Theegala CS, Negulescu II, Rusch KA. Aerobic biodegradation of polyhydroxybutyrate in compost. *Environ Eng Sci* 2011;28:477-88.
- [28] Vieira AC, Marques AT, Guedes RM, Tita V. 4D Numerical analysis of scaffolds: a new approach. In: Fernandes PR, Bartolo PJ, editors. *Computational Methods in Applied Sciences*. Vol 31. 2014. p. 69-95.
- [29] Mainil-Varlet P, Curtis R, Gogolewski S. Effect of in vivo and in vitro degradation on molecular and mechanical properties of various low-molecular-weight polylactides. *J Biomed Mater Res* 1997;36:360-80.
- [30] Buchanan FJ, editor. *Degradation rate of bioresorbable materials*. Cambridge UK: Woodhead Publishing Ltd; 2008. 424 pp.
- [31] Gleadall A, Pan JZ, Krufft MA, Kellomaki M. Degradation mechanisms of bioresorbable polyesters. Part 1. Effects of random scission, end scission and autocatalysis. *Acta Biomater* 2014;10:2223-32.
- [32] Gopferich A. Mechanisms of polymer degradation and erosion. *Biomaterials* 1996;17:103-14.
- [33] Vroman I, Tighzert L. Biodegradable Polymers. *Materials* 2009;2:307-44.
- [34] Chandra R, Rustgi R. Biodegradable polymers. *Prog Polym Sci* 1998;23:1273-335.
- [35] Vieira AC, Guedes RM, Tita V. Considerations for the design of polymeric biodegradable products. *J Polym Eng* 2013;33:293-302.
- [36] Kuhn W. The kinetics of the decomposition of high molecular chains. *Ber Dtsch Chem Ges* 1930;63:1503-9.
- [37] Costache AD, Ghosh J, Knight DD, Kohn J. Computational Methods for the Development of Polymeric Biomaterials. *Adv Eng Mater* 2010;12:B3-B17.
- [38] Sackett CK, Narasimhan B. Mathematical modeling of polymer erosion: Consequences for drug delivery. *Int J Pharm* 2011;418:104-14.
- [39] Siepmann J, Gopferich A. Mathematical modeling of bioerodible, polymeric drug delivery systems. *Adv Drug Deliv Rev* 2001;48:229-47.

- [40] Arifin DY, Lee LY, Wang CH. Mathematical modeling and simulation of drug release from microspheres: Implications to drug delivery systems. *Adv Drug Deliv Rev* 2006;58:1274-325.
- [41] Farrar D. Modelling of the degradation processes for bioresorbable materials. In: Buchanan CM, editor. *Degradation rate of bioresorbable materials: Prediction and Evaluation*. Cambridge, England: Woodhead Publishing; 2008. p. 183-206.
- [42] Lao LL, Venkatraman SS, Peppas NA. Modeling of drug release from biodegradable polymer blends. *Eur J Pharm Biopharm* 2008;70:796-803.
- [43] Versypt ANF, Pack DW, Braatz RD. Mathematical modeling of drug delivery from autocatalytically degradable PLGA microspheres - a review. *J Controlled Release* 2013;165:29-37.
- [44] Grassi M, Grassi G. Application of mathematical modeling in sustained release delivery systems. *Expert Opin Drug Delivery* 2014;11:1299-321.
- [45] Zhang HB, Zhou L, Zhang WJ. Control of scaffold degradation in tissue engineering: a review. *Tissue Eng Part B* 2014;20:492-502.
- [46] Peppas NA, Narasimhan B. Mathematical models in drug delivery: how modeling has shaped the way we design new drug delivery systems. *J Controlled Release* 2014;190:75-81.
- [47] Zong XH, Wang ZG, Hsiao BS, Chu B, Zhou JJ, Jamiolkowski DD, Muse E, Dormier E. Structure and morphology changes in absorbable poly(glycolide) and poly(glycolide-*co*-lactide) during in vitro degradation. *Macromolecules* 1999;32:8107-14.
- [48] Kobayashi S, Yamaji S. Analytical prediction of hydrolysis behavior of tricalcium phosphate/poly-*L*-lactic acid composites in simulated body environment. *Adv Compos Mater* 2014;23:211-23.
- [49] von Burkersroda F, Schedl L, Gopferich A. Why degradable polymers undergo surface erosion or bulk erosion. *Biomaterials* 2002;23:4221-31.
- [50] Valenzuela LM, Michniak B, Kohn J. Variability of water uptake studies of biomedical polymers. *J Appl Polym Sci* 2011;121:1311-20.
- [51] Albertsson AC, Karlsson S. Aspects of biodeterioration of inert and degradable polymers. *Int Biodeterior Biodegrad* 1993;31:161-70.
- [52] Gautieri A, Mezzananza A, Motta A, Redealli A, Vesentini S. Atomistic modeling of water diffusion in hydrolytic biomaterials. *J Mol Model* 2012;18:1495-502.

- [53] Schmitt EA, Flanagan DR, Linhardt RJ. Importance of distinct water environments in the hydrolysis of poly(*D,L*-lactide-*co*-glycolide). *Macromolecules* 1994;27:743-8.
- [54] Jiang L, Zhang J. Biodegradable polymers and polymer blends. In: Ebnesajjad S, editor. *Handbook of Biopolymers and Biodegradable Plastics*. Boston: William Andrew Publishing; 2013. p. 109-28.
- [55] Jiang L, Zhang J. Biodegradable and biobased polymers. In: Myer K, editor. *Applied Plastics Engineering Handbook*. Oxford: William Andrew Publishing; 2011. p. 145-58.
- [56] Japar S, Salit MS. The development and properties of biodegradable and sustainable polymers. *J Polym Mater* 2012;29:153-65.
- [57] Leja K, Lewandowicz G. Polymer biodegradation and biodegradable polymers - a review. *Pol J Environ Stud* 2010;19:255-66.
- [58] Rudnik E. Biodegradability Testing of Compostable Polymer Materials. In: Ebnesajjad S, editor. *Handbook of Biopolymers and Biodegradable Plastics*. A volume in *Plastics Design Library*. Boston: William Andrew Publishing; 2013. p. 213-63.
- [59] Averous L, Pollet E. Biorenewable nanocomposites. *MRS Bull* 2011;36:703-10.
- [60] Shah AA, Hasan F, Hameed A, Ahmed S. Biological degradation of plastics: A comprehensive review. *Biotechnol Adv* 2008;26:246-65.
- [61] Yu L, Dean K, Li L. Polymer blends and composites from renewable resources. *Prog Polym Sci* 2006;31:576-602.
- [62] St. Pierre T, Chiellini E. Biodegradability of synthetic polymers used for medical and pharmaceutical applications: Part 1 - Principles of hydrolysis mechanisms. *J Bioact Compat Polym* 1986;1:467-97.
- [63] Park K, Shalaby WSW, Park H. *Biodegradable hydrogels for drug delivery*. Lancaster: Technomic Publications; 1993. 257 pp.
- [64] Tsuji H, Yamada T. Blends of aliphatic polyesters. VIII. Effects of Poly(*L*-lactide-*co*- $\epsilon$ -caprolactone) on enzymatic hydrolysis of poly(*L*-lactide), poly( $\epsilon$ -caprolactone), and their blend films. *J Appl Polym Sci* 2003;87:412-9.
- [65] Jenkins MJ, Cao Y, Howell L, Leeke GA. Miscibility in blends of poly (3-hydroxybutyrate-*co*-3-hydroxyvalerate) and poly( $\epsilon$ -caprolactone) induced by melt blending in the presence of supercritical CO<sub>2</sub>. *Polymer* 2007;48:6304-10.
- [66] Huneault MA, Li HB. Preparation and properties of extruded thermoplastic starch/polymer blends. *J Appl Polym Sci* 2012;126:E96-E108.



- [67] Li S, Vert M. Biodegradation of aliphatic polyesters. In: Scott G, editor. Degradable Polymers. 2nd ed: Kluwer Academic Publishers; 2002. p. 43-87.
- [68] Vert M, Li SM, Spenlehauer G, Guerin P. Bioresorbability and biocompatibility of aliphatic polyesters. *J Mater Sci Mater Med* 1992;3:432-46.
- [69] Nair LS, Laurencin CT. Biodegradable polymers as biomaterials. *Prog Polym Sci* 2007;32:762-98.
- [70] Jones D, editor. *Injectable fillers: Principles and practice*. West Sussex: Wiley-Blackwell; 2010.. 192 pp.
- [71] Mishra GP, Kinser R, Wierzbicki IH, Alany RG, Alani AWG. In situ gelling polyvalerolactone-based thermosensitive hydrogel for sustained drug delivery. *Eur J Pharm Biopharm* 2014;88:397-405.
- [72] Song Z, Zhu W, Yang F, Liu N, Feng R. Preparation, characterization, in vitro release, and pharmacokinetic studies of curcumin-loaded mPEG–PVL nanoparticles. *Polym Bull* 2014;72:75-91.
- [73] Tang D, Macosko CW, Hillmyer MA. Thermoplastic polyurethane elastomers from bio-based poly( $\delta$ -decalactone) diols. *Polym Chem* 2014;5:3231-7.
- [74] Martello MT, Schneiderman DK, Hillmyer MA. Synthesis and melt processing of sustainable poly( $\epsilon$ -decalactone)-block-poly(lactide) multiblock thermoplastic elastomers. *ACS Sustain Chem Eng* 2014;2:2519-26.
- [75] Zhang JQ, Kasuya K, Takemura A, Isogai A, Iwata T. Properties and enzymatic degradation of poly(acrylic acid) grafted polyhydroxyalkanoate films by plasma-initiated polymerization. *Polym Degrad Stab* 2013;98:1458-64.
- [76] Amass W, Amass A, Tighe B. A review of biodegradable polymers: Uses, current developments in the synthesis and characterization of biodegradable polyesters, blends of biodegradable polymers and recent advances in biodegradation studies. *Polym Int* 1998;47:89-144.
- [77] Vert M. Aliphatic polyesters: Great degradable polymers that cannot do everything. *Biomacromolecules* 2005;6:538-46.
- [78] Braud C, Bunel C, Vert M. Poly( $\beta$ -malic acid): a new polymeric drug-carrier. *Polym Bull* 1985;13:293-9.
- [79] Anonymous, The Dow Chemical Company. CARBOWAX™ Polyethylene Glycols <http://www.dow.com/scripts/litorder.asp?filepath=polyglycols/pdfs/noreg/118-01789.pdf> 2011.. 12 pp. accessed February 2017.

- [80] Niaounakis M. Biopolymers: reuse, recycling, and disposal. Amsterdam: Elsevier Ltd; 2013.. 413 pp.
- [81] Huang SJ, Pavlisko J, Hong E. Poly(enamine-amides) and poly(enamine-ketones). *Polym Prepr (Am Chem Soc, Div Polym Chem)* 1978;19(2):57-62.
- [82] Huang SJ, Ho LH, Hong E, Kitchen O. Hydrophilic-hydrophobic biodegradable polymers: release characteristics of hydrogen-bonded, ring-containing polymer matrices. *Biomaterials* 1994;15:1243-7.
- [83] Huang SJ, Smith DA, Koberstein JT. Hydrophilic/Hydrophobic Copolymers: Fluorinated Hydrogels as Biomaterials. In: Chiellini E, Solaro R, editors. *Biodegradable Polymers and Plastics*. Boston, MA: Springer US; 2003. p. 213-21.
- [84] Rinaudo M. Chitin and chitosan: Properties and applications. *Prog Polym Sci* 2006;31:603-32.
- [85] Gooday GW. Physiology of microbial degradation of chitin and chitosan. *Biodegradation* 1990;1:177-90.
- [86] Harish Prashanth KV, Tharanathan RN. Chitin/chitosan: modifications and their unlimited application potential—an overview. *Trends Food Sci Technol* 2007;18:117-31.
- [87] Kean T, Thanou M. Biodegradation, biodistribution and toxicity of chitosan. *Adv Drug Deliv Rev* 2010;62:3-11.
- [88] Leonard F, Kulkarni RK, Brandes G, Nelson J, Cameron JJ. Synthesis and degradation of poly (alkyl  $\alpha$ -cyanoacrylates). *J Appl Polym Sci* 1966;10:259-72.
- [89] Yang SC, Bhide M, Crispe IN, Pierce RH, Murthy N. Polyketal Copolymers: A New Acid-Sensitive Delivery Vehicle for Treating Acute Inflammatory Diseases. *Bioconjug Chem* 2008;19:1164-9.
- [90] Fu K, Pack DW, Klibanov AM, Langer R. Visual evidence of acidic environment within degrading poly-(lactic-co-glycolic acid) (PLGA) microspheres. *Pharm Res* 2000;17:100-6.
- [91] Gopferich A, Tessmar J. Polyanhydride degradation and erosion. *Adv Drug Deliv Rev* 2002;54:911-31.
- [92] Kumar N, Langer RS, Domb AJ. Polyanhydrides: an overview. *Adv Drug Deliv Rev* 2002;54:889-910.
- [93] Heffernan MJ, Murthy N. Polyketal nanoparticles: a new pH-sensitive biodegradable drug delivery vehicle. *Bioconjug Chem* 2005;16:1340-2.

- [94] Lee S, Yang SC, Heffernan MJ, Taylor WR, Murthy N. Polyketal microparticles: a new delivery vehicle for superoxide dismutase. *Bioconjug Chem* 2007;18:4-7.
- [95] Tomlinson R, Klee M, Garrett S, Heller J, Duncan R, Brocchini S. Pendant Chain Functionalized Polyacetals That Display pH-Dependent Degradation: A Platform for the Development of Novel Polymer Therapeutics. *Macromolecules* 2002;35:473-80.
- [96] Kohn J, Langer R. Poly(iminocarbonates) as potential biomaterials. *Biomaterials* 1986;7:176-82.
- [97] Li C, Kohn J. Synthesis of poly(iminocarbonates): degradable polymers with potential applications as disposable plastics and as biomaterials. *Macromolecules* 1989;22:2029-36.
- [98] Artham T, Doble M. Biodegradation of aliphatic and aromatic polycarbonates. *Macromol Biosci* 2008;8:14-24.
- [99] Ingle NP, Cong H, King MW Barbed suture technology. In: King MW, Gupta BS, Guidoin R, editors. *Biotextiles as Medical Implants*. Cambridge: Woodhead Publishing; 2013.. p. 366-407.
- [100] Prior TD, Grace DL, MacLean JB, Allen PW, Chapman PG, Day A. Correction of hallux abductus valgus by Mitchell's metatarsal osteotomy: comparing standard fixation methods with absorbable polydioxanone pins. *Foot* 1997;7:121-5.
- [101] Lyu S, Sparer R, Untereker D. Analytical solutions to mathematical models of the surface and bulk erosion of solid polymers. *J Polym Sci Part B Polym Phys* 2005;43:383-97.
- [102] Grizzi I, Garreau H, Li S, Vert M. Hydrolytic degradation of devices based on poly(*D,L*-lactic acid) size-dependence. *Biomaterials* 1995;16:305-11.
- [103] Mohammadi Y, Jabbari E. Monte Carlo simulation of degradation of porous poly(lactide) scaffolds, 1 Effect of porosity on pH. *Macromol Theory Simul* 2006;15:643-53.
- [104] Lam CXF, Savalani MM, Teoh SH, Huttmacher DW. Dynamics of in vitro polymer degradation of polycaprolactone-based scaffolds: accelerated versus simulated physiological conditions. *Biomed Mater* 2008;3:1-15.
- [105] Li SM, Garreau H, Vert M. Structure-property relationships in the case of the degradation of massive poly(alpha-hydroxy acids) in aqueous-media: 3. Influence of the morphology of poly(*L*-lactic acid). *J Mater Sci Mater Med* 1990;1:198-206.

- [106] Li SM, Garreau H, Vert M. Structure property relationships in the case of the degradation of massive aliphatic poly-(alpha-hydroxy acids) in aqueous-media: 1. Poly(*D,L*-lactic acid). *J Mater Sci Mater Med* 1990;1:123-30.
- [107] Li SM, Garreau H, Vert M. Structure property relationships in the case of the degradation of massive poly(alpha-hydroxy acids) in aqueous-media. 2. Degradation of lactide-glycolide copolymers - Pla37.5ga25 and Pla75ga25. *J Mater Sci Mater Med* 1990;1:131-9.
- [108] Vert M, Li S, Garreau H, Mauduit J, Boustta M, Schwach G, Engel R, Coudane J. Complexity of the hydrolytic degradation of aliphatic polyesters. *Angew Makromol Chem* 1997;247:239-53.
- [109] Tsuji H, Saeki T, Tsukegi T, Daimon H, Fujie K. Comparative study on hydrolytic degradation and monomer recovery of poly(*L*-lactic acid) in the solid and in the melt. *Polym Degrad Stab* 2008;93:1956-63.
- [110] Pitt CG, Shah SS. Manipulation of the rate of hydrolysis of polymer-drug conjugates: The secondary structure of the polymer. *J Controlled Release* 1996;39:221-9.
- [111] Siparsky GL, Voorhees KJ, Dorgan JR, Schilling K. Water transport in polylactic acid (PLA), PLA/polycaprolactone copolymers, and PLA polyethylene glycol blends. *J Environ Polym Degrad* 1997;5:125-36.
- [112] Martens AA, Besseling NAM, Rueb S, Sudholter EJR, Spaink HP, de Smet LCPM. Random scission of polymers: numerical simulations, and experiments on hyaluronan hydrolysis. *Macromolecules* 2011;44:2559-67.
- [113] Charlier A, Leclerc B, Couarraze G. Release of mifepristone from biodegradable matrices: experimental and theoretical evaluations. *Int J Pharm* 2000;200:115-20.
- [114] Ballauff M, Wolf BA. Degradation of chain molecules: 1. Exact solution of the kinetic-equations. *Macromolecules* 1981;14:654-8.
- [115] Chen YH, Zhou SW, Li Q. Mathematical modeling of degradation for bulk-erosive polymers: Applications in tissue engineering scaffolds and drug delivery systems. *Acta Biomater* 2011;7:1140-9.
- [116] Karst D, Yang YQ. Molecular modeling study of the resistance of PLA to hydrolysis based on the blending of PLLA and PDLA. *Polymer* 2006;47:4845-50.
- [117] Perale G, Arosio P, Moscatelli D, Barri V, Muller M, Maccagnan S, Masi M. A new model of resorbable device degradation and drug release: Transient 1-dimension diffusional model. *J Controlled Release* 2009;136:196-205.

- [118] Soares JS, Zunino P. A mixture model for water uptake, degradation, erosion and drug release from polydisperse polymeric networks. *Biomaterials* 2010;31:3032-42.
- [119] Thombre AG, Himmelstein KJ. A simultaneous transport-reaction model for controlled drug delivery from catalyzed bioerodible polymer matrices. *AIChE J* 1985;31:759-66.
- [120] Antheunis H, van der Meer JC, de Geus M, Heise A, Koning CE. Autocatalytic equation describing the change in molecular weight during hydrolytic degradation of aliphatic polyesters. *Biomacromolecules* 2010;11:1118-24.
- [121] Antheunis H, van der Meer JC, de Geus M, Kingma W, Koning CE. Improved mathematical model for the hydrolytic degradation of aliphatic polyesters. *Macromolecules* 2009;42:2462-71.
- [122] Wang Y, Pan JZ, Han XX, Sinka C, Ding LF. A phenomenological model for the degradation of biodegradable polymers. *Biomaterials* 2008;29:3393-401.
- [123] Han XX, Pan JZ. A model for simultaneous crystallization and biodegradation of biodegradable polymers. *Biomaterials* 2009;30:423-30.
- [124] Gleadall A, Pan JZ, Atkinson H. A simplified theory of crystallization induced by polymer chain scissions for biodegradable polyesters. *Polym Degrad Stab* 2012;97:1616-20.
- [125] Heljak MK, Swieszkowski W, Kurzydowski KJ. Modeling of the degradation kinetics of biodegradable scaffolds: The effects of the environmental conditions. *J Appl Polym Sci* 2014;131:1-7.
- [126] Agrawal CM, McKinney JS, Lanctot D, Athanasiou KA. Effects of fluid flow on the in vitro degradation kinetics of biodegradable scaffolds for tissue engineering. *Biomaterials* 2000;21:2443-52.
- [127] Zhao AY, Hunter SK, Rodgers VGJ. Theoretical prediction of induction period from transient pore evolution in polyester-based microparticles. *J Pharm Sci* 2010;99:4477-87.
- [128] Batycky RP, Hanes J, Langer R, Edwards DA. A theoretical model of erosion and macromolecular drug release from biodegrading microspheres. *J Pharm Sci* 1997;86:1464-77.
- [129] Lemaire V, Belair J, Hildgen P. Structural modeling of drug release from biodegradable porous matrices based on a combined diffusion/erosion process. *Int J Pharm* 2003;258:95-107.

- [130] Arosio P, Busini V, Perale G, Moscatelli D, Masi M. A new model of resorbable device degradation and drug release - Part I: Zero order model. *Polym Int* 2008;57:912-20.
- [131] Nishida H, Yamashita M, Nagashima M, Hattori N, Endo T, Tokiwa Y. Theoretical prediction of molecular weight on autocatalytic random hydrolysis of aliphatic polyesters. *Macromolecules* 2000;33:6595-601.
- [132] Casalini T, Rossi F, Lazzari S, Perale G, Masi M. Mathematical modeling of PLGA microparticles: from polymer degradation to drug release. *Mol Pharmacol* 2014;11:4036-48.
- [133] Guaita M, Chiantore O, Luda MP. Monte-Carlo simulations of polymer degradations: 1. Degradations without volatilization. *Macromolecules* 1990;23:2087-92.
- [134] Emsley AM, Heywood RJ. Computer modeling of the degradation of linear-polymers. *Polym Degrad Stab* 1995;49:145-9.
- [135] Gopferich A, Langer R. Modeling monomer release from bioerodible polymers. *J Controlled Release* 1995;33:55-69.
- [136] Siepmann J, Faisant N, Benoit JP. A new mathematical model quantifying drug release from bioerodible microparticles using Monte Carlo simulations. *Pharm Res* 2002;19:1885-93.
- [137] Siepmann J, Peppas NA. Mathematical modeling of controlled drug delivery. *Adv Drug Deliv Rev* 2001;48:137-8.
- [138] Bose SM, Git Y. Mathematical modelling and computer simulation of linear polymer degradation: simple scissions. *Macromol Theory Simul* 2004;13:453-73.
- [139] Gleadall A, Pan J. Computer simulation of polymer chain scission in biodegradable polymers. *J Biotechnol Biomater* 2013;3:1-5.
- [140] Sanz-Herrera JA, Garcia-Aznar JM, Doblare M. On scaffold designing for bone regeneration: A computational multiscale approach. *Acta Biomater* 2009;5:219-29.
- [141] Rothstein SN, Federspiel WJ, Little SR. A unified mathematical model for the prediction of controlled release from surface and bulk eroding polymer matrices. *Biomaterials* 2009;30:1657-64.
- [142] Lin ZL, Luo J, Chen ZJ, Yi J, Jiang HL, Tu KH, Wang LQ. A Monte Carlo simulation study of the effect of chain length on the hydrolysis of poly(lactic acid). *Chin J Polym Sci* 2013;31:1554-62.
- [143] Bertrand N, Leclair G, Hildgen P. Modeling drug release from bioerodible microspheres using a cellular automaton. *Int J Pharm* 2007;343:196-207.

- [144] Yu RX, Chen HL, Chen TN, Zhou XY. Modeling and simulation of drug release from multi-layer biodegradable polymer microstructure, in three dimensions. *Simul Model Pract Theory* 2008;16:15-25.
- [145] Barat A, Crane M, Ruskin HJ. Quantitative multi-agent models for simulating protein release from PLGA bioerodible nano- and microspheres. *J Pharm Biomed Anal* 2008;48:361-8.
- [146] Knight B. Lack of evidence for an autocatalytic point in the degradation of cellulose acetate. *Polym Degrad Stab* 2014;107:219-22.
- [147] Ding AG, Shenderova A, Schwendeman SP. Prediction of microclimate pH in poly(lactic-*co*-glycolic acid) films. *J Am Chem Soc* 2006;128:5384-90.
- [148] Schusser S, Menzel S, Backer M, Leinhos M, Poghossian A, Wagner P, Schoning MJ. Degradation of thin poly(lactic acid) films: Characterization by capacitance-voltage, atomic force microscopy, scanning electron microscopy and contact-angle measurements. *Electrochim Acta* 2013;113:779-84.
- [149] Keller SS, Gammelgaard L, Jensen MP, Schmid S, Davis ZJ, Boisen A. Micromechanical sensors for the measurement of biopolymer degradation. 2011 IEEE 24th Int Confer Micro Electro Mech Syst (MEMS). 2011. p. 457-60.
- [150] Hopfenburg HB. Controlled release from erodible slabs, cylinders and spheres. In: Paul DR, Harris FW, editors. *Controlled release polymeric formulations*. 33. New York, N.Y: Washington: The Society; 1976. p. 26-32.
- [151] Cooney DO. Effect of geometry on dissolution of pharmaceutical tablets and other solids - surface detachment kinetics controlling. *AIChE J* 1972;18:446-9.
- [152] Lee PI. Diffusional release of a solute from a polymeric matrix - approximate analytical solutions. *J Membr Sci* 1980;7:255-75.
- [153] Larobina D, Mensitieri G, Kipper MJ, Narasimhan B. Mechanistic understanding of degradation in bioerodible polymers for drug delivery. *AIChE J* 2002;48:2960-70.
- [154] Kipper MJ, Narasimhan B. Molecular description of erosion phenomena in biodegradable polymers. *Macromolecules* 2005;38:1989-99.
- [155] Zygourakis K, Markenscoff PA. Computer-aided design of bioerodible devices with optimal release characteristics: A cellular automata approach. *Biomaterials* 1996;17:125-35.
- [156] Zygourakis K. Development and temporal evolution of erosion fronts in bioerodible controlled release devices. *Chem Eng Sci* 1990;45:2359-66.

- [157] Gopferich A, Langer R. Modeling of polymer erosion. *Macromolecules* 1993;26:4105-12.
- [158] Gopferich A, Langer R. The influence of microstructure and monomer properties on the erosion mechanism of a class of polyanhydrides. *J Polym Sci Part A Polym Chem* 1993;31:2445-58.
- [159] Domanskyi S, Poetz KL, Shipp DA, Privman V. Reaction-diffusion degradation model for delayed erosion of cross-linked polyanhydride biomaterials. *Phys Chem Chem Phys* 2015;17:13215-22.
- [160] Pitt CG, Gratzel MM, Kimmel JL, Surles J SA. Aliphatic polyesters II. The degradation of poly(*D,L*-lactide), poly( $\epsilon$ -caprolactone), and their copolymers in vivo. *Biomaterials* 1982;2:215-20.
- [161] Bellenger V, Ganem M, Mortaigne B, Verdu J. Lifetime prediction in the hydrolytic aging of polyesters. *Polym Degrad Stab* 1995;49:91-7.
- [162] Gleadall A, Pan JZ, Krufft MA, Kellomaki M. Degradation mechanisms of bioresorbable polyesters. Part 2. Effects of initial molecular weight and residual monomer. *Acta Biomater* 2014;10:2233-40.
- [163] Codari F, Lazzari S, Soos M, Storti G, Morbidelli M, Moscatelli D. Kinetics of the hydrolytic degradation of poly(lactic acid). *Polym Degrad Stab* 2012;97:2460-6.
- [164] Weir NA, Buchanan FJ, Orr JF, Farrar DF, Dickson GR. Degradation of poly-*L*-lactide. Part 2: Increased temperature accelerated degradation. *Proc Inst Mech Eng, Part H* 2004;218:321-30.
- [165] Deng M, Zhou J, Chen G, Burkley D, Xu Y, Jamiolkowski D, Barbolt T. Effect of load and temperature on in vitro degradation of poly(glycolide-*co-L*-lactide) multifilament braids. *Biomaterials* 2005;26:4327-36.
- [166] Tsuji H. Autocatalytic hydrolysis of amorphous-made polylactides: Effects of *L*-lactide content, tacticity, and enantiomeric polymer blending. *Polymer* 2002;43:1789-96.
- [167] Weir NA, Buchanan FJ, Orr JF, Dickson GR. Degradation of poly-*L*-lactide. Part 1: in vitro and in vivo physiological temperature degradation. *Proc Inst Mech Eng, Part H* 2004;218:307-19.
- [168] Lewitus DY, Rios F, Rojas R, Kohn J. Molecular design and evaluation of biodegradable polymers using a statistical approach. *J Mater Sci Mater Med* 2013;24:2529-35.



- [169] Zaikov GE, Iordanskiĭ AL, Markin VS. Diffusion and chemical reactions. In: Zaikov GE, Iordanskiĭ AL, Markin VS, editors. Diffusion of Electrolytes in Polymers. Utrecht, The Netherlands: VSP BV; 1988. p. 223-60.
- [170] Shen E, Kipper MJ, Dziadul B, Lim MK, Narasimhan B. Mechanistic relationships between polymer microstructure and drug release kinetics in bioerodible polyanhydrides. *J Controlled Release* 2002;82:115-25.
- [171] Tsuji H, Mizuno A, Ikada Y. Properties and morphology of poly(*L*-lactide). III. Effects of initial crystallinity on long-term in vitro hydrolysis of high molecular weight poly(*L*-lactide) film in phosphate-buffered solution. *J Appl Polym Sci* 2000;77:1452-64.
- [172] Tsuji H, Ikada Y. Properties and morphology of poly(*L*-lactide) 4. Effects of structural parameters on long-term hydrolysis of poly(*L*-lactide) in phosphate-buffered solution. *Polym Degrad Stab* 2000;67:179-89.
- [173] Tsuji H. In vitro hydrolysis of blends from enantiomeric poly(lactide)s Part 1. Well-stereo-complexed blend and non-blended films. *Polymer* 2000;41:3621-30.
- [174] Ding LF, Davidchack RL, Pan JZ. A molecular dynamics study of Young's modulus change of semi-crystalline polymers during degradation by chain scissions. *J Mech Behav Biomed Mater* 2012;5:224-30.
- [175] Hayman D, Bergerson C, Miller S, Moreno M, Moore JE. The effect of static and dynamic loading on degradation of PLLA stent fibers. *J Biomech Eng* 2014;136:081006/1-9.
- [176] Karjalainen T, HiljanenVainio M, Malin M, Seppala J. Biodegradable lactone copolymers. 3. Mechanical properties of  $\epsilon$ -caprolactone and lactide copolymers after hydrolysis in vitro. *J Appl Polym Sci* 1996;59:1299-304.
- [177] Wang Y, Han XX, Pan JZ, Sinka C. An entropy spring model for the Young's modulus change of biodegradable polymers during biodegradation. *J Mech Behav Biomed Mater* 2010;3:14-21.
- [178] de Oca HM, Ward IM. Structure and mechanical properties of PGA crystals and fibers. *Polymer* 2006;47:7070-7.
- [179] Shirazi RN, Ronan W, Rochev Y, McHugh P. Modelling the degradation and elastic properties of poly(lactic-*co*-glycolic acid) films and regular open-cell tissue engineering scaffolds. *J Mech Behav Biomed Mater* 2016;54:48-59.

- [180] Gleadall A. Mechanical properties of biodegradable polymers for medical applications. In: Pen J, editor. *Modelling Degradation of Bioresorbable Polymeric Medical Devices*. Amsterdam: Elsevier Ltd; 2015. p. 163-99.
- [181] Gleadall A. *Modelling degradation of biodegradable polymers and their mechanical properties*. PhD thesis. Leicester: The University of Leicester; 2015. 268 pp.
- [182] Duek EAR, Zavaglia CAC, Belangero WD. In vitro study of poly(lactic acid) pin degradation. *Polymer* 1999;40:6465-73.
- [183] Chen C, Ju SP, Huang WC, Lin JS, Chen CC. Prediction of the variation of PGA strength during hydrolysis by a combination of empirical equation, density functional theory calculation, and molecular dynamics simulation. *AIP Adv* 2014;4:0771041/1-12.
- [184] Vieira AC, Marques AT, Guedes RM, Tita V. Material model proposal for biodegradable materials. *Procedia Eng* 2011;10:1597-602.
- [185] Vieira AC, Guedes RM, Tita V. Constitutive modeling of biodegradable polymers: Hydrolytic degradation and time-dependent behavior. *Int J Solids Struct* 2014;51:1164-74.
- [186] Vieira AC, Guedes RM, Tita V. Constitutive models for biodegradable thermoplastic ropes for ligament repair. *Compos Struct* 2012;94:3149-59.
- [187] Soares JS, Rajagopal KR, Moore JE. Deformation-induced hydrolysis of a degradable polymeric cylindrical annulus. *Biomech Model Mechanobiol* 2010;9:177-86.
- [188] Vieira AC. Modeling hydrolytic degradation of PLA devices. In: Piemonte V, editor. *Poly(lactic Acid): Synthesis, Properties and Applications*. New York: Nova Science publishers, Inc.; 2012. p. 143-60.
- [189] Tang CY, Wang ZW, Tsui CP, Bai YF, Gao B, Wu H. Damage modeling of degradable polymers under bulk erosion. *J Appl Polym Sci* 2013;128:2658-65.
- [190] Gopferich A. Polymer bulk erosion. *Macromolecules* 1997;30:2598-604.
- [191] Deroine M, Le Duigou A, Corre YM, Le Gac PY, Davies P, Cesar G, Bruzard S. Accelerated ageing and lifetime prediction of poly(3-hydroxybutyrate-co-3-hydroxyvalerate) in distilled water. *Polym Test* 2014;39:70-8.
- [192] Rittie L, Perbal B. Enzymes used in molecular biology: a useful guide. *J Cell Commun Signal* 2008;2:25-45.
- [193] Nelson DL, Lehninger AL, Cox MM. *Principles of biochemistry*. New York: W.H. 2013. 1198 pp.

- [194] Eubeler JP, Bernhard M, Knepper TP. Environmental biodegradation of synthetic polymers II. Biodegradation of different polymer groups. *Trends Anal Chem* 2010;29:84-100.
- [195] Banerjee A, Chatterjee K, Madras G. Enzymatic degradation of polymers: a brief review. *Mater Sci Technol* 2014;30:567-73.
- [196] Pranamuda H, Tokiwa Y, Tanaka H. Polylactide degradation by an *Amycolatopsis* sp. *Appl Environ Microbiol* 1997;63:1637-40.
- [197] Averous L. Synthesis, properties, environmental and biomedical applications of polylactic acid. In: Ebnesajjad S, editor. *Handbook of Biopolymers and Biodegradable Plastics; Processing, properties and applications*. United States: Elsevier Ltd.; 2013. p. 171-88.
- [198] Azevedo HS, Reis RL. Understanding the enzymatic degradation of biodegradable polymers and strategies to control their degradation rate. **In: Reis RL, Román, JS, editors. Biodegradable Systems in Tissue Engineering and Regenerative Medicine. Boca Raton: CRC Press; 2005. p. 177-201.**
- [199] Chanprateep S, Shimizu H, Shioya S. Characterization and enzymatic degradation of microbial copolyester P(3HB-*co*-3HV)s produced by metabolic reaction model-based system. *Polym Degrad Stab* 2006;91:2941-50.
- [200] Agrawal CM, Huang D, Schmitz JP, Athanasiou KA. Elevated temperature degradation of a 50:50 copolymer of PLA-PGA. *Tissue Eng* 1997;3:345-52.
- [201] McLaren AD. Enzyme reactions in structurally restricted systems IV. The digestion of insoluble substrates by hydrolytic enzymes. *Enzymologia* 1963;26:237-46.
- [202] Duguay DG, Labow RS, Santerre JP, Mclean DD. Development of a mathematical-model describing the enzymatic degradation of biomedical polyurethanes: 1. Background, rationale and model formulation. *Polym Degrad Stab* 1995;47:229-49.
- [203] Mukai K, Yamada K, Doi Y. Kinetics and mechanism of heterogeneous hydrolysis of poly[(*R*)-3-hydroxybutyrate] film by PHA depolymerases. *Int J Biol Macromol* 1993;15:361-6.
- [204] Timmins MR, Lenz RW, Fuller RC. Heterogeneous kinetics of the enzymatic degradation of poly(beta-hydroxyalkanoates). *Polymer* 1997;38:551-62.
- [205] Scandola M, Focarete ML, Frisoni G. Simple kinetic model for the heterogeneous enzymatic hydrolysis of natural poly(3-hydroxybutyrate). *Macromolecules* 1998;31:3846-51.

- [206] Tayal A, Kelly RM, Khan SA. Rheology and molecular weight changes during enzymatic degradation of a water-soluble polymer. *Macromolecules* 1999;32:294-300.
- [207] Zeng J, Chen XS, Liang QZ, Xu XL, Jing XB. Enzymatic degradation of poly(*L*-lactide) and poly( $\epsilon$ -caprolactone) electrospun fibers. *Macromol Biosci* 2004;4:1118-25.
- [208] Zeng J, Yang LX, Liang QZ, Zhang XF, Guan HL, Xu XL, Chen XS, Jing XB. Influence of the drug compatibility with polymer solution on the release kinetics of electrospun fiber formulation. *J Controlled Release* 2005;105:43-51.
- [209] Arvanitoyannis I, Nakayama A, Kawasaki N, Yamamoto N. Novel star-shaped polylactide with glycerol using stannous octoate or tetraphenyl tin as catalyst: 1. Synthesis, characterization and study of their biodegradability. *Polymer* 1995;36:2947-56.
- [210] Arvanitoyannis I, Nakayama A, Psomiadou E, Kawasaki N, Yamamoto N. Synthesis and degradability of a novel aliphatic polyester based on *L*-lactide and sorbitol: 3. *Polymer* 1996;37:651-60.
- [211] Numata K, Srivastava RK, Finne-Wistrand A, Albertsson AC, Doi Y, Abe H. Branched poly(lactide) synthesized by enzymatic polymerization: Effects of molecular branches and stereochemistry on enzymatic degradation and alkaline hydrolysis. *Biomacromolecules* 2007;8:3115-25.
- [212] Numata K, Finne-Wistrand A, Albertsson AC, Doi Y, Abe H. Enzymatic degradation of monolayer for poly(lactide) revealed by real-time atomic force microscopy: Effects of stereochemical structure, molecular weight, and molecular branches on hydrolysis rates. *Biomacromolecules* 2008;9:2180-5.
- [213] Vasanthan N, Gezer H. Thermally induced crystallization and enzymatic degradation studies of poly (*L*-lactic acid) films. *J Appl Polym Sci* 2013;127:4395-401.
- [214] Bikiaris DN, Papageorgiou GZ, Achilias DS. Synthesis and comparative biodegradability studies of three poly(alkylene succinate)s. *Polym Degrad Stab* 2005;91:31-43.
- [215] Yamashita K, Kikkawa Y, Kurokawa K, Doi Y. Enzymatic degradation of poly(*L*-lactide) film by proteinase K: Quartz crystal microbalance and atomic force microscopy study. *Biomacromolecules* 2005;6:850-7.

- [216] Suyama T, Tokiwa Y, Ouichanpagdee P, Kanagawa T, Kamagata Y. Phylogenetic affiliation of soil bacteria that degrade aliphatic polyesters available commercially as biodegradable plastics. *Appl Environ Microbiol* 1998;64:5008-11.
- [217] Tokiwa Y, Suzuki T. Hydrolysis of polyesters by lipases. *Nature* 1977;270:76-8.
- [218] Murphy CA, Cameron JA, Huang SJ, Vinopal RT. Fusarium polycaprolactone depolymerase is cutinase. *Appl Environ Microbiol* 1996;62:456-60.
- [219] Kulkarni A, Reiche J, Kratz K, Kamusewitz H, Sokolov IM, Lendlein A. Enzymatic chain scission kinetics of poly( $\epsilon$ -caprolactone) monolayers. *Langmuir* 2007;23:12202-7.
- [220] Ozsagiroglu E, Iyisan B, Avcibasi Guvenilir Y. Comparing the in-vitro biodegradation kinetics of commercial and synthesized polycaprolactone films in different enzyme solutions. *Ekoloji* 2013;22:90-6.
- [221] Marten E, Müller RJ, Deckwer WD. Studies on the enzymatic hydrolysis of polyesters I. Low molecular mass model esters and aliphatic polyesters. *Polym Degrad Stab* 2003;80:485-501.
- [222] Castilla-Cortázar I, Más-Estellés J, Meseguer-Dueñas JM, Escobar Ivirico JL, Marí B, Vidaurre A. Hydrolytic and enzymatic degradation of a poly( $\epsilon$ -caprolactone) network. *Polym Degrad Stab* 2012;97:1241-8.
- [223] Sekosan G, Vasanthan N. Morphological changes of annealed poly-epsilon-caprolactone by enzymatic degradation with lipase. *J Polym Sci Part B Polym Phys* 2010;48:202-11.
- [224] Hayashi T, Nakayama K, Mochizuki M, Masuda T. Studies on biodegradable poly(hexano-6-lactone) fibers. Part 3. Enzymatic degradation in vitro - (IUPAC technical report). *Pure Appl Chem* 2002;74:869-80.
- [225] Jiang N, Jiang SD, Hou Y, Yan SK, Zhang GZ, Gan ZH. Influence of chemical structure on enzymatic degradation of single crystals of PCL-*b*-PEO amphiphilic block copolymer. *Polymer* 2010;51:2426-34.
- [226] Lee CW, Kimura Y, Chung JD. Mechanism of enzymatic degradation of poly(butylene succinate). *Macromol Res* 2008;16:651-8.
- [227] Jendrossek D. Peculiarities of PHA granules preparation and PHA depolymerase activity determination. *Appl Microbiol Biotechnol* 2007;74:1186-96.
- [228] Kasuya K, Inoue Y, Doi Y. Adsorption kinetics of bacterial PHB depolymerase on the surface of polyhydroxyalkanoate films. *Int J Biol Macromol* 1996;19:35-40.

- [229] Kasuya KI, Inoue Y, Yamada K, Doi Y. Kinetics of surface hydrolysis of poly[(*R*)-3-hydroxybutyrate] film by PHB depolymerase from *Alcaligenes faecalis* T1. *Polym Degrad Stab* 1995;48:167-74.
- [230] Guerin P, Renard E, Langlois V. Degradation of natural and artificial poly[(*R*)-3-hydroxyalkanoate]s: From biodegradation to hydrolysis. In: Chen GGQ, editor. *Plastics from Bacteria: Natural Functions and Applications. Microbiology Monographs Vol. 14*, Berlin: Springer-Verlag; 2010. p. 283-321.
- [231] Knoll M, Hamm TM, Wagner F, Martinez V, Pleiss J. The PHA depolymerase engineering database: A systematic analysis tool for the diverse family of polyhydroxyalkanoate (PHA) depolymerases. *BMC Bioinf* 2009;10:1-8.
- [232] Hiraishi T, Komiya N, Matsumoto N, Abe H, Fujita M, Maeda M. Degradation and adsorption characteristics of PHB depolymerase as revealed by kinetics of mutant enzymes with amino acid substitution in substrate-binding domain. *Biomacromolecules* 2010;11:113-9.
- [233] Sudesh K, Abe H, Doi Y. Synthesis, structure and properties of polyhydroxyalkanoates: biological polyesters. *Prog Polym Sci* 2000;25:1503-55.
- [234] Murase T, Iwata T, Doi Y. Atomic force microscopy investigation of poly[(*R*)-3-hydroxybutyrate] lamellar single crystals: Relationship between molecular weight and enzymatic degradation behavior. *Macromol Biosci* 2001;1:275-81.
- [235] Murase T, Suzuki Y, Doi Y, Iwata T. Nonhydrolytic fragmentation of a poly[(*R*)-3-hydroxybutyrate] single crystal revealed by use of a mutant of polyhydroxybutyrate depolymerase. *Biomacromolecules* 2002;3:312-7.
- [236] Iwata T, Doi Y. Crystal structure and biodegradation of aliphatic polyester crystals. *Macromol Chem Phys* 1999;200:2429-42.
- [237] Su FY, Iwata T, Tanaka F, Doi Y. Crystal structure and enzymatic degradation of poly(4-hydroxybutyrate). *Macromolecules* 2003;36:6401-9.
- [238] Numata K, Hirota T, Kikkawa Y, Tsuge T, Iwata T, Abe H, Doi Y. Enzymatic degradation processes of lamellar crystals in thin films for poly[(*R*)-3-hydroxybutyric acid] and its copolymers revealed by real-time atomic force microscopy. *Biomacromolecules* 2004;5:2186-94.
- [239] Numata K, Abe H, Doi Y. Enzymatic processes for biodegradation of poly(hydroxyalkanoate)s crystals. *Can J Chem* 2008;86:471-83.

- [240] Abe H, Doi Y, Aoki H, Akehata T. Solid-state structures and enzymatic degradabilities for melt-crystallized films of copolymers of (*R*)-3-hydroxybutyric acid with different hydroxyalkanoic acids. *Macromolecules* 1998;31:1791-7.
- [241] Yamashita K, Funato T, Suzuki Y, Teramachi S, Doi Y. Characteristic interactions between poly(hydroxybutyrate) depolymerase and poly [(*R*)-3-hydroxybutyrate] film studied by a quartz crystal microbalance. *Macromol Biosci* 2003;3:694-702.
- [242] Yu J, Plackett D, Chen LXL. Kinetics and mechanism of the monomeric products from abiotic hydrolysis of poly[(*R*)-3-hydroxybutyrate] under acidic and alkaline conditions. *Polym Degrad Stab* 2005;89:289-99.
- [243] Ishida K, Asakawa N, Inoue Y. Structure, properties and biodegradation of some bacterial copoly(hydroxyalkanoate)s. *Macromol Symp* 2005;224:47-58.
- [244] Doi Y, Kanesawa Y, Kunioka M, Saito T. Biodegradation of microbial copolyesters: poly(3-hydroxybutyrate-*co*-3-hydroxyvalerate) and poly(3-hydroxybutyrate-*co*-4-hydroxybutyrate). *Macromolecules* 1990;23:26-31.
- [245] Luo S, Netravali AN. A study of physical and mechanical properties of poly(hydroxybutyrate-*co*-hydroxyvalerate) during composting. *Polym Degrad Stab* 2003;80:59-66.
- [246] Hermida EB, Yashchuk O, Miyazaki SS. Changes in the mechanical properties of compression moulded samples of poly(3-hydroxybutyrate-*co*-3-hydroxyvalerate) degraded by *Streptomyces omiyaensis* SSM 5670. *Polym Degrad Stab* 2009;94:267-71.
- [247] Zhang JQ, Kasuya K, Hikima T, Takata M, Takemura A, Iwata T. Mechanical properties, structure analysis and enzymatic degradation of uniaxially cold-drawn films of poly[(*R*)-3-hydroxybutyrate-*co*-4-hydroxybutyrate]. *Polym Degrad Stab* 2011;96:2130-8.
- [248] Tanaka T, Iwata T. Physical properties, structure analysis, and enzymatic degradation of poly[(*R*)-3-hydroxybutyrate-*co*-(*R*)-3-hydroxyvalerate] films and fibres. In: Khemani K, Scholz C, editors. *Degradable Polymer and Materials: Principles and Practice* 2nd ed. Washington, DC: American Chemical Society; 2012. p. 171-85.
- [249] Kumagai Y, Kanesawa Y, Doi Y. Enzymatic degradation of microbial poly(3-hydroxybutyrate) films. *Macromol Chem Phys* 1992;193:53-7.
- [250] Abe H, Doi Y. Side-chain effect of second monomer units on crystalline morphology, thermal properties, and enzymatic degradability for random copolyesters of (*R*)-3-

- hydroxybutyric acid with (*R*)-3-hydroxyalkanoic acids. *Biomacromolecules* 2002;3:133-8.
- [251] Li ZG, Lin H, Ishii N, Chen GQ, Inoue Y. Study of enzymatic degradation of microbial copolyesters consisting of 3-hydroxybutyrate and medium-chain-length 3-hydroxyalkanoates. *Polym Degrad Stab* 2007;92:1708-14.
- [252] Yoshie N, Nakasato K, Fujiwara M, Kasuya K, Abe H, Doi Y, Inoue Y. Effect of low molecular weight additives on enzymatic degradation of poly(3-hydroxybutyrate). *Polymer* 2000;41:3227-34.
- [253] Danjaji ID, Nawang R, Ishiaku US, Ismail H, Ishak ZAMM. Degradation studies and moisture uptake of sago-starch-filled linear low-density polyethylene composites. *Polym Test* 2002;21:75-81.
- [254] Russo MAL, Truss R, Halley PJ. The enzymatic hydrolysis of starch-based PVOH and polyol plasticised blends. *Carbohydr Polym* 2009;77:442-8.
- [255] Yew GH, Yusof AMM, Ishak ZAM, Ishiaku US. Water absorption and enzymatic degradation of poly(lactic acid)/rice starch composites. *Polym Degrad Stab* 2005;90:488-500.
- [256] Li M, Witt T, Xie F, Warren FJ, Halley PJ, Gilbert RG. Biodegradation of starch films: The roles of molecular and crystalline structure. *Carbohydr Polym* 2015;122:115-22.
- [257] Edwards CH, Warren FJ, Milligan PJ, Butterworth PJ, Ellis PR. A novel method for classifying starch digestion by modelling the amylolysis of plant foods using first-order enzyme kinetic principles. *Food Funct* 2014;5:2751-8.
- [258] Butterworth PJ, Warren FJ, Ellis PR. Human alpha-amylase and starch digestion: An interesting marriage. *Starch/Starke* 2011;63:395-405.
- [259] Adeleye OO, Ologhobo AD, Iji PA. Prediction of starch hydrolysis in native starches studied in vitro. *Starch/Starke* 2014;66:502-7.
- [260] Lopez-Rubio A, Flanagan BM, Shrestha AK, Gidley MJ, Gilbert EP. Molecular rearrangement of starch during in vitro digestion: Toward a better understanding of enzyme resistant starch formation in processed starches. *Biomacromolecules* 2008;9:1951-8.
- [261] Shrestha AK, Ng CS, Lopez-Rubio A, Blazek J, Gilbert EP, Gidley MJ. Enzyme resistance and structural organization in extruded high amylose maize starch. *Carbohydr Polym* 2010;80:699-710.



- [262] Zheng Y, Zhang HX, Yao C, Hu LL, Peng YJ, Shen J. Study on physicochemical and in-vitro enzymatic hydrolysis properties of ginkgo (*Ginkgo biloba*) starch. *Food Hydrocolloids* 2015;48:312-9.
- [263] Dash M, Chiellini F, Ottenbrite RM, Chiellini E. Chitosan—A versatile semi-synthetic polymer in biomedical applications. *Prog Polym Sci* 2011;36:981-1014.
- [264] Puls J, Wilson SA, Holter D. Degradation of Cellulose Acetate-Based Materials: A Review. *J Polym Environ* 2011;19:152-65.
- [265] Reese ET. Biological degradation of cellulose derivatives. *Ind Eng Chem* 1957;49:89-93.
- [266] Cantor PA, Mechalias BJ. Biological degradation of cellulose acetate reverse-osmosis membranes. *J Polym Sci Part C Polym Symp* 1969;28:225-41.
- [267] Gardner RM, Buchanan CM, Komarek R, Dorschel D, Boggs C, White AW. Compostability of cellulose acetate films. *J Appl Polym Sci* 1994;52:1477-88.
- [268] Liu CC, Zhang AY, Ye L, Feng ZG. Self-healing biodegradable poly(urea-urethane) elastomers based on hydrogen bonding interactions. *Chin J Polym Sci* 2012;31:251-62.
- [269] Gunatillake P, Mayadunne R, Adhikari R. Recent developments in biodegradable synthetic polymers. In: El-Gewely MR, editor. *Biotechnol Ann Rev*. Vol 12. Hungary: Elsevier B.V.; 2006. p. 301-47.
- [270] Linhardt A, König M, Schöfberger W, Brüggemann O, Andrianov A, Teasdale I. Biodegradable Polyphosphazene Based Peptide-Polymer Hybrids. *Polymers* 2016;8:1-16.
- [271] Watanabe Y, Hamada N, Morita M, Tsujisaka Y. Purification and properties of a polyvinyl alcohol-degrading enzyme produced by a strain of *Pseudomonas*. *Arch Biochem Biophys* 1976;174:575-81.
- [272] Deroiné M, Le Duigou A, Corre YM, Le Gac PY, Davies P, César G, Bruzard S. Seawater accelerated ageing of poly(3-hydroxybutyrate-co-3-hydroxyvalerate). *Polym Degrad Stab* 2014;105:237-47.
- [273] Anonymous. ASTM D5338-98 (Reapproved 2003): Standard test method for determining aerobic biodegradation of plastic materials under controlled composting conditions. West Conshohocken, PA: ASTM International; 2003. 7 pp.
- [274] Anonymous. ASTM D5988-12 Standard test method for determining aerobic biodegradation of plastic materials in soil. West Conshohocken, PA: ASTM International; 2012. 6 pp.

- [275] Anonymous. BS EN 13432:2000 Packaging. Requirements for packaging recoverable through composting and biodegradation - Test scheme and evaluation criteria for the final acceptance of packaging. Brussels: CEN; 2000. 26 pp. ISBN 0 580 36765 7.
- [276] Kyrikou I, Briassoulis D. Biodegradation of agricultural plastic films: A critical review. *J Polym Environ* 2007;15:125-50.
- [277] Karlsson S, Albertsson AC. Biodegradable polymers and environmental interaction. *Polym Eng Sci* 1998;38:1251-3.
- [278] Woolnough CA, Yee LH, Charlton T, Foster LJR. Environmental degradation and biofouling of 'green' plastics including short and medium chain length polyhydroxyalkanoates. *Polym Int* 2010;59:658-67.
- [279] Doi Y, Kasuya K, Abe H, Koyama N, Ishiwatari S, Takagi K, Yoshida Y. Evaluation of biodegradabilities of biosynthetic and chemosynthetic polyesters in river water. *Polym Degrad Stab* 1996;51:281-6.
- [280] Hayes DG, Dharmalingam S, Wadsworth LC, Leonas KK, Miles C, Inglis DA. Biodegradable agricultural mulches derived from biopolymers. *ACS Symp Ser* 2012;1114:201-23.
- [281] Lunt J. Large-scale production, properties and commercial applications of polylactic acid polymers. *Polym Degrad Stab* 1998;59:145-52.
- [282] Hakkarainen M. Aliphatic polyesters: Abiotic and biotic degradation and degradation products. *Adv Polym Sci* 2002;157:113-38.
- [283] Tokiwa Y, Calabia BP. Biodegradability and biodegradation of poly(lactide). *Appl Microbiol Biotechnol* 2006;72:244-51.
- [284] Kale G, Auras R, Singh SP. Comparison of the degradability of poly(lactide) packages in composting and ambient exposure conditions. *Packag Technol Sci* 2007;20:49-70.
- [285] Ghorpade VM, Gennadios A, Hanna MA. Laboratory composting of extruded poly(lactic acid) sheets. *Bioresour Technol* 2001;76:57-61.
- [286] Sangwan P, Wu DY. New insights into polylactide biodegradation from molecular ecological techniques. *Macromol Biosci* 2008;8:304-15.
- [287] Briassoulis D, Rudnik E. Comparative biodegradation in soil behavior of two biodegradable polymers based on renewable resources. *J Polym Environ* 2011;19:18-39.

- [288] Briassoulis D, Rudnik E. Degradation behaviour of poly(lactic acid) films and fibres in soil under Mediterranean field conditions and laboratory simulations testing. *Ind Crops Prod* 2011;33:648-58.
- [289] Agarwal M, Koelling KW, Chalmers JJ. Characterization of the degradation of polylactic acid polymer in a solid substrate environment. *Biotechnol Prog* 1998;14:517-26.
- [290] Pranamuda H, Tsuchii A, Tokiwa Y. Poly (*L*-lactide)-degrading enzyme produced by *Amycolatopsis* sp. *Macromol Biosci* 2001;1:25-9.
- [291] Masaki K, Kamini NR, Ikeda H, Iefuji H. Cutinase-like enzyme from the yeast *Cryptococcus* sp strain S-2 hydrolyzes polylactic acid and other biodegradable plastics. *Appl Environ Microbiol* 2005;71:7548-50.
- [292] Watanabe M, Kawai F, Tsuboi S, Nakatsu S, Ohara H. Study on enzymatic hydrolysis of polylactic acid by endogenous depolymerization model. *Macromol Theory Simul* 2007;16:619-26.
- [293] Saadi Z, Rasmont A, Cesar G, Bewa H, Benguigui L. Fungal degradation of poly(*L*-lactide) in soil and in compost. *J Polym Environ* 2012;20:273-82.
- [294] Saadi Z, Cesar G, Bewa H, Benguigui L. Fungal degradation of poly(butylene adipate-*co*-terephthalate) in soil and in compost. *J Polym Environ* 2013;21:893-901.
- [295] Karamanlioglu M, Robson GD. The influence of biotic and abiotic factors on the rate of degradation of poly(lactic) acid (PLA) coupons buried in compost and soil. *Polym Degrad Stab* 2013;98:2063-71.
- [296] Ho KLG, Pometto AL. Temperature effects on soil mineralization of polylactic acid plastic in laboratory respirometers. *J Environ Polym Degrad* 1999;7:101-8.
- [297] Ho KLG, Pometto AL, Gadea-Rivas A, Briceno JA, Rojas A. Degradation of polylactic acid (PLA) plastic in Costa Rican soil and Iowa State University compost rows. *J Environ Polym Degrad* 1999;7:173-7.
- [298] Ho KLG, Pometto AL, Hinz PN. Effects of temperature and relative humidity on polylactic acid plastic degradation. *J Environ Polym Degrad* 1999;7:83-92.
- [299] Ho KLG, Pometto AL, Hinz PN, Gadea-Rivas A, Briceno JA, Rojas A. Field exposure study of polylactic acid (PLA) plastic films in the banana fields of Costa Rica. *J Environ Polym Degrad* 1999;7:167-72.
- [300] Cook WJ, Cameron JA, Bell JP, Huang SJ. Scanning electron-microscopic visualization of biodegradation of polycaprolactones by fungi. *J Polym Sci Part C Polym Lett* 1981;19:159-65.

- [301] Tsuji H, Suzuyoshi K. Environmental degradation of biodegradable polyesters 1. Poly( $\epsilon$ -caprolactone), poly[(*R*)-3-hydroxybutyrate], and poly(*L*-lactide) films in controlled static seawater. *Polym Degrad Stab* 2002;75:347-55.
- [302] Kijchavengkul T, Auras R, Rubino M, Ngouajio M, Fernandez RT. Assessment of aliphatic-aromatic copolyester biodegradable mulch films. Part II: Laboratory simulated conditions. *Chemosphere* 2008;71:1607-16.
- [303] Kijchavengkul T, Auras R, Rubino M, Ngouajio M, Fernandez RT. Assessment of aliphatic-aromatic copolyester biodegradable mulch films. Part I: field study. *Chemosphere* 2008;71:942-53.
- [304] Kijchavengkul T, Auras R, Rubino M, Alvarado E, Camacho Montero JR, Rosales JM. Atmospheric and soil degradation of aliphatic-aromatic polyester films. *Polym Degrad Stab* 2010;95:99-107.
- [305] Stloukal P, Verney V, Commereuc S, Rychly J, Matisova-Rychla L, Pis V, Koutny M. Assessment of the interrelation between photooxidation and biodegradation of selected polyesters after artificial weathering. *Chemosphere* 2012;88:1214-9.
- [306] Bilck AP, Grossmann MVE, Yamashita F. Biodegradable mulch films for strawberry production. *Polym Test* 2010;29:471-6.
- [307] Abe M, Kobayashi K, Honma N, Nakasaki K. Microbial degradation of poly(butylene succinate) by *Fusarium solani* in soil environments. *Polym Degrad Stab* 2010;95:138-43.
- [308] Koitabashi M, Noguchi MT, Sameshima-Yamashita Y, Hiradate S, Suzuki K, Yoshida S, Watanabe T, Shinozaki Y, Tsushima S, Kitamoto HK. Degradation of biodegradable plastic mulch films in soil environment by phylloplane fungi isolated from gramineous plants. *AMB Express* 2012;2:1-10.
- [309] Thirmizir MZA, Ishak ZAM, Mat Taib R, Rahim S, Jani SM. Natural weathering of kenaf bast fibre-filled poly(butylene succinate) composites: effect of fibre loading and compatibiliser addition. *J Polym Environ* 2011;19:263-73.
- [310] Sakai W, Tsutsumi N. Photodegradation and radiation degradation. In: Auras R, Lim L-T, Selke SEM, Tsuji H, editors. *Poly(Lactic Acid): Synthesis, Structures, Properties, Processing, and Applications*. John Wiley & Sons, Inc; 2010. p. 413-21.
- [311] Bocchini S, Fukushima K, Di Blasio A, Fina A, Frache A, Geobaldo F. Polylactic acid and polylactic acid-based nanocomposite photooxidation. *Biomacromolecules* 2010;11:2919-26.

- [312] Morse MC, Liao Q, Criddle CS, Frank CW. Anaerobic biodegradation of the microbial copolymer poly(3-hydroxybutyrate-*co*-3-hydroxyhexanoate): Effects of comonomer content, processing history, and semi-crystalline morphology. *Polymer* 2011;52:547-56.
- [313] Sang BI, Hori K, Tanji Y, Unno H. Fungal contribution to in situ biodegradation of poly(3-hydroxybutyrate-*co*-3-hydroxyvalerate) film in soil. *Appl Microbiol Biotechnol* 2002;58:241-7.
- [314] Sang BI, Hori K, Tanji Y, Unno H. A kinetic analysis of the fungal degradation process of poly(3-hydroxybutyrate-*co*-3-hydroxyvalerate) in soil. *Biochem Eng J* 2001;9:175-84.
- [315] Hong LW, Yu J. Environmental factors and kinetics of microbial degradation of poly(3-hydroxybutyrate-*co*-3-hydroxyvalerate) in an aqueous medium. *J Appl Polym Sci* 2003;87:205-13.
- [316] Arcos-Hernandez MV, Laycock B, Pratt S, Donose BC, Nikolic MAL, Luckman P, Werker A, Lant PA. Biodegradation in a soil environment of activated sludge derived polyhydroxyalkanoate (PHBV). *Polym Degrad Stab* 2012;97:2301-12.
- [317] Tsuji H, Suzuyoshi K, Tezuka Y, Ishida T. Environmental degradation of biodegradable polyesters: 3. Effects of alkali treatment on biodegradation of poly( $\epsilon$ -caprolactone) and poly[(*R*)-3-hydroxybutyrate] films in controlled soil. *J Polym Environ* 2003;11:57-65.
- [318] Casarin SA, Agnelli JAM, Malmonge SM, Rosario F. Biodegradable PHB/copolyester blends - biodegradation in soil. *Polim Cienc Tecnol* 2013;23:115-22.
- [319] Rosa DS, Lotto NT, Lopes DR, Guedes CGF. The use of roughness for evaluating the biodegradation of poly-beta-(hydroxybutyrate) and poly- $\beta$ -(hydroxybutyrate-*co*-  $\beta$ -valerate). *Polym Test* 2004;23:3-8.
- [320] Mergaert J, Anderson C, Wouters A, Swings J, Kersters K. Biodegradation of polyhydroxyalkanoates. *FEMS Microbiol Rev* 1992;103:317-21.
- [321] Molitoris HP, Moss ST, deKoning GJM, Jendrossek D. Scanning electron microscopy of polyhydroxyalkanoate degradation by bacteria. *Appl Microbiol Biotechnol* 1996;46:570-9.
- [322] Lim SP, Gan SN, Tan IKP. Degradation of medium-chain-length polyhydroxyalkanoates in tropical forest and mangrove soils. *Appl Biochem Biotechnol* 2005;126:23-33.

- [323] Abou-Zeid DM, Muller RJ, Deckwer WD. Degradation of natural and synthetic polyesters under anaerobic conditions. *J Biotechnol* 2001;86:113-26.
- [324] Kasuya K, Takagi K, Ishiwatari S, Yoshida Y, Doi Y. Biodegradabilities of various aliphatic polyesters in natural waters. *Polym Degrad Stab* 1998;59:327-32.
- [325] Doi Y, Kanesawa Y, Tanahashi N, Kumagai Y. Biodegradation of microbial polyesters in the marine-environment. *Polym Degrad Stab* 1992;36:173-7.
- [326] Doi Y, Abe H. Structural effects on biodegradation of aliphatic polyesters. *Macromol Symp* 1997;118:725-31.
- [327] Ho YH, Gan SN, Tan IKP. Biodegradation of a medium-chain-length polyhydroxyalkanoate in tropical river water. *Appl Biochem Biotechnol* 2002;102:337-47.
- [328] Boskhomdzhieva AP, Bonartseva AP, Makhinaa TK, Myshkinaa VL, Ivanova EA, Bagrovb DV, Filatovaa EV, Bonartsevaaa GA. Biodegradation kinetics of poly(3-hydroxybutyrate) based biopolymer systems. *Biochemistry (Moscow) Suppl Ser B* 2010;4:177-83.
- [329] Eldsater C, Karlsson S, Albertsson AC. Effect of abiotic factors on the degradation of poly(3-hydroxybutyrate-co-3-hydroxyvalerate) in simulated and natural composting environments. *Polym Degrad Stab* 1999;64:177-83.
- [330] Thellen C, Coyne M, Froio D, Auerbach M, Wirsén C, Ratto JA. A processing, characterization and marine biodegradation study of melt-extruded polyhydroxyalkanoate (PHA) films. *J Polym Environ* 2008;16:1-11.
- [331] Kaplan DL, Mayer JM, Greenberger M, Gross R, McCarthy S. Degradation methods and degradation kinetics of polymer-films. *Polym Degrad Stab* 1994;45:165-72.
- [332] Mergaert J, Webb A, Anderson C, Wouters A, Swings J. Microbial-degradation of poly(3-hydroxybutyrate) and poly(3-hydroxybutyrate-co-3-hydroxyvalerate) in soils. *Appl Environ Microbiol* 1993;59:3233-8.
- [333] Mergaert J, Wouters A, Anderson C, Swings J. In-situ biodegradation of poly(3-hydroxybutyrate) and poly(3-hydroxybutyrate-co-3-hydroxyvalerate) in natural-waters. *Can J Microbiol* 1995;41:154-9.
- [334] Voinova O, Gladyshev M, Volova TG. Comparative study of PHA degradation in natural reservoirs having various types of ecosystems. *Macromol Symp* 2008;269:34-7.
- [335] Volova TG, Boyandin AN, Vasil'ev AD, Karpov VA, Kozhevnikov IV, Prudnikova SV, Rudnev VP, Xuan BB, Dung VVT, Gitel'zon II. Biodegradation of

- polyhydroxyalkanoates (PHAs) in the South China Sea and identification of PHA-degrading bacteria. *Microbiology* 2011;80:252-60.
- [336] Volova TG, Boyandin AN, Vasiliev AD, Karpov VA, Prudnikova SV, Mishukova OV, Boyarskikh UA, Filipenko ML, Rudnev VP, Bui BX, Vu VD, Gitelson II. Biodegradation of polyhydroxyalkanoates (PHAs) in tropical coastal waters and identification of PHA-degrading bacteria. *Polym Degrad Stab* 2010;95:2350-9.
- [337] Volova TG, Gladyshev MI, Trusova MY, Zhila NO. Degradation of polyhydroxyalkanoates and the composition of microbial destructors under natural conditions. *Microbiology* 2006;75:593-8.
- [338] Volova TG, Gladyshev MI, Trusova MY, Zhila NO. Degradation of polyhydroxyalkanoates in eutrophic reservoir. *Polym Degrad Stab* 2007;92:580-6.
- [339] Rutkowska M, Krasowska K, Heimowska A, Adamus G, Sobota M, Musiol M, Janeczek H, Sikorska W, Krzan A, Zagar E, Kowalczyk M. Environmental degradation of blends of atactic poly[(*R,S*)-3-hydroxybutyrate] with natural PHBV in baltic sea water and compost with activated sludge. *J Polym Environ* 2008;16:183-91.
- [340] Riggi E, Santagata G, Malinconico M. Bio-based and biodegradable plastics for use in crop production. *Recent Pat Food, Nutr Agric* 2011;3:49-63.
- [341] Bastioli C, Floridi G, Del Tredici G. Biodegradable multiphase compositions based on starch. US 20100003434 A1 2010. 7 pp.
- [342] Briassoulis D. Mechanical behaviour of biodegradable agricultural films under real field conditions. *Polym Degrad Stab* 2006;91:1256-72.
- [343] Martin-Closas L, Pelacho AM, Picuno P, Rodriguez D. Properties of new biodegradable plastics for mulching, and characterization of their degradation in the laboratory and in the field. *Acta Hort* 2008;801 275-82.
- [344] Fernando WC, Suyama K, Itoh H, Tanaka A, Yamamoto A. Degradation of an acylated starch-plastic mulch film in soil and impact on soil microflora. *Soil Sci Plant Nutr* 2002;48:701-9.
- [345] Kapanen A, Schettini E, Vox G, Itavaara M. Performance and environmental impact of biodegradable films in agriculture: A field study on protected cultivation. *J Polym Environ* 2008;16:109-22.
- [346] Calmon A, Guillaume S, Bellon-Maurel V, Feuilloley P, Silvestre F. Evaluation of material biodegradability in real conditions-development of a burial test and an analysis methodology based on numerical vision. *J Environ Polym Degrad* 1999;7:157-66.

- [347] Andrady AL, Pegram JE, Olson TM. Research and development of two marine-degradable biopolymers. Research Triangle Institute Report Accession Number AD-A254 051. 1992. 47 pp.
- [348] Gan ZH, Kuwabara K, Abe H, Iwata T, Doi Y. The role of polymorphic crystal structure and morphology in enzymatic degradation of melt-crystallized poly(butylene adipate) films. *Polym Degrad Stab* 2005;87:191-9.
- [349] Nakamura H, Nakamura T, Noguchi T, Imagawa K. Photodegradation of PEEK sheets under tensile stress. *Polym Degrad Stab* 2006;91:740-6.
- [350] Ikada E. Relationship between photodegradability and biodegradability of some aliphatic polyesters. *J Photopolym Sci Technol* 1999;12:251-6.
- [351] Janorkar AV, Metters AT, Hirt DE. Degradation of Poly(*L*-Lactide) films under ultraviolet-induced photografting and sterilization conditions. *J Appl Polym Sci* 2007;106:1042-7.
- [352] Zaidi L, Kaci M, Bruzaud S, Bourmaud A, Grohens Y. Effect of natural weather on the structure and properties of polylactide/Cloisite 30B nanocomposites. *Polym Degrad Stab* 2010;95:1751-8.
- [353] Briassoulis D. The effects of tensile stress and the agrochemical Vapam on the ageing of low density polyethylene (LDPE) agricultural films. Part I. Mechanical behaviour. *Polym Degrad Stab* 2005;88:489-503.
- [354] Griffin GJL. Synthetic-polymers and the living environment. *Pure Appl Chem* 1980;52:399-407.
- [355] Kockott D. Natural and artificial weathering of polymers. *Polym Degrad Stab* 1989;25:181-208.
- [356] Scheirs J. *Compositional and Failure Analysis of Polymers*. Chichester: John Wiley & Sons Ltd: 2000.. 806 pp.
- [357] Farias RF, Canedo EL, Wellen RMR, Rabello MS. Environmental stress cracking of poly(3-hydroxybutyrate) under contact with sodium hydroxide. *Mater Res (Sao Carlos, Braz)* 2015;18:258-66.
- [358] Li X, Chu C, Chu PK. Effects of external stress on biodegradable orthopedic materials: A review. *Bioact Mater* 2016;1:77-84.
- [359] Zhao Y, Qiu D, Yang Y, Tang G, Fan Y, Yuan X. Degradation of electrospun poly(*L*-lactide) membranes under cyclic loading. *J Appl Polym Sci* 2012;124:E258-E66.



- [360] Yang Y, Tang G, Zhao Y, Yuan X, Fan Y. Effect of Cyclic Loading on In Vitro Degradation of Poly(*L*-lactide-*co*-glycolide) Scaffolds. *J Biomater Sci Polym Ed* 2010;21:53-66.
- [361] Thompson DE, Mauli Agrawal C, Athanasiou K. The effect of dynamic compressive loading on biodegradable implants of 50-50% polylactic acid-polyglycolic acid. *Tissue Eng* 1996;2:61-74.
- [362] Nicodemus GD, Shiptet KA, Kaltz SR, Bryant SJ. Dynamic compressive loading influences degradation behavior of PEG-PLA hydrogels. *Biotechnol Bioeng* 2009;102:948-59.
- [363] Arm DM, Tencer AF. Effects of cyclical mechanical stress on the controlled release of proteins from a biodegradable polymer implant. *J Biomed Mater Res* 1997;35:433-41.
- [364] Rajagopal KR, Srinivasa AR, Wineman AS. On the shear and bending of a degrading polymer beam. *Int J Plast* 2007;23:1618-36.
- [365] Soares JS, Moore JEJ, Rajagopal KR. Constitutive Framework for Biodegradable Polymers with Applications to Biodegradable Stents. *ASAIO J* 2008;54:295-301.
- [366] Soares JS, Moore JE, Rajagopal KR. Modeling of deformation-accelerated breakdown of polylactic acid biodegradable stents. *J Med Device* 2010;4:041007/1-10.

Fig. 1. Steps involved in polymer biodegradation by hydrolysis. Under a surface erosion mechanism ( $\lambda' > D; L > L_{crit}$ ), polymer is eroded from the surface and the core polymeric material remains intact (average molecular weight  $M_n$  and mechanical property), until the load bearing capability decreases steadily as the thickness of the polymer is less than the critical thickness. At this point the mechanism of erosion shifts to bulk erosion ( $\lambda' < D; L < L_{crit}$ ), where the time to failure becomes dominated by the rate of auto-acceleration of hydrolysis where  $M_n$  reaches a critical value  $M_e$ . From this point, the polymer depolymerises into water-soluble products oligomer and monomers, followed by assimilation by micro-organisms into biomass or mineralised to  $CO_2$ ,  $H_2O$ ,  $CH_4$  and other metabolic products.  $L$  is the thickness of the specimen,  $L_{crit}$  is the critical sample thickness,  $\lambda'$  is the pseudo first order rate of hydrolysis and  $D$  is the diffusion coefficient. Surface and bulk erosion plots from [6], Copyright 2014. Reproduced with permission from Future Medicine Ltd.

Fig. 2. Schematic illustration of three types of erosion phenomenon: (a) surface erosion with a growing hydrolysis front (e.g. enzymes), (b) bulk erosion with autocatalysis due to retained degradation products (e.g. PLA), (c) bulk erosion without autocatalysis (e.g. PLA-co-PCL) where water diffusion and catalyst is faster than the reaction rate (based on [49]).  $L_{crit}$  is the critical sample thickness,  $\lambda'$  is the pseudo first order rate of hydrolysis and  $D$  is the diffusion coefficient. [28], Copyright 2014. Reproduced with permission from Springer Science + Business Media.

Fig. 3. 'Flow diagram' showing processes involved in hydrolytic degradation of bulk eroding polymers. Shaded boxes refer to the most frequently measured properties. Dotted lines/boxes indicate processes applicable only to semi-crystalline polymers. [41], Copyright 2008, Reproduced with permission from Woodhead Publishing Ltd.

- Fig. 4. Comparison of the degradation processes: matrix morphology and acid catalyst concentration ( $\beta = 3$ , where  $\beta$  is a parameter that regulates the autocatalysis effect for matching the modelling results to known experimental data), based on equation (22) herein. Only a quarter of the polymer matrix is considered because of the double symmetry, in which the lower left corner of design domain is the centre of the whole polymer film. Size of design domain: left, 3 mm; middle, 0.2 mm; right, 10  $\mu\text{m}$ . [115], Copyright 2011. Reproduced with permission from Elsevier Ltd.
- Fig. 5. Model to simulate monomer release from polyanhydride matrices using Monte Carlo techniques according to [39, 135]. Illustration of matrix porosity calculations from erosion simulations, [135], Copyright 1995. Reproduced with permission from Elsevier Ltd.
- Fig. 6. Simulation of polymer erosion using a Monte Carlo model (black pixels, non-eroded areas; white pixels, eroded areas). [32], Copyright 1996. Reproduced with permission from Elsevier Ltd.
- Fig. 7. Plots of calculated tensile strength vs time of hydrolysis for different initial molecular weights using equation (42). [18], Copyright 2002. Reproduced with permission from Elsevier Ltd.
- Fig. 8. Flowchart of numerical simulation used for degradation behaviour and mechanical properties of PLGA films and tissue engineering scaffolds.  $C_m$  is the mole concentration of monomers;  $[E]$  concentration of ester groups;  $[E]_0$  the initial concentration of ester groups,  $C_m^B$  diffusion of monomers and accounts for dissociation of acid end group;  $k_1$  the non-catalytic reaction rate constant;  $k_2$  the autocatalytic reaction rate constant,  $\overline{M}_n$  number average molecular weight,  $\overline{M}_{n0}$  initial number average molecular weight, N number of polymer chains per unit volume,  $N_{chains}$  total number of polymer chains,  $R_{scissions}$  ratio of random scissions

to end scissions;  $\bar{M}_e$  critical molecular weight for chain entanglement,  $N_{total}$  sum of polymer units in a group of chains,  $m$  molar mass of repeat unit,  $n$  total number of chains in a group of chains,  $E$  the Young's modulus;  $E_0$  initial Young's modulus,  $k_b$  Boltzmann's constant;  $T$  temperature,  $N$  number of polymer chains per unit volume,  $N_0$  initial number of polymer chains,  $D_0$  intrinsic diffusion coefficient. [179], Copyright 2016. Adapted with permission from Elsevier Ltd.

Fig. 9. Modelling of mechanical properties for PGA over time; (A) Molecular weight variation profiles with degradation time for PGA with different initial molecular weights; (B) Variations in ultimate strength ratios for PGA-1700 under external loads of 0, 440, 540 MPa, at 300K with degradation time; (C) Temperature effect on PGA-1700 strength with degradation time. [183], Copyright 2014. Reproduced with permission from AIP Publishing.

Fig. 10. Modelling of changes in mechanical properties over time using three different approaches for the degradation of PLA-PCL fibres. [9], Copyright 2011. Reproduced with permission from Elsevier Ltd.

Fig. 11. The prediction of changes in mechanical properties over time for porous polymers with different architectures. The different architectures include a face-centred-cube arrangement of spherical pores with corner pores (model A), a regular packing of cubic pores (model B) and a face-centred cubic arrangement of spherical pores without corner pores (model C). Variation of (a) strain, (b) Young's modulus, and (c) damage  $d$  of the three micro-cell models with time. [189], Copyright 2011. Reproduced with permission from John Wiley & Sons Inc.

Fig. 12. Evolution of the stress-at-break (a) and strain-at-break (b) as a function of molecular weight for PHBV aged in distilled water at 25, 30, 40 and 50°C. [191], Copyright 2014. Reproduced with permission from Elsevier Ltd.

Fig. 13. Schematic model of the enzymatic degradation behaviour of flat-on lamellar crystal in P(3HB) melt crystallized thin films by PHB depolymerase from *R. pickettii* T1 at 20°C. (A): Flat-on lamellar crystal composed of both amorphous and crystalline phases in a phosphate buffer solution before enzymatic degradation. Two arrows indicate loose chain-packing region. [238], Copyright 2004. Reproduced with permission from the American Chemical Society.

Fig. 14. Relationship between the erosion rate of crystalline phase and the lamellar thickness: (○) P(3HB); (●) P(3HB-co-6 mole % 3HV); (▲) P(3HV)-co-6 mol % 3HHx); (Δ) P(3HB-co-6 mol % mcl-3HA). [250], Copyright 2002. Reproduced with permission from the American Chemical Society.

Fig. 15. Enzymatic hydrolysis of amylose by amylase [34].

Fig. 16. Enzymatic, non-hydrolytic degradation of cellulose [34].

Fig. 17. Abiotic and biotic degradation of PLA during compositing. [197], Copyright 2011. Reproduced with permission from Elsevier Ltd.

Fig. 18. Biodegradation of PCL by *Penicillium funiculosum* showing areas of severe biodegradation near mycelium. Complete degradation of amorphous and crystalline regions seen; magnification 1080X. [300], Copyright 1981. Reproduced with permission from John Wiley and Sons, Inc.

Fig.1

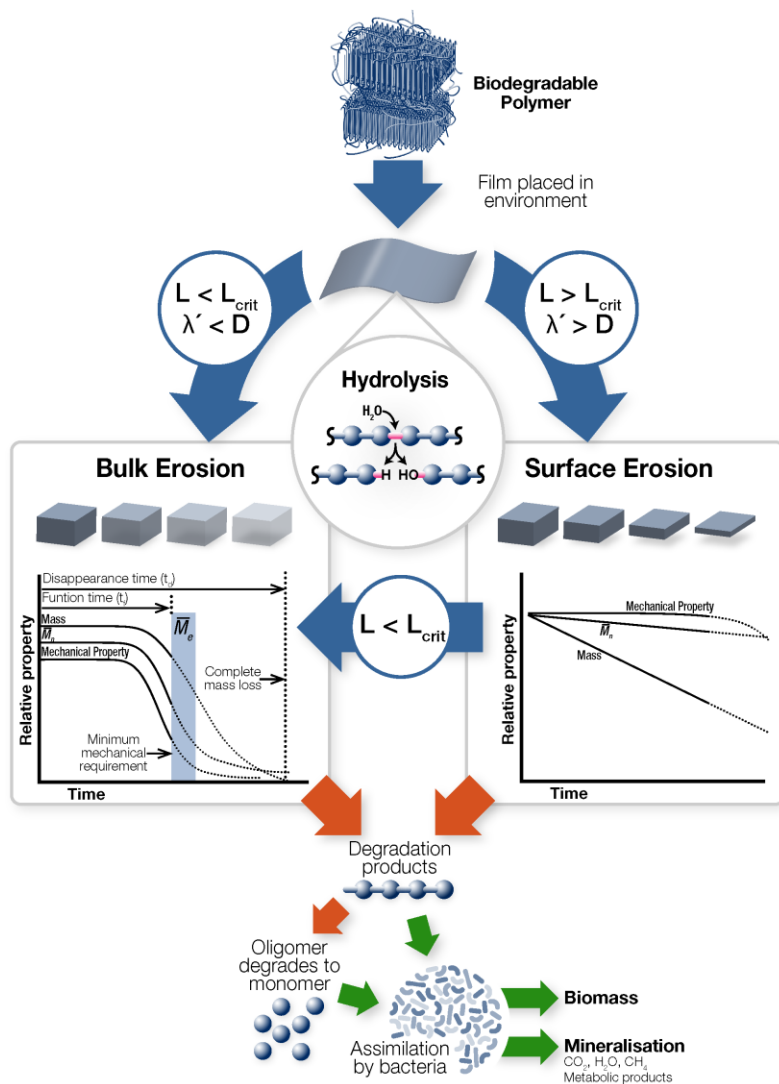
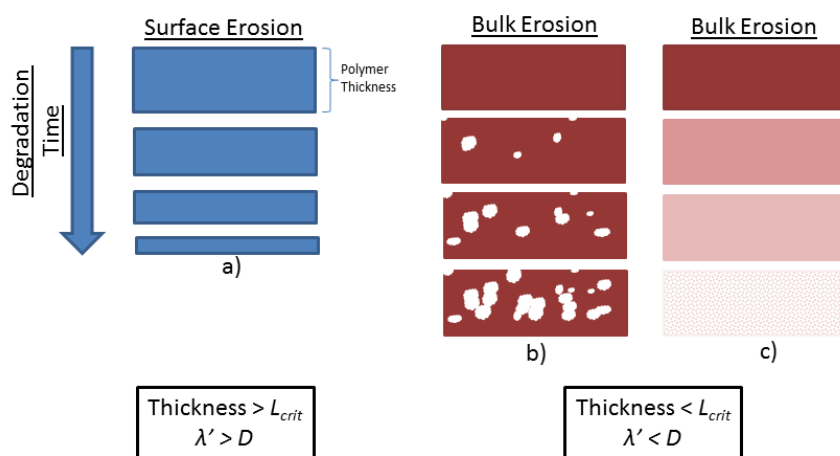


Fig.2



Critical sample thickness  $L_{crit} = (D/\lambda')^{1/2}$ ,  $D$  is the diffusion coefficient of water and  $\lambda'$  the pseudo first order hydrolysis rate constant

Fig.3

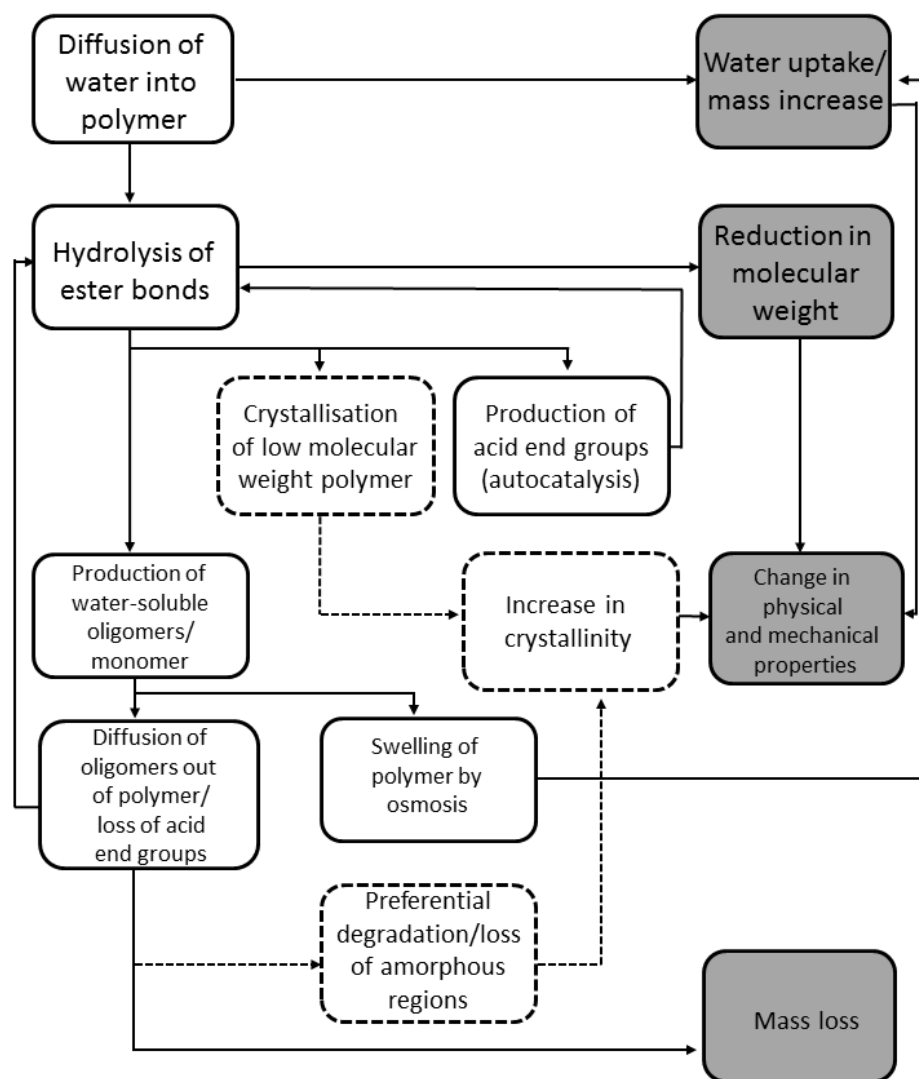




Fig.4

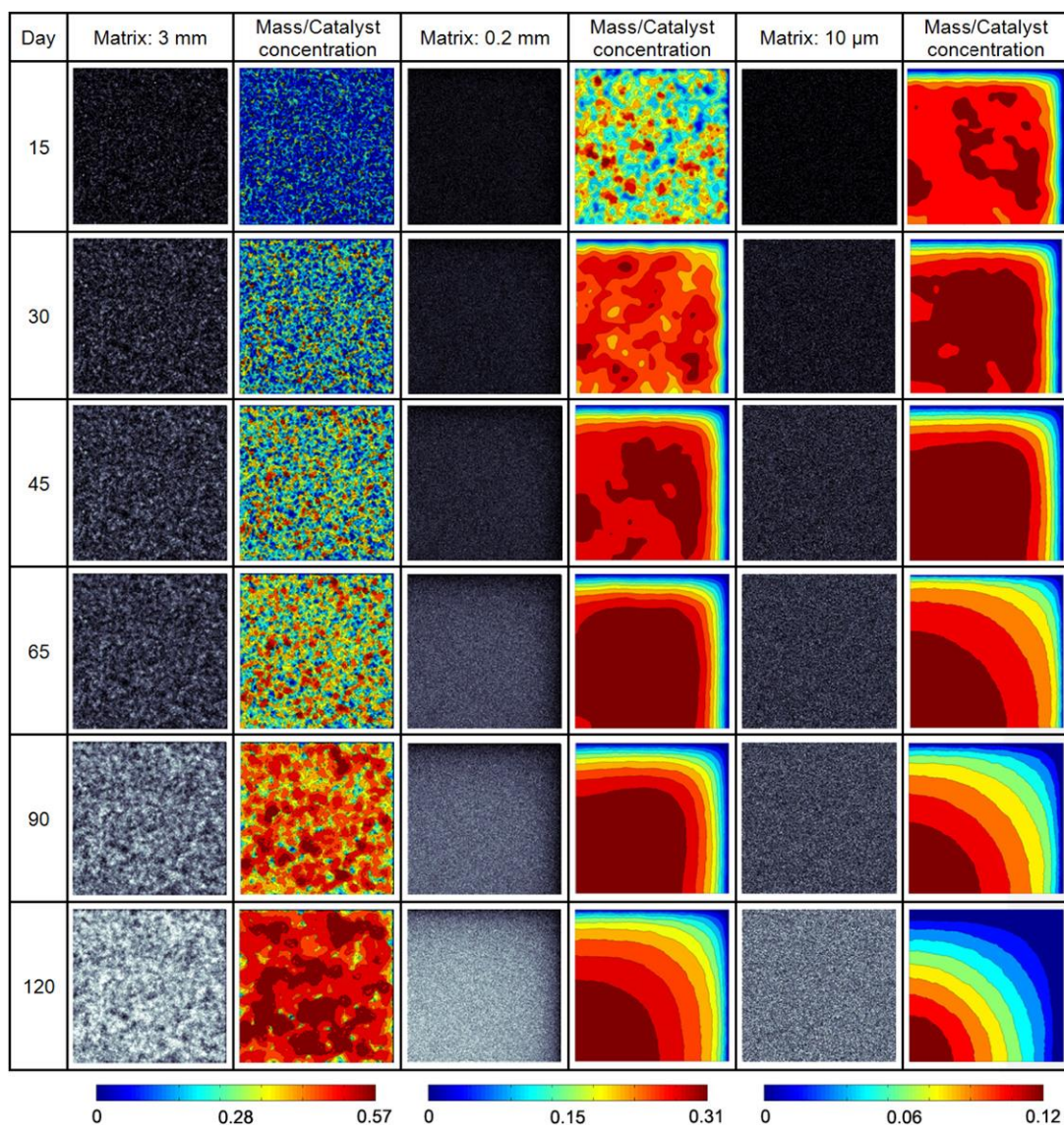


Fig.5

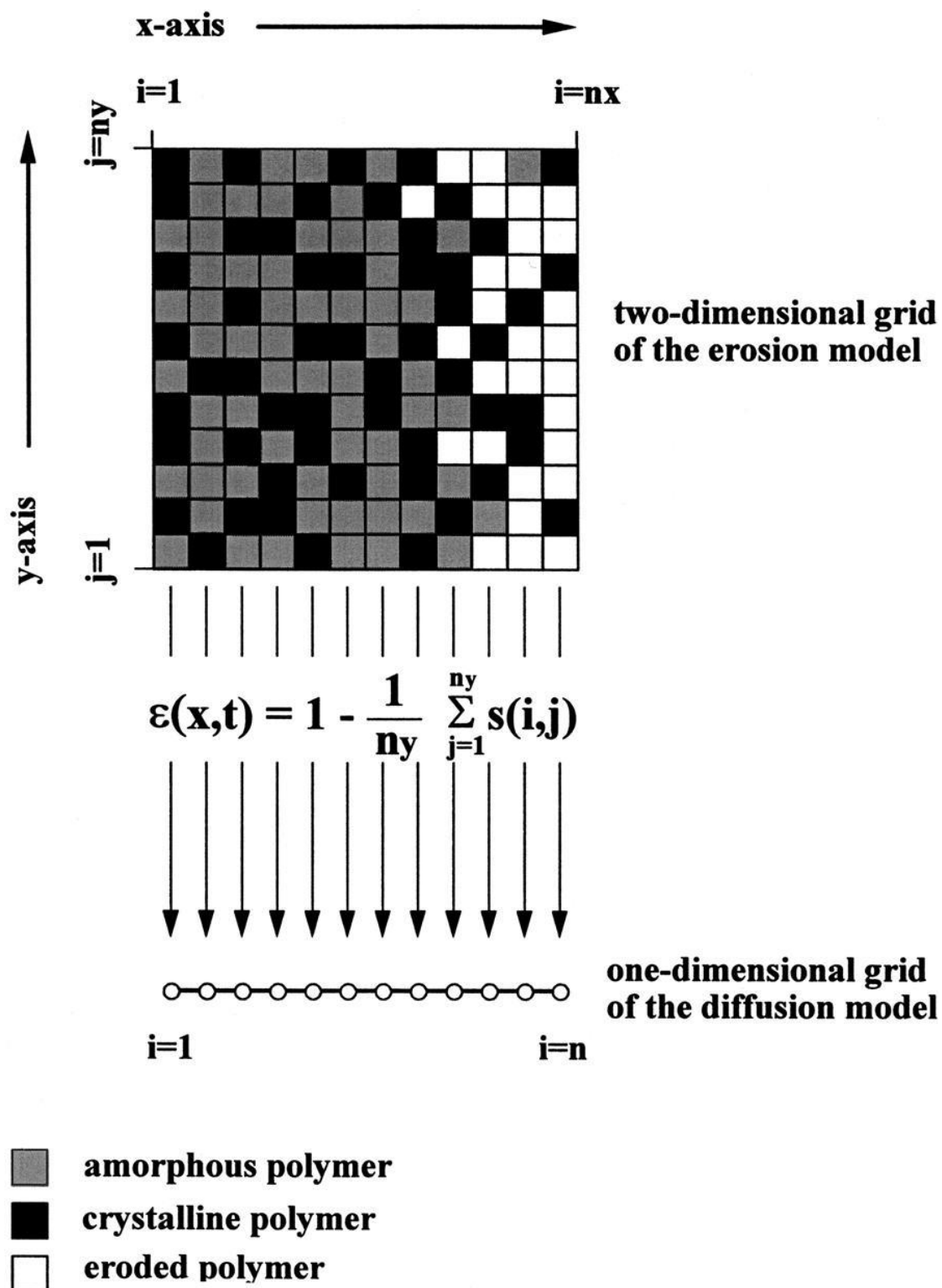


Fig.6

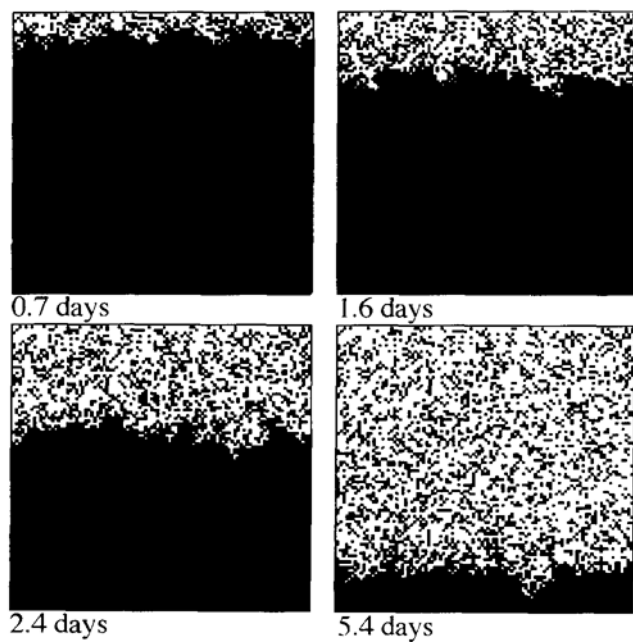


Fig.7

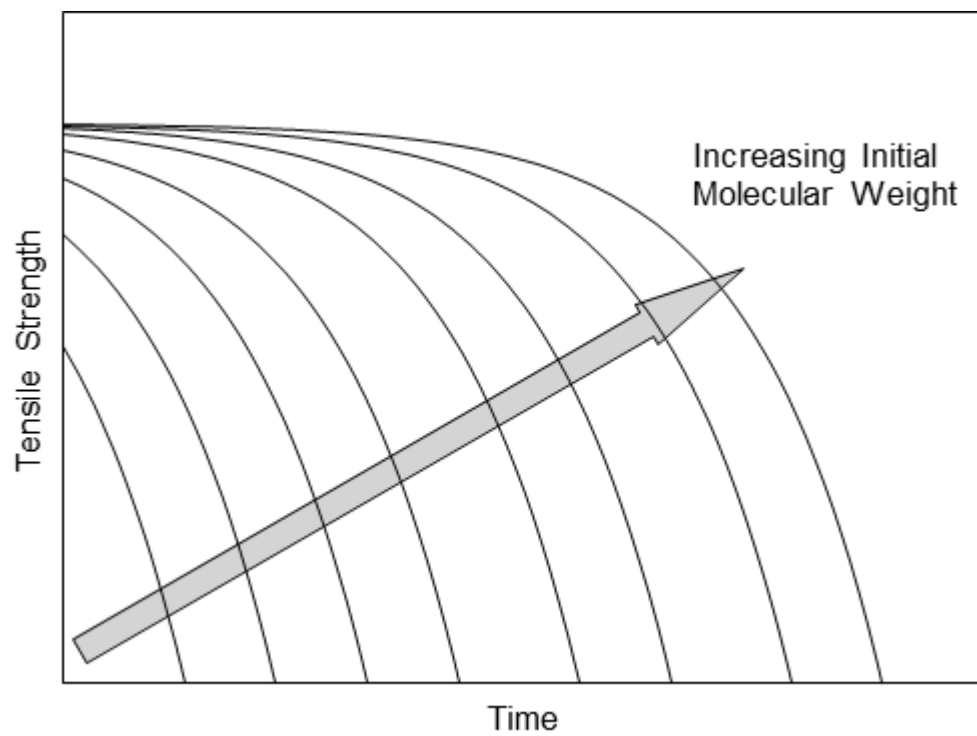


Fig.8

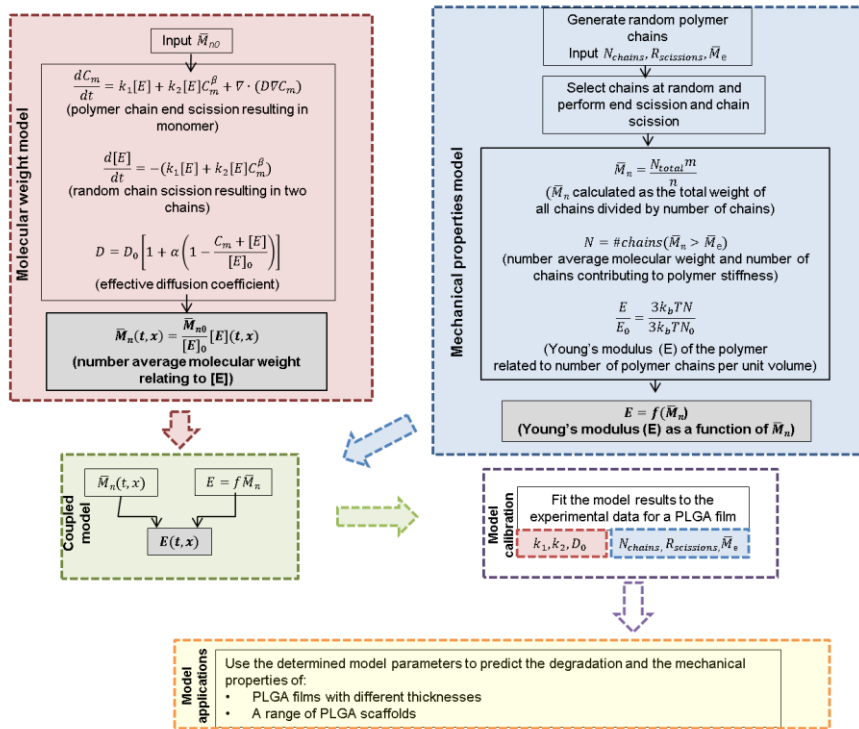


Fig.9

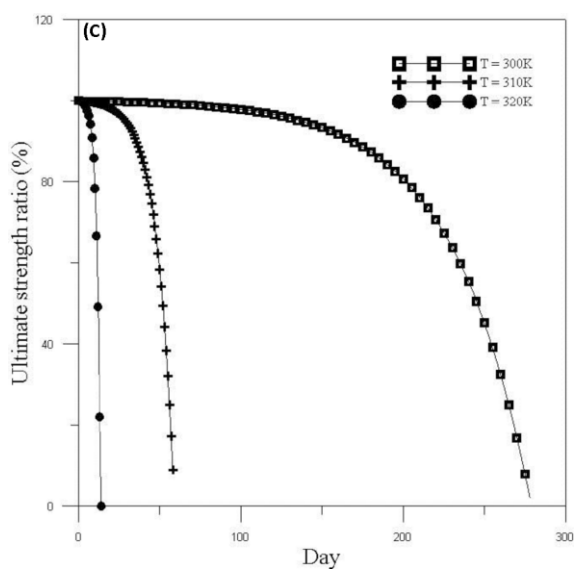
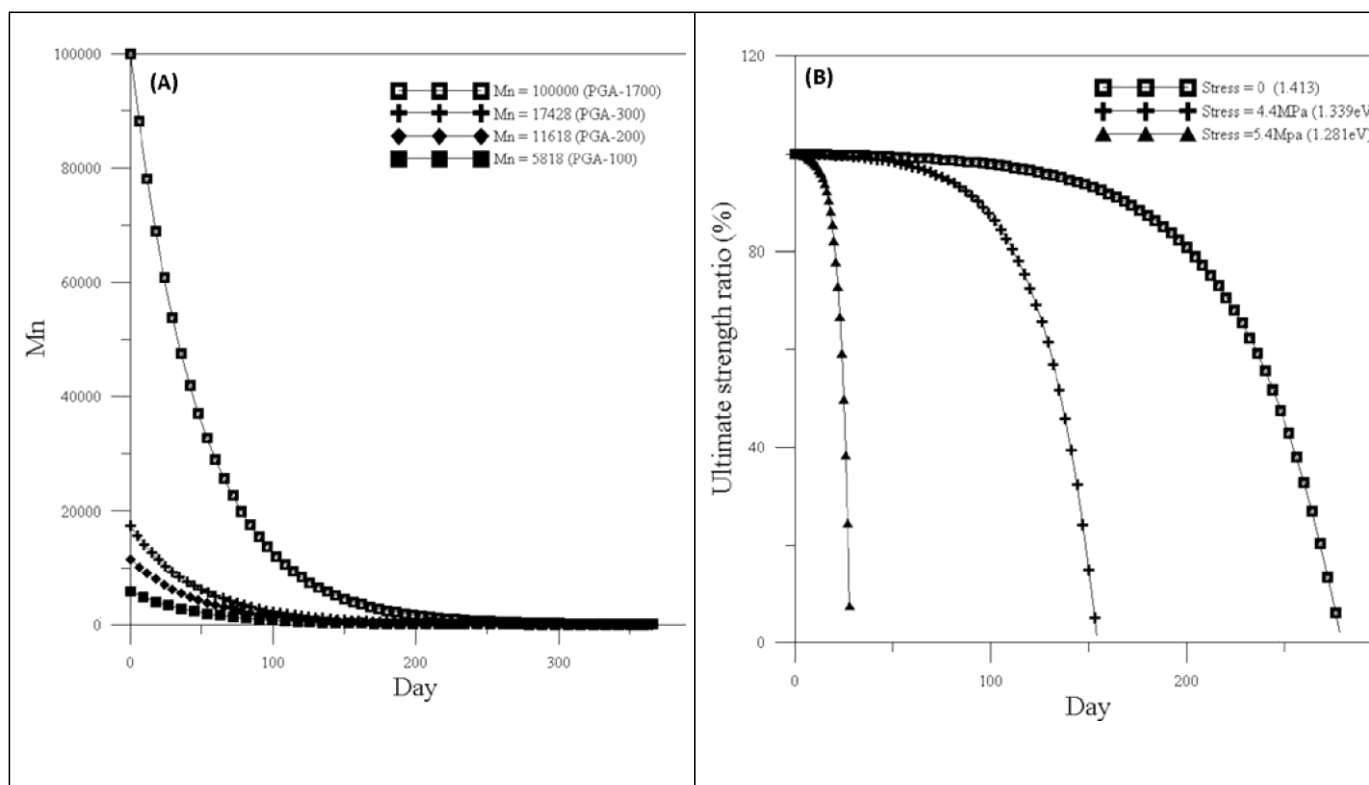


Fig.10

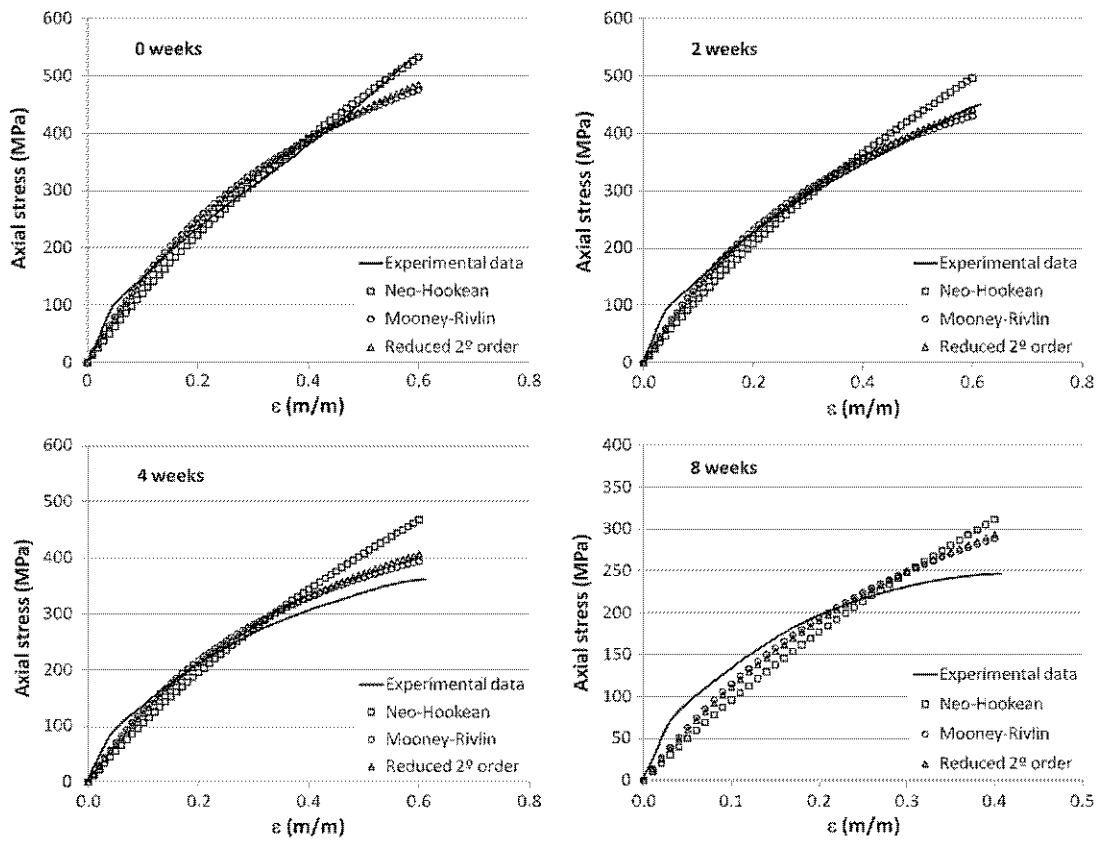


Fig.11

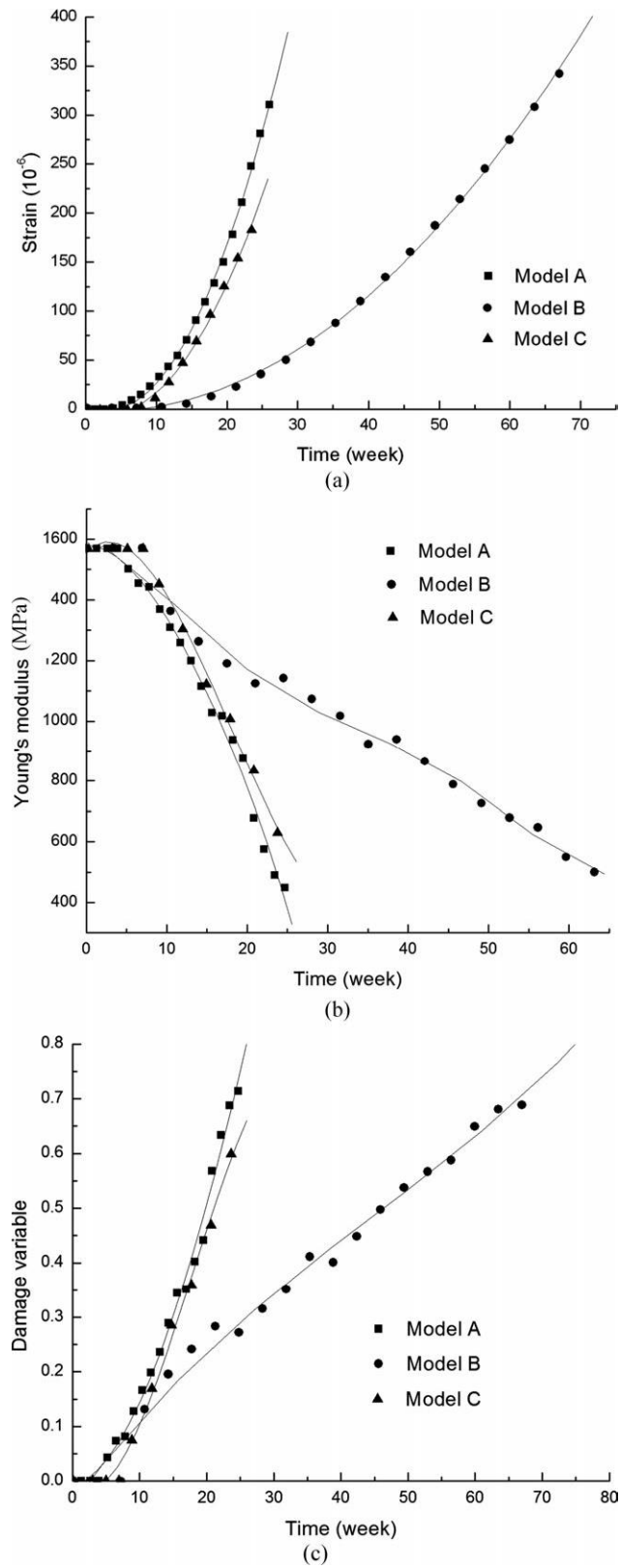




Fig.12

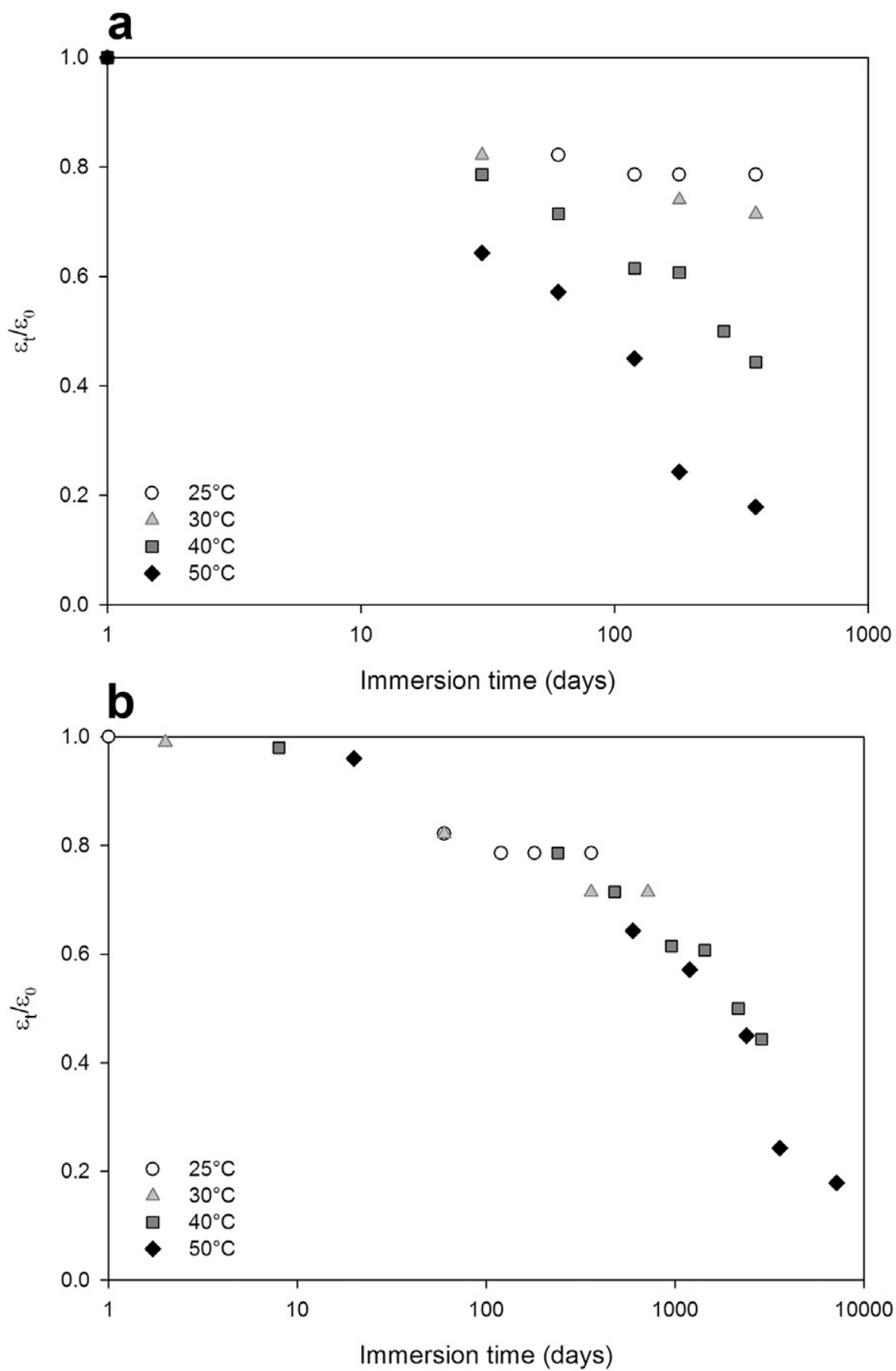


Fig.13

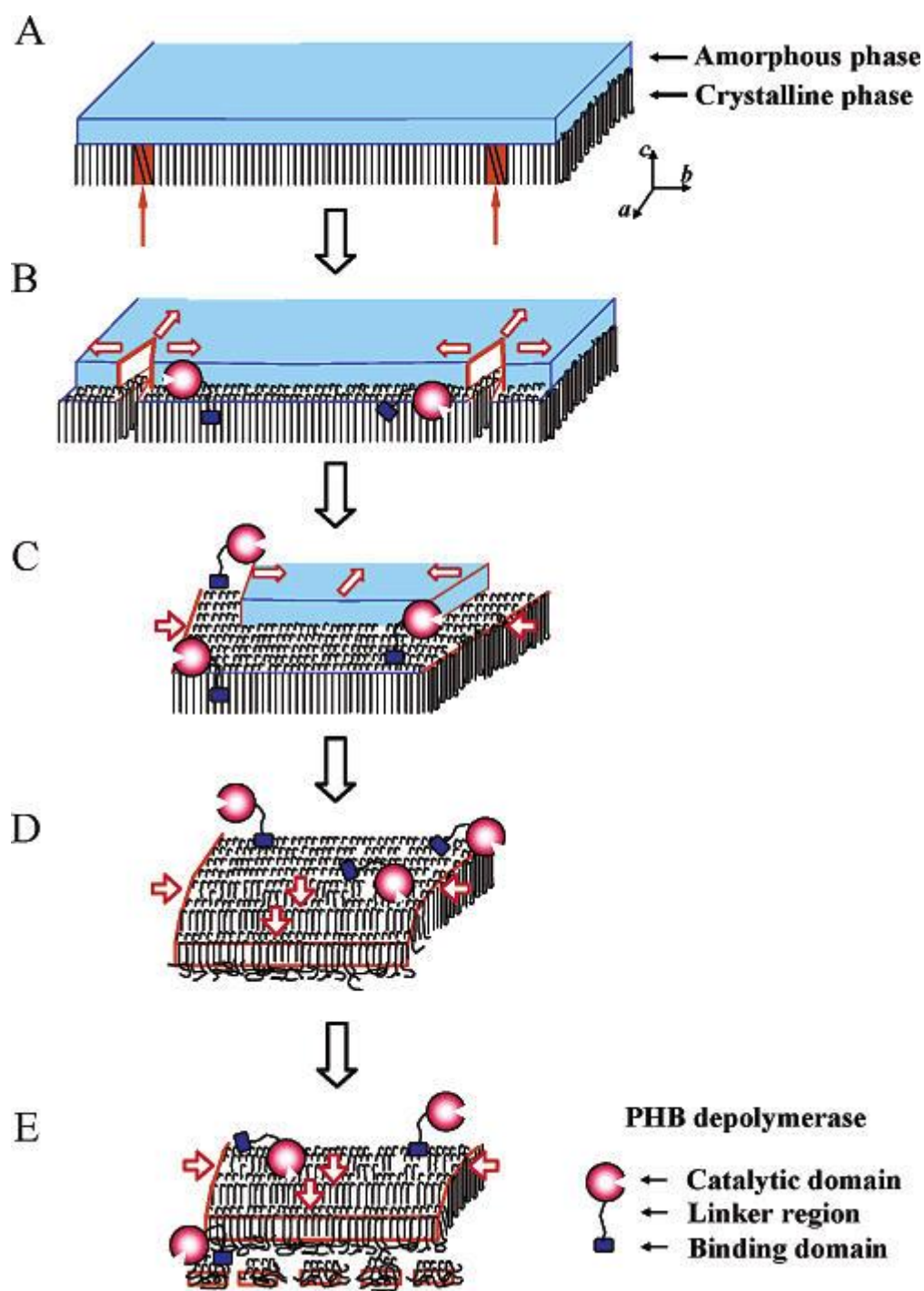


Fig.14

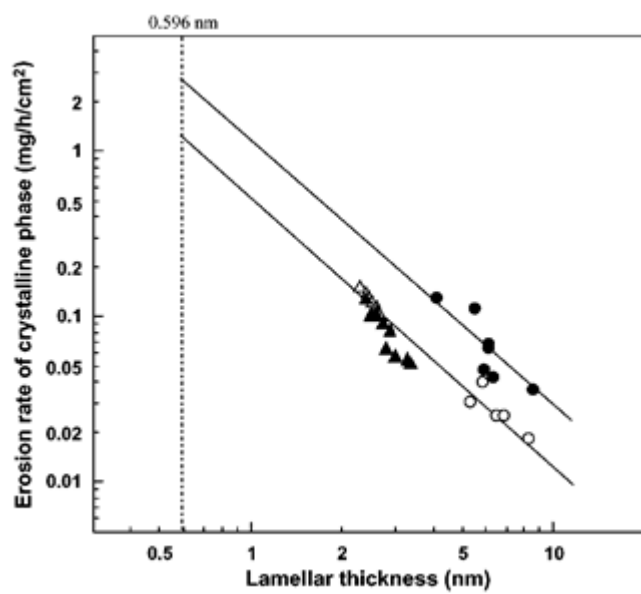


Fig.15

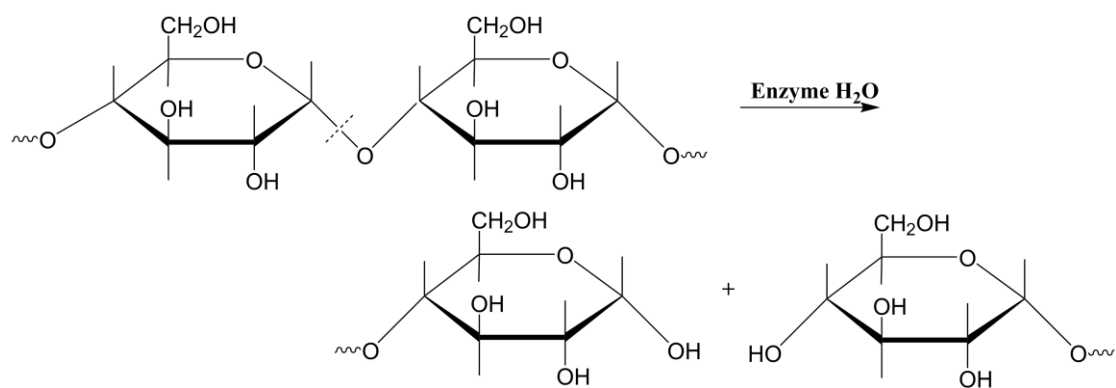


Fig.16

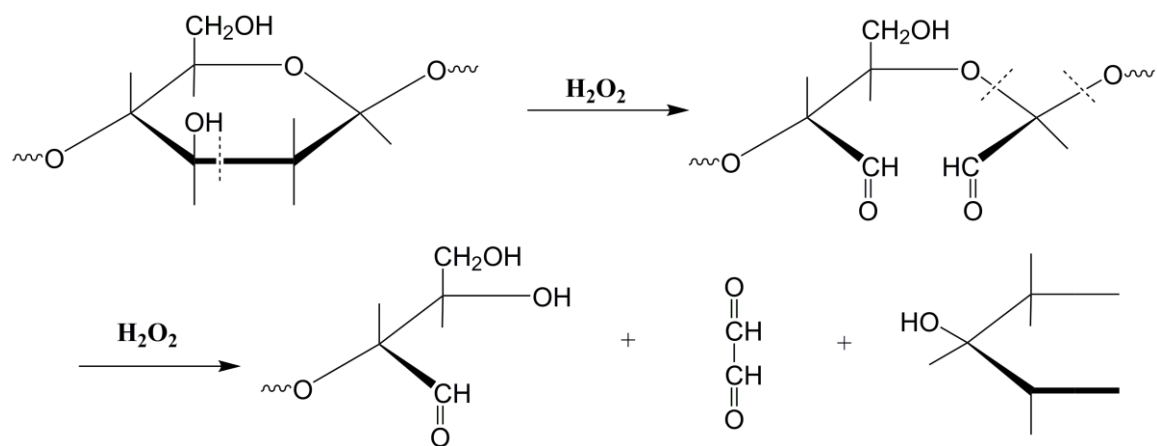


Fig.17

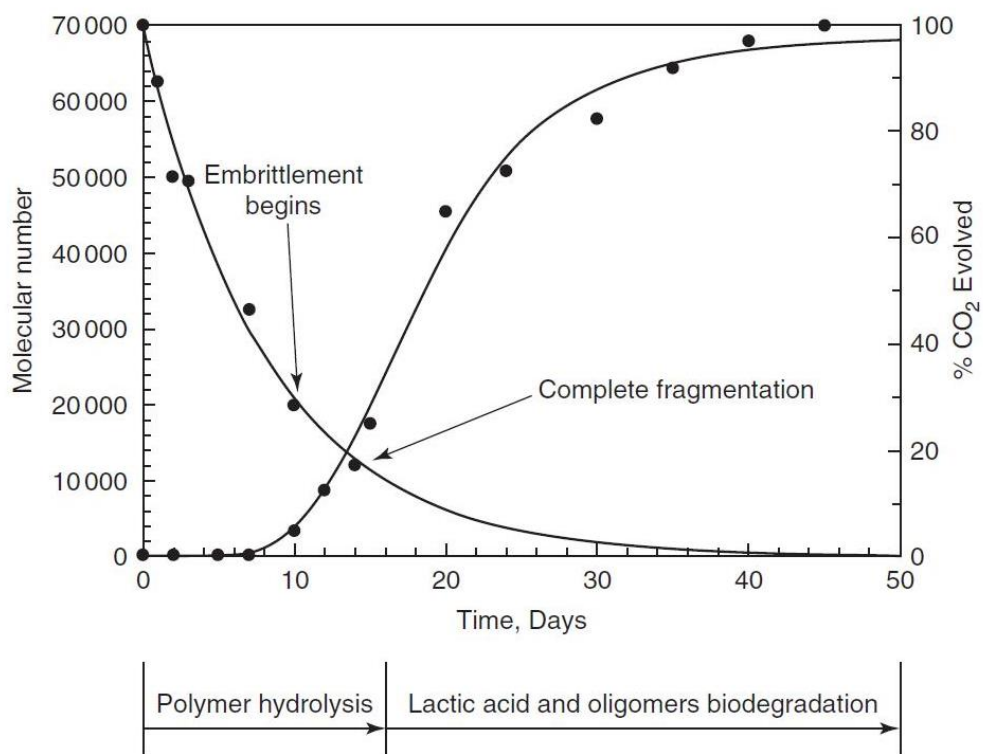


Fig.18

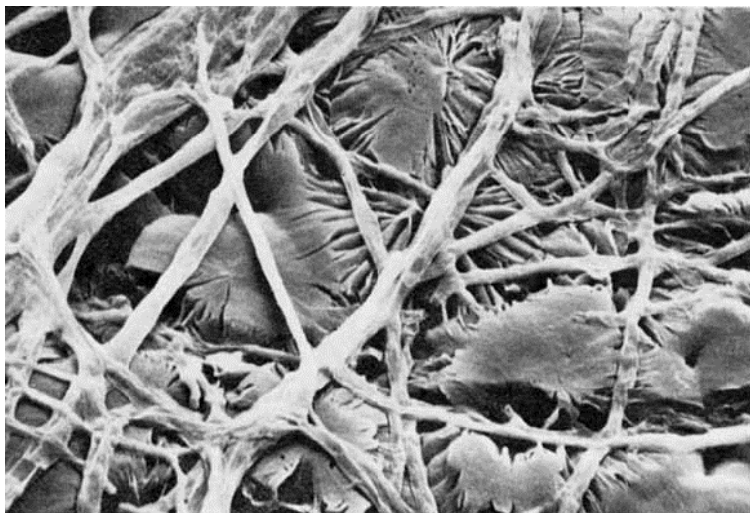
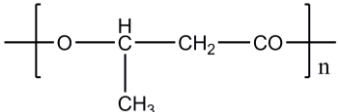
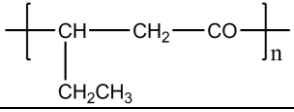
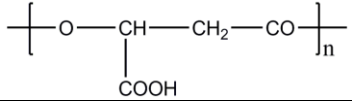
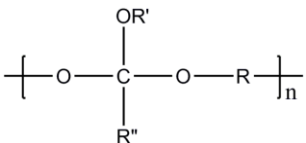
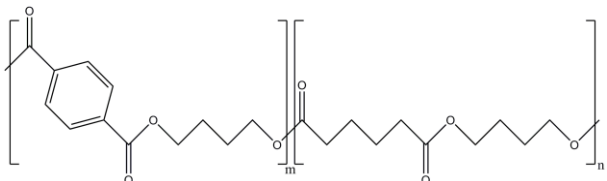
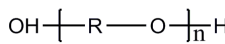
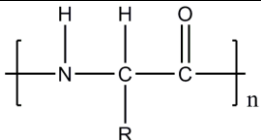
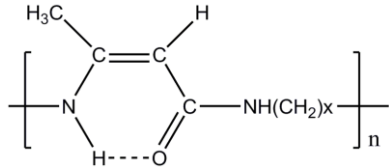
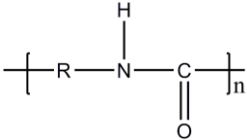
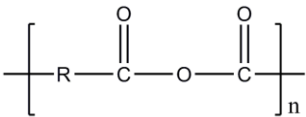
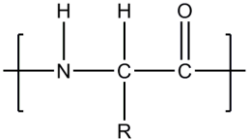
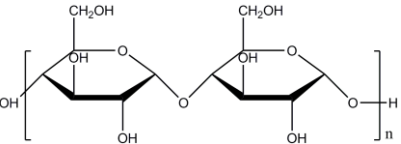
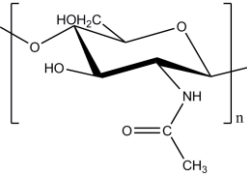


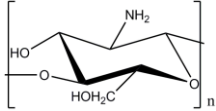
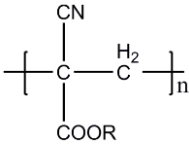
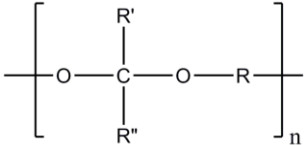
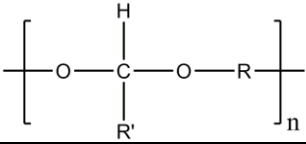
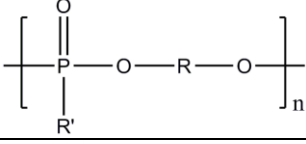
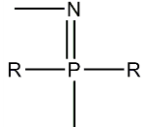
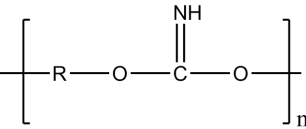
Table 1. Classes of biodegradable polymers.

Type	Chemical Structure	Comments	Examples	Reference
Poly( $\epsilon$ -caprolactone) (PCL)		Generally prepared from the ring opening polymerisation of $\epsilon$ -caprolactone. Degradation <i>in vivo</i> is much slower than poly( $\alpha$ -hydroxy acid)s.	Tailored lifetime and properties by blending of PCL with: poly(L-lactic acid), poly(3-hydroxybutyrate-co3-hydroxyvalerate), thermoplastic starch.	[34, 64-66]
Poly(glycolic acid) (PGA)		High crystallinity (45-55%), high tensile modulus, poor solubility in organic solvents. Excellent fibre forming ability. $T_g$ 35-40°C and melting point >200°C. High rate of degradation and acidic degradation products.	Several glycolide copolymers units have been developed to overcome the inherent disadvantages of PGA, such as a 90% glycolic acid (GA) and 10% L-lactic acid (LA) copolymer that was initially used for the development of the multifilament suture Vicryl®. A modified version of the suture, Vicryl Rapid® is an irradiated version of the suture to increase the rate of degradation. PANACRYL® is another commercially developed suture from the co-polymer with a higher LA/GA ratio in order to decrease the rate of degradation.	[67-69]
Poly(lactic acid) (PLA)		Poly(lactic acid) undergoes slow hydrolytic degradation via the bulk erosion when the thickness of the device is less than the critical sample thickness and the rate of water diffusion is greater than the rate of hydrolysis of the ester backbone.	Poly(L-lactide) (PLLA), poly(DL-lactide) (PDLLA). Sculptra®, an injectable form of PLLA is FDA approved for the restoration or correction of facial fat loss or lipoatrophy in people with the human immunodeficiency virus.	[67, 69, 70]
Polyvalerolactone (PVL)		Biodegradable but at a slow rate.	Biodegradable copolymers poly(ethylene glycol)/polyvalerolactone/poly(ethylene glycol) (PEG/PVL/PEG) for drug delivery applications.	[67, 71, 72]
Poly( $\epsilon$ -decalactone)		Amorphous, low $T_g$ aliphatic polyester that can be utilised as a soft segment in thermoplastic polyurethanes (TPU).	Poly( $\epsilon$ -decalactone)- <i>block</i> -poly(lactide) multiblock thermoplastic elastomers.	[67, 73, 74]



Type	Chemical Structure	Comments	Examples	Reference
Poly(3-hydroxybutyrate) (PHB)		A bacterial polyester (polyhydroxyalkanoate) that is highly crystalline with a melting temperature of 180°C and a $T_g \sim 5^\circ\text{C}$ .	Copolymers have better processability and degradation rate eg. poly(3-hydroxybutyrate-co-3-hydroxyvalerate) (PHBV copolymers).	[67, 75]
Polyhydroxyvalerate (PHV)		A bacterial polyester (polyhydroxyalkanoate) produced in plant cells or by fermentation.	The copolymer PHBV is produced commercially as Biopol <sup>®</sup> .	[67, 76]
Poly( $\beta$ -malic acid) (PMLA)		An aliphatic polyester that can generate metabolites during degradation and water soluble irrespective of pH.	PMLA 100 is water-soluble at all pH, and degrades rapidly under physiological conditions.	[67, 77, 78]
Poly(ortho esters) (POE)		Degradation occurs via surface erosion when the device thickness is greater than the critical sample thickness and the rate of hydrolysis is more rapid than the rate of water diffusion into the device. Ortho ester linkages are hydrolytically labile and their the rate of degradation, pH sensitivity, and glass transition temperatures can be controlled by using diols with varying levels of chain flexibility.	Poly(ortho esters) were developed by the ALZA corporation (Alzamer <sup>®</sup> ) as a hydrophobic, surface eroding polymer for drug delivery applications.	[69, 76]
Aromatic copolyesters		Obtained by polycondensation between 1,4-butanediol and a mixture of adipic acid and terephthalic acid.	Poly(butylene adipate-co-adipate-terephthalate) (PBAT) is produced commercially as Ecoflex <sup>®</sup> F Blend C1200.	[33]
Polyethers		Water soluble if the carbon chain is short. Increased molecular weight of poly(ethylene oxide) (PEO), also referred to as poly(ethylene glycol) (PEG), reduces the rate of hydrolysis.	The Dow Chemical Company formulates a wide range of poly(ethylene glycol) products under the CARBOWAX <sup>™</sup> range.	[76, 79]
Polyamides (PA)		High crystallinity and strong interchain interactions (cf more flexible polyesters with analogous structures), resulting in lower rates of biodegradation.	Rilsan <sup>®</sup> (PA 11, Arkema), Rilsan <sup>®</sup> Clear G830 Rnew (PA, Arkema), Grilamid 1S (PA 1010, EMS-GRIVORY), VESTAMID <sup>®</sup> Terra DD (PA 610, Evonik).	[34, 76, 80]

Type	Chemical Structure	Comments	Examples	Reference
Poly(amide-enamines)		Hydrophobic polymer degradable by hydrolysis and biodegradation by fungi and bacteria.	Hydrogen-bond copolyesters containing poly(enol-ketones) and poly(amide-enamine) are used as drug release matrices.	[34, 81-83]
Polyurethanes (PU)		Biodegradability depends on whether the prepolymer is a polyester or a polyether. Has the structural characteristics of both polyesters and polyamides.	Hydrophilic ether urethanes.	[34, 76]
Polyanhydrides		Degradation mainly by surface erosion when the device thickness is greater than the critical sample thickness and the rate of hydrolysis is more rapid than the rate of water diffusion into the device and controlled by varying the amount of hydrophobic or hydrophilic monomers.	Poly(bis( <i>p</i> -carboxyphenoxy)alkane anhydride).	[49, 76]
Polypeptides and proteins		Naturally occurring polyamides (polypeptides) containing amino acid units.	Natural proteins, collagen, gelatin.	[76]
Polysaccharides		Basic sugar units joined by glycoside linkages; hydrolysed abiotically and by enzymes.	Naturally occurring starches and different forms of cellulose.	[76]
Chitin		Also referred to as poly( <i>N</i> -acetyl- $\beta$ - <i>D</i> -glucosamine) and depending on its source, can occur as two allomorphs, namely the $\alpha$ and $\beta$ forms with the $\alpha$ form most common. Most of degradation occurs by bacteria and fungi, where some microorganisms solely degrade chitin via the hydrolysis of glucosidic bonds.	Derivatives of chitin are of biomedical and therapeutic significance. Chitin has been chemically modified by depolymerisation, acylation and grafting of functional groups to alter properties such as water solubility, swelling, immuno-enhancing effects.	[84, 85]

Type	Chemical Structure	Comments	Examples	Reference
Chitosan		Also referred to as poly(D-glucosamine), is a deacetylated derivative of chitin that can degrade via oxidation–reduction depolymerisation and free radical degradation however are unlikely to be a significant source or degradation <i>in vivo</i> . Chitosan can be degraded by enzymes which hydrolyse glucosamine–glucosamine, glucosamine– <i>N</i> -acetyl-glucosamine and <i>N</i> -acetyl-glucosamine– <i>N</i> -acetyl-glucosamine linkages.	Chitosan- <i>graft</i> -copolymers with acrylic, vinyl, nonvinyl groups have been used as slow-release drug carriers. Grafting poly(ethylene glycol) (PEG) onto chitosan has been used to prepare water-soluble chitosan derivatives, to be used as a carrier of anticancer drugs.	[86, 87]
Polycyanoacrylates		Prepared by anionic polymerization. Hydrolysable surgical adhesive.	Poly(alkylcyanoacrylate), poly(ethyl cyanoacrylate).	[33, 34, 88]
Polyketals		Degrade into neutral compounds comprised of acetone and diols and may avoid the inflammation associated with acidic products of polyester materials.	Poly(1,4-phenyleneacetone dimethyleneketal (PPADK), poly(cyclohexane-1,4-diyl acetone dimethylene ketal) (PCADK).	[89-94]
Polyacetals		First prepared by the reaction of a diol (poly(ethylene glycol)) and a divinyl ether (tri(ethylene glycol) divinyl ether) using an acid catalyst, displaying pH dependent degradation.	Amino-polyacetals.	[95]
Polyphosphoesters		Degrade under physiological conditions by hydrolytic and enzymatic cleavage of the phosphate bonds in the backbone to phosphate, alcohol and diols.	Synthetic flexibility of polyphosphoesters allows co-polymers such as poly(lactide-co-ethyl phosphate).	[69]
Polyphosphazenes (PPHOS)		Degradation rate is controlled by varying the amount of hydrolytically unstable side groups (R).	Poly((imidazolyl)methylphenoxy phosphazene) and poly((ethyl glycinato)(methylphenoxy)phosphazene).	[49]
Poly(imino-carbonates)		Derived by replacing the carbonyl oxygen of a carbonate by an imino group, causing a high degree of hydrolytic instability to the polymer without significantly affecting the mechanical properties of the material.	Poly(bisphenol A-iminocarbonate).	[96, 97]

Type	Chemical Structure	Comments	Examples	Reference
Polycarbonates	$\left[ \text{R}-\text{O}-\overset{\text{O}}{\parallel}{\text{C}}-\text{O} \right]_n$	The carbonate bond in aliphatic polycarbonates is readily biodegradable.	Poly(ethylene carbonate), poly(propylene carbonate), poly(butylene carbonate), poly(hexamethylene carbonate).	[98]
Poly(1,4-dioxane-2-one) (PDO)	$\left[ \text{O}-(\text{CH}_2)_2-\text{O}-\text{CO}-\text{CO} \right]_n$	Biocompatible polymer with good flexibility and tensile strength for medical applications.	Degradable suture (Biosyn <sup>®</sup> ), PGA/PTMC/PDO (60%:26%:14%); where PTMC is poly(trimethylene carbonate).	[69, 99]
Poly(1,3-dioxane-2-one) (PDO)	$\left[ \text{O}-(\text{CH}_2)_3-\text{O}-\text{CO} \right]_n$	Breaks down into glycoxylate which is excreted in urine or converted into glycine and subsequently into carbon dioxide and water; similar to polyglycolides. Strength is lost in 1–2 months and mass is lost within 6–12 months by hydrolytic degradation.	Maxon <sup>®</sup> (67.5/32.5 PGA/poly(1,3-dioxane-2-one) copolymer).	[67]
Poly( <i>para</i> -dioxanone) (PDS)	$\left[ \text{O}-(\text{CH}_2)_2-\text{O}-\text{CH}_2-\text{CO} \right]_n$	Used traditionally as a monofilament suture or as a biodegradable ligating clip. Degrades in the body by a nonenzymatic hydrolysis mechanism.	Monofilament suture (PDS <sup>®</sup> ) developed in the 1980s. Also used as fixation screws for small bone and osteochondral fragments (Orthosorb Absorbable Pins <sup>®</sup> ).	[67, 69, 100]

Table 2. Classes of hydrolysable bonds and corresponding half-lives [32, 62, 63]. [32], Copyright 1996,. Reproduced with permission from Elsevier Ltd.

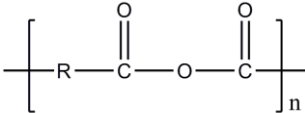
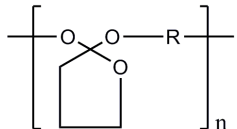
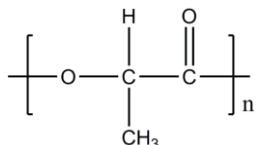
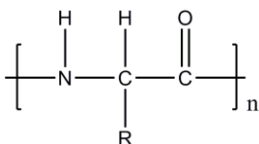
Polymer	Chemical Structure	Half-life <sup>a</sup>
Polyanhydrides		0.1 hours
Poly(ortho esters)		4 hours
Polyesters		3.3 years
Polyamides		83 000 years

Table 3. Estimated values of  $\varepsilon$  (dependence of the erosion number) and  $L_{crit}$  (critical device dimension) for selected degradable polymers. [49].

Copyright 2002. Reproduced with permission from Elsevier Ltd.

Chemical Structure	Polymer	$\lambda$ (s <sup>-1</sup> )	$\varepsilon^a$	$L_{crit}^a$
$\left[ \text{R}-\overset{\text{O}}{\parallel}{\text{C}}-\text{O}-\overset{\text{O}}{\parallel}{\text{C}} \right]_n$	Polyanhydride	$1.9 \times 10^{-3}$ [63]	11 515	75 $\mu\text{m}$
$\left[ \begin{array}{c} \text{R}' \\   \\ \text{O}-\text{C}-\text{O}-\text{R} \\   \\ \text{R}'' \end{array} \right]_n$	Polyketal	$6.4 \times 10^{-5}$ [63]	387	0.4 mm
$\left[ \begin{array}{c} \text{OR} \\   \\ \text{O}-\text{C}-\text{O}-\text{R} \\   \\ \text{R} \end{array} \right]_n$	Poly(ortho ester)	$4.8 \times 10^{-5}$ [63]	291	0.6 mm
$\left[ \begin{array}{c} \text{H} \\   \\ \text{O}-\text{C}-\text{O}-\text{R} \\   \\ \text{R}' \end{array} \right]_n$	Polyacetal	$2.7 \times 10^{-8}$ [63]	0.16	2.4 cm

$\left[ \text{O} - (\text{CH}_2)_5 - \overset{\text{O}}{\parallel}{\text{C}} \right]_n$	Poly( $\epsilon$ -caprolactone)	$9.7 \times 10^{-8}$ [160]	0.1	1.3 cm
$\left[ \text{O} - \overset{\text{H}}{\underset{\text{R}}{\text{C}}} - \overset{\text{O}}{\parallel}{\text{C}} \right]_n$	Poly( $\alpha$ -hydroxy esters)	$6.6 \times 10^{-9}$ [63]	$4.0 \times 10^{-2}$	7.4 cm
$\left[ \overset{\text{H}}{\text{N}} - \overset{\text{H}}{\underset{\text{R}}{\text{C}}} - \overset{\text{O}}{\parallel}{\text{C}} \right]_n$	Polyamide	$2.6 \times 10^{-13}$ [63]	$1.5 \times 10^{-6}$	13.4 m

Table 4. Influence of dynamic stress on the degradation behaviour of biodegradable polymers. [358], Copyright 2016. Adapted with permission from KeAi Communications C.

Polymers	Dynamic stress mode	Frequency	Degradation conditions	Main degradation effects	Reference
PLLA	Compression	1 Hz	Electrospun membranes were immersed in buffered proteinase K at 37°C and pH 8.6. Load locomotion of 0.60 mm for 2, 4, 6, 8 and 10 hours.	No significant influence on the degradation in the early period and promote degradation in the following stage.	[359]
70:30 PLGA	Compression	1 Hz	Porous PLGA scaffolds were in a buffered solution at 37°C and pH 7.4 under dynamic and static loading for 12 weeks.	A faster reduction in mass, dimensions of the PLGA scaffolds, while the relative molecular weight decreased slower in the first week and faster in the following stages.	[360]
50:50 PLGA	Compression	0.5 Hz	PLGA implants with and without	Lower molecular weight loss of the	[361]



Polymers	Dynamic stress mode	Frequency	Degradation conditions	Main degradation effects	Reference
			protein mimic under static and dynamic compression conditions in buffer at 37°C for up to 6 weeks.	loaded specimens compared to the nonloaded specimens in a week immersion.	
Poly(lactic acid)- <i>b</i> -poly(ethylene glycol)- <i>b</i> -poly(lactic acid) with methacrylate end groups	Compression	0.3 Hz, 1 Hz, and 3 Hz	Gel cylinders loaded statically or dynamically with impermeable or permeable platens on top of the gel.	The frequency has no influence at the low cross-linked gels while a higher frequency suggested a faster degradation at the high cross-linked gels.	[362]
PLLA	Tension	1 Hz	Fibers were degraded in buffer at 45°C, loaded axially with free hanging 50g and 100g weights.	A faster degradation under load condition.	[175]

Polymers	Dynamic stress mode	Frequency	Degradation conditions	Main degradation effects	Reference
50:50 PLGA	Bending	0.4 Hz	Release of proteins from cylinders in buffer at loading of 720 cycles/day.	No significant influence on mass loss and molecular weight. Release of protein attributed to stress concentration resulting in microcracks.	[363]